TURBULENCE MODULATION IN PARTICLE-LADEN FLOWS: THE DERIVATION AND VALIDATION OF A DISSIPATION TRANSPORT EQUATION

By

JOHN D. SCHWARZKOPF

A dissertation submitted in partial fulfillment of
the requirements for the degree of

DOCTOR OF PHILOSOPHY

WASHINGTON STATE UNIVERSITY
School of Mechanical and Materials Engineering

DECEMBER 2008

To the Faculty of Washington State University:

The members of the Committee appointed to examine the dissertation of JOHN D. SCHWARZKOPF find it satisfactory and recommend that it be accepted.

_____
Chair

_____

_____

_____

ACKNOWLEDGMENTS

I would like to acknowledge Professor James Riley of the University of Washington. Professor Riley was kind enough to provide a copy of the DNS code. He was also very helpful in answering questions about the code and kind enough to allow us to visit him to modify the code. I am also grateful to his graduate student, Saensuk Wetchagarun, who was a tremendous help in altering the code.

I would also like to acknowledge my committee members. First I would like to thank the chair of my committee, Professor Prashanta Dutta, for his support and immense help in writing and publishing papers. I would also like to thank Professor David Wollkind for many fruitful discussions on topics of the derivation. I would also like to thank Professor Steve Penoncello of the University of Idaho for his support and fruitful discussions during the conceptual phase. And last but not least, I would like to thank my mentor Professor Clayton Crowe, who encouraged me to pursue a graduate degree, taught me, challenged me, supported me and encouraged me in scholarly activity throughout this research project. To him I am very grateful.

TURBULENCE MODULATION IN PARTICLE-LADEN FLOWS: THE DERIVATION AND VALIDATION OF A DISSIPATION TRANSPORT EQUATION

Abstract

by John D. Schwarzkopf, Ph.D.
Washington State University
December 2008

Chair: Prashanta Dutta

In this research, a volume averaged dissipation transport equation is developed for particle laden turbulent flows. The derivation process identifies an additional production of dissipation term that is due to the presence of particles and three new coefficients. The coefficient for the production of dissipation due to the presence of particles was found from experimental data involving homogeneous turbulence generation by particles. The coefficient for the dissipation of dissipation was found to contain an additional term due to the presence of particles within a homogeneous turbulent decay. The coefficient associated with the production by mean velocity gradients was found analytically, but the data needed to determine this coefficient was lacking the necessary parameters. A numerical model was developed and compared to the experimental data of particle laden turbulent channel flow. The first stage of the model shows promise and agrees reasonably well with the experimental data.

TABLE OF CONTENTS

LIST OF TABLES

LIST OF FIGURES

NOMENCLATURE

C	particle concentration
$C_{\varepsilon 1}$	production of dissipation coefficient in time averaged dissipation model
$C'_{\varepsilon 1}$	production of dissipation coefficient in volume averaged dissipation model
$C_{\varepsilon 2}$	dissipation of dissipation coefficient in time averaged dissipation model
$C'_{\varepsilon 2}$	dissipation of dissipation coefficient in volume averaged dissipation model
$C_{\varepsilon 3}$	production of dissipation coefficient (due to particles) in volume averaged dissipation model
D	particle diameter [m]
f	drag factor
k	turbulent kinetic energy [m^2/s^2]
n	number of particles per unit volume [$1/m^3$], or particle number if used in a summation format
n_i, n_k	unit vectors
N	total number of particles within a control volume
NS_i	Navier-Stokes equations
P	pressure [N/m^2]
$P_{( )}$	shear production term
Re_r	relative Reynolds number between dispersed and continuous phase
St	Stokes number
S_d	surfaces of the dispersed phase

U_i Stokes relative velocity [m/sec]

u_i instantaneous velocity of the continuous phase medium [m/s]

$\overline{u_i}$ time averaged velocity of the single phase medium [m/s]

u'_i fluctuation velocity of the single phase medium [m/s]

$\langle u_i \rangle$ volume average velocity of the continuous phase medium [m/s]

δu_i volume deviation velocity of the continuous phase medium [m/s]

u_τ shear velocity [m/s]

u^+ non-dimensional velocity in wall coordinates

v_i instantaneous velocity of the dispersed phase medium [m/s]

$\langle v_i \rangle$ volume average velocity of the dispersed phase medium [m/s]

δv_i volume deviation velocity of the dispersed phase medium [m/s]

V volume [m^3]

y^+ non-dimensional wall coordinate

Greek symbols

α volume fraction associated with a phase

β_V hydrodynamic drag coefficient

δ_{ij} Kronecker delta

ε dissipation [m^2/s^3]

η Kolmogorov length scale [m]

μ dynamic viscosity [N s/m^2]

ν kinematic viscosity [m^2/s]

ρ density [kg/m^3]

$\sigma_{( )}$ turbulent Schmidt number

τ viscous shear stress [N/m^2]

$\tau_{( )}$ response time in relation to subscript [s]

Averaging definitions:

$\langle B \rangle = \frac{1}{V_c}\int_{V_c} B dV$ Phase volume average of property B

$\overline{B} = \frac{1}{V}\int_{V_c} B dV$ Local volume average of property B

$\overline{\overline{B}} = \frac{1}{T}\int_{T} B dt$ Local time average of property B

$\overline{B} = \alpha_c \langle B \rangle$ Relation of the local volume average to the phase average of property B

Subscripts:

c related to the continuous phase

d related to the dispersed phase

n related to the particle number

p related to the particle

r relative

t related to time averaging

T the turbulent form

w at or related to the wall

Scripts:

$\tilde{B}$ non-dimensional form of property B

κ_i wavenumber vector

Dedication

This dissertation is dedicated to my parents, Ed and Suzan Gates, my wife Rebecca and my two sons, Ryan and Zackary, all of whom supported my decision to pursue this degree.

CHAPTER ONE

INTRODUCTION AND OBJECTIVE

1.1 Introduction

In a short review of the modeling status on particle laden turbulence, Eaton (2006) states that many models have been developed to understand turbulence modulation associated with dilute particle laden flows, yet there still remains a need for a general model that can account for factors such as particle size, relative Reynolds number, volume fraction, number density, mass density, surface roughness, etc. The mechanisms responsible for turbulence modulation, or the effect of particles on carrier phase turbulence, are not well understood. As particles are introduced, the statistics of the continuous phase turbulence are altered. Depending on particle characteristics such as size, density, mass loading and relative velocity difference, the level of turbulent kinetic energy (TKE) and dissipation changes relative to the corresponding un-laden flow. Gore and Crowe (1989) showed that the ratio of particle diameter to the size of the most energetic eddies (D/L_e) can be used to distinguish augmentation and attenuation of turbulence intensity. The primary reason for the modulation of turbulence is attributed to the altered dissipation within the continuous phase caused by the work done at the surfaces of the particles (Eaton 2006). The modulation of turbulence in particle laden

flows has been demonstrated by extensive experimentation over the last decades [Hosokawa, et al. (1998); Savolainen, et al. (1998); Sheen, et al. (1993); Tsuji, et al. (1984); Varakasin, et al. (1998), Lee and Durst (1982), Mizukami, et al. (1992), Parthasarathy and Faeth (1990), Chen and Faeth (2000), Lance and Bataille (1982), Kenning and Crowe (1997)]. However, a turbulence model that adequately predicts these modulations over a wide range of conditions is still lacking.

1.2 Motivation and Applications

The motivation for this work is based on understanding the fundamental physics behind multi-phase flows. There are several applications of this fundamental work. Chen and Wood (1985) note that two-phase gas-solid suspension flows are inherent in chemical engineering applications such as spray drying, cyclone separation, pneumatic conveying, pulverized coal gasification and combustion. Crowe (2000) claims that turbulence is a responsible for mixing of chemical species, heat transfer and shear stresses in the continuous phase. A short review of the modeling status was published by Curtis et al. (2004) in which they state that large industries such as the chemical, pharmaceutical, agricultural, and mining industries can benefit from an understanding of particle-laden turbulent flows. Curtis et al. (2004) lists several areas of investigation that could benefit industry; these include turbulent-gas flow interactions, particle clustering, particle shape, friction effects, and particle size distribution. Other applications involve biological systems, atomization, and phase-change cooling or heat treatment. There is a wide range of applications for a multi-phase turbulence model; however there does not appear to be a 'general' model that can be applied to a variety of applications.

1.3 Research Objective

The objective of this research project is to develop a volume averaged dissipation transport equation to extend the volume averaged equation set developed by Crowe et al. (1998) and Crowe and Gillandt (1998). Such an equation set is viewed as 'general' and could potentially be applied to a wide range of applications, including homogeneous turbulence decay with particles, homogenous turbulence generation by particles, particle-laden turbulent channel or pipe flow, particle laden jet flow, etc.

1.4 Literature Review

The most robust and widely used model for turbulence in single phase flows has been the two equation k-ε model. The equation for turbulence energy is

$$\frac{Dk}{Dt} = P_k - \varepsilon + \frac{\partial}{\partial x_i}\left[\left(\nu + \frac{\nu_T}{\sigma_k}\right)\frac{\partial k}{\partial x_i}\right] \tag{1.1}$$

where k is the turbulent kinetic energy ($k = \overline{\overline{u'u'}}/2$), P_k is the production of turbulent energy due to the mean velocity gradients, ν_T is the time averaged turbulent viscosity, ε is the time averaged dissipation and σ_ε is the effective Schmidt number for turbulent diffusion. The turbulence energy is affected by diffusion, the production due to mean flow velocity gradients and dissipation. The equation for dissipation is

$$\frac{D\varepsilon}{Dt} = C_{\varepsilon 1}\frac{P_\varepsilon \varepsilon}{k} - C_{\varepsilon 2}\frac{\varepsilon^2}{k} + \frac{\partial}{\partial x_i}\left[\left(\nu + \frac{\nu_T}{\sigma_\varepsilon}\right)\frac{\partial \varepsilon}{\partial x_i}\right] \tag{1.2}$$

where P_ε is the production of dissipation due to the mean velocity gradients, $C_{\varepsilon 1}$ and $C_{\varepsilon 2}$ are empirical constants, and σ_ε is the turbulent Schmidt number for diffusion of dissipation. As with the turbulence energy, the dissipation is affected by diffusion of dissipation, production of dissipation and dissipation of dissipation.

A typical approach to obtain two-equation models for turbulence energy and dissipation in dispersed phase flows is to begin by adding a source term to the single-phase momentum equation to account for the surface effects, namely

$$\frac{\partial}{\partial t}(\rho u_i)+\frac{\partial}{\partial x_j}(\rho u_j u_i)=-\frac{\partial P}{\partial x_i}+\frac{\partial \tau_{ij}}{\partial x_j}-\frac{\alpha_d \rho_d}{\tau_p} f(u_i - v_i) \tag{1.3}$$

where ρ is the material density of the fluid, P is the pressure, τ_{ij} is the shear stress, u_i is the instantaneous carrier phase velocity, v_i is the instantaneous dispersed phase velocity, α_d and ρ_d are the volume fraction and material density of the dispersed phase, f is the drag factor, τ_p is the particle response time and the additional term is recognized as the drag force per unit volume on the continuous phase. The derivations then proceed using the same Reynolds averaging techniques employed for single phase flows. The concept of adding a point force to represent the effect of a cloud of particles is invalid, and Eq. (1.3) cannot be derived from fundamental principles.

A test to assess the viability of a turbulence model for disperse phase flows is to apply the model to the simplest possible flow configuration. This fundamental case would be a uniform, steady, homogeneous flow through a cloud of particles fixed in position over a large region of space with no walls (shown in Figure 1.1). For such a case there would be no diffusion or production due to mean velocity gradients; therefore the production of turbulence by the particles would be equal to the dissipation of turbulence within the fluid. The remainder of this section is focused on applying previously developed turbulence models for particle laden turbulent flows to this fundamental case.

Elghobashi and Abou-Arab (1983) derived a complex turbulent kinetic energy and dissipation equation by assuming that the particulate phase behaved as a continuous medium. They applied Reynolds averaging procedures to the volume averaged equations

for both the continuous and disperse phases. Their work may be appropriate for "dusty gas" conditions, however for flows with low particle mass loading, the assumption of particles behaving as a continuous medium is invalid.

Chen and Wood (1985) followed after the work of Elghobashi and Abou-Arab (1983) and added a force per unit volume to the instantaneous momentum equation and temporal averaged the result. They argued that their equation was valid for dilute flows and they proposed the dissipation transport equation for the continuous phase to be of the form

$$\frac{D\varepsilon}{Dt} = -C_{\varepsilon 1}\overline{\overline{u_i'u_j'}}\frac{\partial \overline{\overline{u_i}}}{\partial x_j}\frac{\varepsilon}{k} - C_{\varepsilon 2}\frac{\varepsilon^2}{k} - C_{\varepsilon 3}\frac{k}{3}\frac{\partial \overline{\overline{u_i}}}{\partial x_i}\frac{\varepsilon}{k} + \frac{\partial}{\partial x_i}\left[\frac{\nu_T}{\sigma_\varepsilon}\frac{\partial \varepsilon}{\partial x_i}\right] + \frac{2\overline{\overline{\rho}}_p}{\rho t_*}\left[\nu\overline{\overline{\frac{\partial u_i'}{\partial x_j}\left(\frac{\partial v_i'}{\partial x_j} - \frac{\partial u_i'}{\partial x_j}\right)}}\right] \tag{1.4}$$

Applying the fundamental case reduces the above equation to

$$0 = -C_{\varepsilon 2}\frac{\varepsilon^2}{k} - \frac{2\overline{\overline{\rho}}_p}{\rho t_*}\varepsilon \tag{1.5}$$

This equation has two solutions for the dissipation; the first solution is the trivial solution $(\varepsilon = 0)$ while the second solution is impossible

$$\varepsilon = -\frac{2\overline{\rho}_p k}{C_{\varepsilon 2}\rho t_*} \tag{1.6}$$

Chen and Wood also proposed the turbulent kinetic energy of the form

$$\begin{aligned}\frac{Dk}{Dt} = &-\overline{\overline{u_i'u_j'}}\frac{\partial \overline{\overline{u_i}}}{\partial x_j} - \frac{k}{3}\frac{\partial \overline{\overline{u_i}}}{\partial x_i} + \frac{\partial}{\partial x_i}\left[\frac{\nu_T}{\sigma_\varepsilon}\frac{\partial k}{\partial x_i}\right] - \varepsilon + \frac{\overline{\overline{\rho}}_p}{\rho_c t_*}\left(\overline{\overline{u_i'v_i'}} - \overline{\overline{u_i'u_i'}}\right) \\ &+ \frac{1}{\rho_c t_*}\left(\left(\overline{\overline{\rho_p' u_i' v_i'}} - \overline{\overline{\rho_p' u_i' u_i'}}\right)\right) + \frac{1}{\rho_c t_*}\left(\overline{\overline{v_i}} - \overline{\overline{u_i}}\right)\overline{\overline{\rho_p' u_j'}}\end{aligned} \tag{1.7}$$

Applying the above equation to the fundamental case and solving for the dissipation results in

$$\varepsilon = -\frac{\overline{\overline{\rho}}_p}{\rho_c t_*}\left(\overline{\overline{u_i' u_i'}}\right) \tag{1.8}$$

which is clearly incorrect.

Yuan and Michaleides (1992) developed an equation to represent the total turbulence modification by particles of the form

$$\Delta E_k = -\frac{\pi}{12} d^3 \rho_p (u-v)^2 \left[1 - \exp\left(-2f\frac{\tau}{\tau_p}\right)\right] + \frac{\pi}{12} d^2 \rho f(l_w)\left(u^2 - v^2\right) \tag{1.9}$$

The terms on the right hand side of Eq. (1.9) are the work done on the particle and the kinetic energy. Applying Eq. (1.9) to the fundamental case and assuming that the particles are large such that $\tau_p >> \tau$, results in

$$\Delta E_k = \frac{\pi}{12} d^2 \rho f(l_w) u^2 \tag{1.10}$$

which predicts an increase in turbulence kinetic energy. If $\tau_p << \tau$, and the particle diameter is on the order of the wake dimension ($f(l_w)$), then

$$\Delta E_k = \frac{\pi}{12} d^3 u^2 \left(\rho - \rho_p\right) \tag{1.11}$$

which suggests that the change in kinetic energy is related to the difference in density between the particle and the fluid. They also claim that the model agrees well with the findings of Gore and Crowe (1989).

Yarin and Hesteroni (1994) claim that the turbulence intensity is given by

$$\frac{\sqrt{u'^2}}{U_{rel}} = const\left(\frac{\alpha_d}{\alpha_c} c_D^{3/2}\right)^{4/9} \tag{1.12}$$

where U_{rel} is the relative velocity between the particle and carrier phase and α_d/α_c is the ratio of volume fractions. Their model compares well with experimental data for high relative Reynolds numbers but appears to be several factors off for flows with low

relative Reynolds number (Crowe, 2001). However, when applied to the idealized case, the above correlation shows an increase in turbulence intensity, yielding the correct results.

Similar to the work of Chen and Wood (1985), Kulick et al. (1993), Fessler and Eaton (1995), and Eaton (1995) show an additional dissipation term due to the presence of particles of the form

$$\varepsilon_p = \frac{\overline{\overline{c}}}{\rho\tau_p}\left(\overline{\overline{u_i'u_i'}} - \overline{\overline{u_i'v_i'}}\right) + \frac{1}{\rho\tau_p}\left(\overline{\overline{c'u_i'u_i'}} - \overline{\overline{c'u_i'v_i'}}\right) + \frac{1}{\rho\tau_p}\left(\overline{u}_i - \overline{v}_i\right)\overline{\overline{c'u_i'}} \tag{1.13}$$

where c is the particle concentration. Applying this equation to the fundamental case where the mean and fluctuating particle velocity are zero and since the particles are fixed in position, the fluctuating particle concentration is zero, reduces the above equation to

$$\varepsilon_p = \frac{\overline{\overline{c}}}{\rho\tau_p}\overline{\overline{(u_i'u_i')}} \tag{1.14}$$

They show from a Reynolds averaging process that the change in kinetic energy is comprised of the single phase effects minus the dissipation due to particles, which is shown to be of the form (Eaton 1995)

$$\frac{Dk}{Dt} = \left.\frac{Dk}{Dt}\right|_{s-phase} - \varepsilon_p \tag{1.15}$$

Substituting in Eq. (1.14) into Eq. (1.15), applying the fundamental case to the single phase terms, and solving for the fluid dissipation shows

$$\varepsilon_{fluid} = -\frac{\overline{\overline{c}}}{\rho\tau_p}\overline{\overline{(u_i'u_i')}} \tag{1.16}$$

which is clearly incorrect.

Crowe and Gillant (1998) proposed a turbulent kinetic energy equation for particle laden turbulent flows. They argue that Reynolds averaging procedures do not apply to particle laden flow because this process does not account for the effects of neighboring particles. They assert that volume averaging or ensemble averaging are the correct procedures to obtain the transport equations for turbulent properties within the carrier phase of particle laden flows. Their turbulent kinetic energy is shown to be of the form

$$\alpha_c \frac{Dk}{Dt} = -\alpha_c \left\langle \delta u_i \delta u_j \right\rangle \frac{\partial \langle u_i \rangle}{\partial x_j} - \frac{\beta_V}{\rho}\left[\left\langle \delta u_i \delta v_i \right\rangle - \left\langle \delta v_i \delta v_i \right\rangle\right] + \frac{\beta_V}{\rho}\left[\langle u_i \rangle - \langle v_i \rangle\right]^2 + \frac{\partial}{\partial x_j}\left(\frac{\sigma_k}{\rho}\frac{\partial k}{\partial x_j}\right) - \alpha_c \varepsilon \quad (1.17)$$

where σ_k is the diffusion coefficient for turbulence energy and a production and redistribution term due to the presence of the particle arises from the volume averaged process. Applying the above equation to the fundamental case and solving for the dissipation results in

$$\varepsilon = \frac{\beta_V}{\alpha_c \rho_c}\left[\langle u_i \rangle\right]^2 \quad (1.18)$$

which shows that production of turbulent energy by particles is balanced with dissipation.

Lain et al. (1999) added an additional production term to the dissipation equation that accounted for the production of dissipation due to the presence of bubbles. They suggested that the effect of the bubbles on the dissipation could be included by incorporating an additional term within the dissipation equation of the form

$$S_{\varepsilon,P} = C_{\varepsilon 3}\frac{\varepsilon}{k} S_{k,P} \quad (1.19)$$

where $S_{k,P}$ represents the modulation terms found within Crowe and Gillandt's volume averaged turbulence kinetic energy equation. Including the modified form of the

dissipation of dissipation term, the dissipation equation provided by Lain, et al. (1999) is shown to be

$$\begin{aligned}&\frac{\partial}{\partial t}(\rho\varepsilon)+\frac{\partial}{\partial x}(\rho U\varepsilon)+\frac{1}{r}\frac{\partial}{\partial r}(\rho rV\varepsilon)=C_{\varepsilon 1}\frac{G_k\varepsilon}{k}-C_{\varepsilon 2}\rho\frac{\varepsilon^2}{k}+\frac{\partial}{\partial x}\left[\left(\mu+\frac{\mu_T}{\sigma_\varepsilon}\right)\frac{\partial\varepsilon}{\partial x}\right]\\&+\frac{1}{r}\frac{\partial}{\partial r}\left[\left(\mu+\frac{\mu_T}{\sigma_\varepsilon}\right)r\frac{\partial\varepsilon}{\partial r}\right]+C_{\varepsilon 3}\frac{\varepsilon}{k}\left[\sum_{i=1}^{3}\frac{\alpha_d\rho_d}{\tau_d(C_D)}\left\{\left[U-\bar{v}\right]^2-\overline{\overline{u_i'v_i'}}+\overline{\overline{v_i'v_i'}}\right\}\right]\end{aligned}\tag{1.20}$$

where U and V are the Reynolds averaged velocity components of the continuous phase, v is the velocity of the bubble phase, $\tau_d(C_D)$ is the bubble response time, μ_T is the turbulent viscosity, the coefficients are identified as: $C_{\varepsilon 1} = 1.44$, $C_{\varepsilon 2} = 1.92$, $C_{\varepsilon 3} = 1.1$, $\sigma_\varepsilon = 1.3$, and G_k is the production of dissipation identified by

$$G_k=\mu_T\left[2\left\{\left(\frac{\partial U}{\partial x}\right)^2+\left(\frac{\partial V}{\partial y}\right)^2+\left(\frac{V}{r}\right)^2\right\}+\left(\frac{\partial U}{\partial r}+\frac{\partial V}{\partial x}\right)^2+\left(r\frac{\partial}{\partial r}\left(\frac{W}{r}\right)\right)^2+\left(\frac{\partial W}{\partial x}\right)^2\right]\tag{1.21}$$

Substituting Eq. (1.21) into Eq. (1.20) and applying the fundamental case to the resultant equation shows

$$\frac{\varepsilon}{k}\left[C_{\varepsilon 3}\left[\sum_{i=1}^{3}\frac{\alpha_d\rho_d}{\tau_d(C_D)}[U]^2\right]-C_{\varepsilon 2}\rho\varepsilon\right]=0\tag{1.22}$$

The above equation has two solutions for the dissipation, the trivial solution and

$$\varepsilon=\frac{C_{\varepsilon 3}}{C_{\varepsilon 2}\rho}\left[\sum_{i=1}^{3}\frac{\alpha_d\rho_d}{\tau_d(C_D)}[U]^2\right]\tag{1.23}$$

which shows the correct result. The coefficient $C_{\varepsilon 3}$ was set to be a constant of 1.1 and the coefficient $C_{\varepsilon 2}$ is the traditional value (1.92); however if this case were applied to the TKE equation, a comparison of the two would show that the above equation does not provide any new information and further requires that $C_{\varepsilon 3} = C_{\varepsilon 2}$. Squires and Eaton

(1992) claim that the coefficient $C_{\varepsilon 3}$ is not a universal constant but potentially a function of bulk density of the dispersed phase.

Zhou and Chen (2001) proposed a Reynolds stress transport equation for the continuous phase of the form

$$\frac{\partial}{\partial t}\left(\rho\overline{\overline{u_i u_j}}\right)+\frac{\partial}{\partial x_k}\left(\rho U_k\overline{\overline{u_i u_j}}\right)=D_{ij}+P_{ij}+G_{p_{ij}}+\Pi_{ij}-\varepsilon_{ij} \tag{1.24}$$

where D_{ij}, P_{ij}, Π_{ij}, and ε_{ij} are the diffusion, production, pressure strain and dissipation rate terms. The term $G_{p_{ij}}$ is the gas phase Reynolds stress due to particle drag force. Zhou and Chen's Reynolds stress model can be reduced to the turbulent kinetic energy model by setting i = j and multiplying by 1/2. Applying the reduced equation to the fundamental case, the co-moving derivative, the production and the diffusion become zero. The particle generation term for this case is reduced to

$$G_{p_{ii}}=-\sum_p\frac{\rho_p}{\tau_{rp}}\left(\overline{\overline{u_i' u_i'}}\right) \tag{1.25}$$

and the pressure strain term is reduced to

$$\Pi_{ii}=0 \tag{1.26}$$

and the dissipation is reduced to

$$\varepsilon_{ii}=\rho\varepsilon \tag{1.27}$$

(It is noted that the equation for ε_{ij} in Zhou and Chen's manuscript is not multiplied by the density of the fluid, thus in Eq. (1.27) a density was added to ensure the correct units). Substituting Eqs. (1.25 – 1.27) into the reduced form of Eq. (1.24) and solving for the dissipation shows

$$\varepsilon=-\frac{1}{\rho}\sum_p\frac{\rho_p}{\tau_{rp}}\left(\overline{\overline{u_i' u_i'}}\right) \tag{1.28}$$

which is clearly impossible since all the terms in the right hand side of the above equation are positive. Likewise, the dissipation model presented by Zhou and Chen (2001) is of the form

$$\rho\frac{D\varepsilon}{Dt}=\frac{\varepsilon}{k}\left[C_{\varepsilon 1}\left(G+G_p\right)-C_{\varepsilon 2}\rho\varepsilon\right]+\frac{\partial}{\partial x_i}\left[C_\varepsilon\frac{k}{\varepsilon}\overline{\overline{u_i'u_j'}}\frac{\partial\varepsilon}{\partial x_j}\right] \tag{1.29}$$

where G is not identified in the manuscript but assumed to be the standard production term, and G_p is source term due to the particles of the form

$$G_p=\sum_p\frac{\rho_p}{\tau_{rp}}\left(\overline{\overline{v_i'u_i'}}-\overline{\overline{u_i'u_i'}}\right) \tag{1.30}$$

Substituting Eq. (1.30) into Eq. (1.29) and applying the resultant equation to the fundamental case shows

$$0=\frac{\varepsilon}{k}\left[-C_{\varepsilon 1}\sum_p\frac{\rho_p}{\tau_{rp}}\left(\overline{\overline{u_i'u_i'}}\right)-C_{\varepsilon 2}\rho\varepsilon\right] \tag{1.31}$$

The above equation has two solutions for the dissipation, the trivial solution and

$$\varepsilon=-\frac{C_{\varepsilon 1}}{\rho C_{\varepsilon 2}}\sum_p\frac{\rho_p}{\tau_{rp}}\left(\overline{\overline{u_i'u_i'}}\right) \tag{1.32}$$

both of which are impossible. Although this equation set does not show that production of dissipation by particles is balanced with dissipation of dissipation in the fluid for the fundamental case, the numerical results do compare well with the experimental data.

Simonin and Squires (2003) proposed a transport equation for the form of turbulent kinetic energy of the continuous phase for dilute particle laden flows. Their equation is shown to be of the form

$$\alpha_c\rho\frac{Dq^2}{Dt}=P+\Gamma+\Pi_{qf}-\alpha_c\rho\varepsilon_v \tag{1.33}$$

where P represents the shear production, Γ represents the turbulent transport, ε_v is a combined dissipation and Π_{qf} is described by

$$\Pi_{qf} = \frac{m_d n_d}{\tau_p}\left\langle v_{r,i} v_{r,i} \right\rangle_p + \frac{m_d n_d}{\tau_p}\left[q_{fp} - 2\tilde{q}_f^2 + V_{r,i} V_{d,i}\right] \tag{1.34}$$

where $v_{r,i}$ is the relative velocity fluctuation and $V_{d,i}$ can be modeled using a gradient transport hypothesis, $\tilde{q}_f^2$ is the kinetic energy of the locally undisturbed fluid velocity and q_{fp} is related to the particle velocity fluctuation. Substituting Eq. (1.34) into Eq. (1.33) and applying the resultant equation to the fundamental case results in

$$\varepsilon_v = \frac{m_d n_d}{\alpha_c \rho \tau_p}\left\langle \tilde{u}_{f,i} \tilde{u}_{f,i} \right\rangle + \frac{m_d n_d}{\alpha_c \rho \tau_p}\left[-2\tilde{q}_f^2\right] \tag{1.35}$$

where $\tilde{u}_{f,i}$ is the local and instantaneous undisturbed velocity of the fluid. The above terms on the right hand side of Eq. (1.35) are equal and opposite, resulting in zero value for the dissipation. It should be noted that they claim that when production is equal to dissipation the equation reduces to

$$\varepsilon_v = \frac{m_d n_d}{\alpha_c \rho \tau_p}\overline{\overline{(u_i' - v_i')^2}} \tag{1.36}$$

which shows that the dissipation is related to the production due to the relative velocity fluctuations and further more would yield the correct result when applied to the fundamental case. However, the terms shown in the work of Simonin and Squires (2003) are not clear, which may account for the discrepancy between Eq. (1.36) and Eq. (1.35).

The turbulent kinetic energy used by Zhang and Reese (2003) is of the form

$$\frac{\partial}{\partial t}(\alpha_c \rho k) + \frac{\partial}{\partial x_j}\left(\alpha_c \rho \overline{\overline{u_j}} k\right) = -\alpha_c \rho \overline{\overline{u_i' u_j'}} \frac{\partial \overline{\overline{u_i}}}{\partial x_j} - \alpha_c \rho \varepsilon + \frac{\partial}{\partial x_j}\left[\alpha_c \left(\mu + \frac{\mu_T}{\sigma_k}\right)\frac{\partial k}{\partial x_j}\right] + [\Delta k] \tag{1.37}$$

where Δk is a source of turbulent kinetic energy due to the presence of particles. The term Δk was studied by Zhang and Reese (2001); in this study, they concluded that the volume averaged terms found by Crowe and Gillant (1998) better matched the experimental data of Tsuji et al. (1984) than the time averaged terms found in the literature. Applying the above equation to the fundamental case and solving for the dissipation yields

$$\varepsilon = \frac{\Delta k}{\alpha_c \rho} = \frac{\beta_0 \langle u_i \rangle^2}{\alpha_c \rho} \tag{1.38}$$

which shows that the dissipation is balanced with the change in production of turbulent kinetic energy produced by the particles. Zhang and Reese (2003) also proposed a dissipation transport equation of the form

$$\frac{\partial}{\partial t}(\alpha_c \rho \varepsilon) + \frac{\partial}{\partial x_j}\left(\alpha_c \rho \overline{\overline{u_j}} \varepsilon\right) = C_{\varepsilon 1} \alpha_c \mu_T \left(\frac{\partial \overline{\overline{u_i}}}{\partial x_j} + \frac{\partial \overline{\overline{u_j}}}{\partial x_i}\right) \frac{\partial \overline{\overline{u_i}}}{\partial x_j} \frac{\varepsilon}{k} - C_{\varepsilon 2} \alpha_c \rho \frac{\varepsilon^2}{k} + \frac{\partial}{\partial x_j}\left[\alpha_c \left(\mu + \frac{\mu_T}{\sigma_\varepsilon}\right) \frac{\partial \varepsilon}{\partial x_j}\right] + C_{\varepsilon 3} \frac{\varepsilon}{k}[\Delta k] \tag{1.39}$$

where Δk is a source of turbulent kinetic energy due to the presence of particles and is modeled after Crowe and Gillant's generation and redistribution terms. Applying the fundamental test to the above equation yields

$$0 = \frac{\varepsilon}{k}\left[C_{\varepsilon 3} \Delta k - C_{\varepsilon 2} \alpha_c \rho \varepsilon\right] \tag{1.40}$$

Again, the above equation has two solutions for the dissipation, the first is the trivial solution and the second is

$$C_{\varepsilon 3} \Delta k = C_{\varepsilon 2} \alpha_c \rho \varepsilon \tag{1.41}$$

which implies that if $C_{\varepsilon 2} = C_{\varepsilon 3}$, then the TKE equation is obtained and no new information is found, or if $C_{\varepsilon 2}$ does not equal $C_{\varepsilon 3}$, then the production of dissipation due to particles does not equal the dissipation of the fluid and this would be incorrect.

Yu, et al. (2006) formed a two-time-scale dissipation model after the work of Zhou and Chen (2001). In the dissipation model, the inverse turbulent time scale of the fluid (ε/k) is replaced by $1/\tau_e$, where τ_e is the minimum of a modified particle response time or the turbulent time scale. This modification does not alter the fundamental error in Zhou and Chen's dissipation equation.

Nasr et al. (2007) added a source term to the turbulent kinetic energy and dissipation equations. The source terms are similar to those proposed by Lain and Sommerfeld (2003) and they were modeled using a Lagrangian tracking technique. For steady flow conditions, their turbulent kinetic energy is of the form

$$\overline{\overline{u}}_j \frac{\partial k}{\partial x_j} = -R_{ij} \frac{\partial \overline{\overline{u}}_i}{\partial x_j} - \varepsilon + \frac{\partial}{\partial x_j}\left[\left(\nu + \frac{\nu_T}{\sigma_k}\right)\frac{\partial k}{\partial x_j}\right] + \left[\overline{\overline{u_i^p S_{ui}^P}} - \overline{\overline{u}}_i \overline{\overline{S_{ui}^P}}\right] \tag{1.42}$$

where R_{ij} is the Reynolds stress, u_i^p is the particle velocity and S_{ui}^P is the drag force of the particle on the fluid. Applying the fundamental case to the above equation shows

$$\varepsilon = -\frac{\gamma}{\rho}\overline{\overline{u_i u_i}} = -\frac{\gamma}{\rho}\left(\overline{\overline{u}}_i \overline{\overline{u}}_i + \overline{\overline{u_i' u_i'}}\right) \tag{1.43}$$

where γ is related to the hydrodynamic drag. Nasr et al. (2007) also proposed a dissipation equation of the form

$$\overline{\overline{u}}_j \frac{\partial \varepsilon}{\partial x_j} = C_{\varepsilon 1} R_{ij} \frac{\partial \overline{\overline{u}}_i}{\partial x_j}\frac{\varepsilon}{k} - C_{\varepsilon 2}\frac{\varepsilon^2}{k} + \frac{\partial}{\partial x_j}\left[\left(\nu + \frac{\nu_T}{\sigma_\varepsilon}\right)\frac{\partial \varepsilon}{\partial x_j}\right] + C_{\varepsilon 3}\frac{\varepsilon}{k}\left[\overline{\overline{u_i^p S_{ui}^P}} - \overline{\overline{u}}_i \overline{\overline{S_{ui}^P}}\right] \tag{1.44}$$

Applying the fundamental case to the above equation shows

$$0 = -C_{\varepsilon 2}\frac{\varepsilon^2}{k} + C_{\varepsilon 3}\frac{\varepsilon}{k}\left[-\overline{\overline{u}}_i \overline{\overline{S_{ui}^P}}\right] \tag{1.45}$$

Solving for the dissipation, two solutions are evident; the trivial solution and

$$\varepsilon = -\frac{C_{\varepsilon 3}}{C_{\varepsilon 2}}\frac{\gamma}{\rho}\overline{\overline{u_i u_i}} = -\frac{C_{\varepsilon 3}}{C_{\varepsilon 2}}\frac{\gamma}{\rho}\left(\overline{\overline{u}}_i \overline{\overline{u}}_i + \overline{\overline{u_i' u_i'}}\right) \tag{1.46}$$

which shows to be no different than Eq. (1.43) and furthermore is impossible. Nasr et al. (2007) compared the model results to experimental data of Kulick (1994). Their results show that when particle-particle and particle-wall collisions are included, the carrier phase turbulence is attenuated; if these collisions are not included, the turbulence is augmented. Overall, their results are in reasonable agreement with the data.

Yan et al. (2007), incorporating some of the ideas proposed in literature, added a source term to account for turbulent production due to wakes. Their model also contains a sink term to account for turbulent attenuation. The proposed model for steady turbulent kinetic energy is of the form

$$\overline{\overline{u}}_j \frac{\partial k}{\partial x_j} = v_T \left(\frac{\partial \overline{\overline{u}}_i}{\partial x_j} + \frac{\partial \overline{\overline{u}}_j}{\partial x_i} \right) \frac{\partial \overline{\overline{u}}_i}{\partial x_j} + \frac{\partial}{\partial x_j} \left[\frac{v_T}{\sigma_k} \frac{\partial k}{\partial x_j} \right] - \varepsilon - \frac{\alpha_d \rho_d}{\rho \tau_p} \left(\overline{\overline{u_i' u_i'}} - \overline{\overline{u_i' v_i'}} \right) + \overline{\overline{u}}_i \frac{\alpha_d \rho_d}{\rho \tau_p} \left(\overline{\overline{u}}_i - \overline{\overline{v}}_i \right) (f-1) \quad (1.47)$$

Applying the above equation to the fundamental case shows

$$\varepsilon = \frac{\alpha_d \rho_d}{\rho \tau_p} \left[\left(\overline{\overline{u}}_i \right)^2 (f-1) - \left(\overline{\overline{u_i' u_i'}} \right) \right] \quad (1.48)$$

which confirms that production by the particles is balanced with dissipation. Yan et al. (2007) also proposed a dissipation equation with an *ad hoc* source term to account for the dissipation production. It is presented as

$$\begin{aligned} \overline{\overline{u}}_j \frac{\partial \varepsilon}{\partial x_j} = {} & C_{\varepsilon 1} \frac{\varepsilon}{k} v_T \left(\frac{\partial \overline{\overline{u}}_i}{\partial x_j} + \frac{\partial \overline{\overline{u}}_j}{\partial x_i} \right) \frac{\partial \overline{\overline{u}}_i}{\partial x_j} + \frac{\partial}{\partial x_j} \left[\frac{v_T}{\sigma_\varepsilon} \frac{\partial \varepsilon}{\partial x_j} \right] - C_{\varepsilon 2} \frac{\varepsilon^2}{k} \\ & - \frac{2\alpha_d \rho_d}{\rho \tau_p} \left[\nu \overline{\overline{\frac{\partial u_i'}{\partial x_j} \left(\frac{\partial u_i'}{\partial x_j} - \frac{\partial v_i'}{\partial x_j} \right)}} \right] + C \frac{\varepsilon}{k} \overline{\overline{u}}_i \frac{\alpha_d \rho_d}{\rho \tau_p} \left(\overline{\overline{u}}_i - \overline{\overline{v}}_i \right) (f-1) \end{aligned} \quad (1.49)$$

where C is a model constant. Applying the fundamental case to the above equation shows

$$0 = -C_{\varepsilon 2} \frac{\varepsilon^2}{k} - \frac{2\alpha_d \rho_d}{\rho \tau_p} \varepsilon + C \frac{\varepsilon}{k} \overline{\overline{u}}_i \frac{\alpha_d \rho_d}{\rho \tau_p} \left(\overline{\overline{u}}_i \right) (f-1) \quad (1.50)$$

Solving for the dissipation shows two solutions, the trivial solution and

$$\varepsilon = \frac{\alpha_d \rho_d}{C_{\varepsilon 2} \rho \tau_p} \left[C \left(\overline{\overline{u}}_i \right)^2 (f-1) - 2k \right] \tag{1.51}$$

The above equation does show that turbulent kinetic energy is proportional to dissipation. By substituting in Eq. (1.48) into Eq. (1.51) the turbulent kinetic energy is shown to be related to the square of the mean velocity. Yan et al. (2007) compared several models [Chen and Wood (1985), Mostafa and Mongia (1988), Lightstone and Hodgson (2004), Yokomine and Shimizu (1995)] but all the models show to be weak in predicting the turbulence intensity for small particles (200 μm). However, the model of Yan et al. (2007) does agree well with large particle data (> 500 μm) of Tsuji et al. (1984). The weakness of these equations is that they contain *ad hoc* terms and may be limited to a small range of applications.

Mohanarangam et al. (2007) obtained an equation for the turbulent kinetic energy of the form

$$\overline{\overline{u}}_j \frac{\partial k}{\partial x_j} = \frac{P_k}{\rho} + \frac{\partial}{\partial x_j} \left[\zeta \nu_T \frac{\partial k}{\partial x_j} \right] - \varepsilon - \frac{f \rho_d}{\rho \tau_p} \left(\overline{\overline{u_i' u_i'}} - \overline{\overline{u_i' v_i'}} \right) \tag{1.52}$$

where ζ is the inverse Prandtl number and P_k is the production due to mean velocity gradients. Applying the above equation to the fundamental case shows

$$\varepsilon = -\frac{f \rho_d}{\rho \tau_p} \left(\overline{\overline{u_i' u_i'}} \right) \tag{1.53}$$

which is incorrect. They also proposed a dissipation of dissipation equation of the form

$$\begin{aligned} \overline{\overline{u}}_j \frac{\partial \varepsilon}{\partial x_j} = C_{\varepsilon 1} \frac{P_k}{\rho} \frac{\varepsilon}{k} + \frac{\partial}{\partial x_j} \left[\zeta \nu_T \frac{\partial \varepsilon}{\partial x_j} \right] - C_{\varepsilon 2} \frac{\varepsilon^2}{k} \\ - R - \frac{2 f \rho_d}{\tau_p \rho} \varepsilon \left(1 - \exp\left(- B_\varepsilon \tau_p \frac{\varepsilon}{k} \right) \right) \end{aligned} \tag{1.54}$$

where R is a function of the rate of strain and B_ε is a constant. Applying the above equation to the fundamental case shows

$$0 = -C_{\varepsilon 2}\frac{\varepsilon^2}{k} - \frac{2f\rho_d}{\tau_p \rho}\varepsilon\left(1 - \exp\left(-B_\varepsilon \tau_p \frac{\varepsilon}{k}\right)\right) \tag{1.55}$$

which again has two solutions, the trivial solution and

$$\varepsilon = -\frac{2f\rho_d k}{C_{\varepsilon 2}\tau_p \rho}\left(1 - \exp\left(-B_\varepsilon \tau_p \frac{\varepsilon}{k}\right)\right) \tag{1.56}$$

The terms within the exponential are positive along with the terms outside; however, here the dissipation is shown to be negative for this fundamental case.

1.5 Traditional Approach to Modeling Turbulence

In the above literature review, many researchers either start from Eq. (1.3) or a volume averaged form of Eq. (1.3) and then apply Reynolds averaging procedures to obtain the equations describing turbulence. Other examples involve incorporating *ad hoc* source and sink terms to account for the measured effects. However, it is apparent that these approaches are flawed. To assess this flaw, let's consider the fundamental physics.

The momentum equations for a continuous fluid can be obtained from Newton's second law by transforming from a Lagrangian to an Eulerian reference frame using the Reynolds transport theorem (RTT), applying Gauss's theorem to convert the surface integrals to volume integrals and including the assumption of a Newtonian fluid, resulting in

$$\int_V \left(\frac{\partial}{\partial t}(\rho u_i) + \frac{\partial}{\partial x_j}(\rho u_j u_i) + \frac{\partial P}{\partial x_i} - \frac{\partial}{\partial x_j}\left(\mu \frac{\partial u_i}{\partial x_j}\right) - \rho g_i\right) dV = 0 \tag{1.57}$$

for an incompressible flow. To ensure that the above equation is valid over an arbitrary volume the integrand is set to zero, resulting in the incompressible form of the Navier-Stokes equations. The above equation set is valid in the continuous portion (i.e. carrier phase) of a particle laden flow. However, in order to apply Eq. (1.57) to particle laden flows, the particle surfaces would need to be treated as boundary conditions. Such treatments for each particle would require enormous computational efforts and advanced grid methods.

To minimize the computational effort, many previous researchers have assumed that a force due to the effects of the particle can be applied to a point in the flow, such as

$$\int_V \left(\frac{\partial}{\partial t}(\rho u_i) + \frac{\partial}{\partial x_j}(\rho u_j u_i) + \frac{\partial P}{\partial x_i} - \frac{\partial}{\partial x_j}\left(\mu \frac{\partial u_i}{\partial x_j} \right) - \rho g_i + F_i \right) dV = 0 \qquad (1.58)$$

where F_i is a force per unit volume due to the presence of particles and the integrand of the above equation is equivalent to Eq. (1.3). However, this force is not defined at an arbitrary point within the continuous phase, see Figure 1.2. The force due to the particle would better be described at a point within the continuous phase by the pressure, shear and body forces acting on the control volume and would require complex grids as described above. The only way to include a force per unit volume is to have a control volume that contains enough particles to provide and effective average, also shown in Figure 1.2. In order to define this force – F_i – at a point, the limiting volume would have to include many particles such that the inter-particle spacing would be comparable to the mean free path of the molecules. This would be considered a mixture of two-fluids rather than a multiphase flow.

It is shown in literature that one approach to obtain the turbulence kinetic energy equation is to multiply the terms within the integrand of Eq. (1.58) by the instantaneous

velocity and decompose the instantaneous terms within the integrand of Eq. (1.58) into mean and fluctuating terms (in time). The result is then temporal averaged and the mechanical kinetic energy equation is subtracted, leaving an equation for the turbulent kinetic energy. This approach would make sense if there were enough particles within the volume of interest such that the particles could be treated as a continuous medium. However, in many industrial applications the particles are not considered a continuous medium, thus limiting the application of this approach.

The two correct approaches for developing the momentum equations and turbulence equations for dispersed phase turbulent flow are volume averaging (Crowe et al. 1998) and ensemble averaging (Zhang and Prosperetti 1994). It has been shown (Crowe et al. 1998) that the additional source term needed in the momentum equations (1.3) to account for the surface effects of particles arises from volume averaging the momentum equation (i.e. a volume larger than the limiting volume is necessary). They also argued that it is not possible to describe the flow properties at a point without the inclusion of the effect of the neighboring particles (illustrated in Figure 1.2). Volume averaging provides a scheme to include the effects of the dispersed phase without the necessity of including the details of the surface interaction. Crowe, et al. (1998) and Slattery (1972) provide a detailed description of the volume average concept.

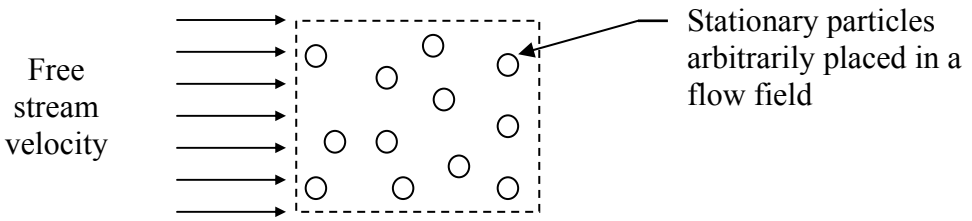

Figure 1.1: An idealized case for testing turbulence models where a mean fluid flow approaches a bed of stationary particles within a large volume of fluid having no walls. For such a case, the flow is homogeneous and therefore turbulence production must balance with dissipation.

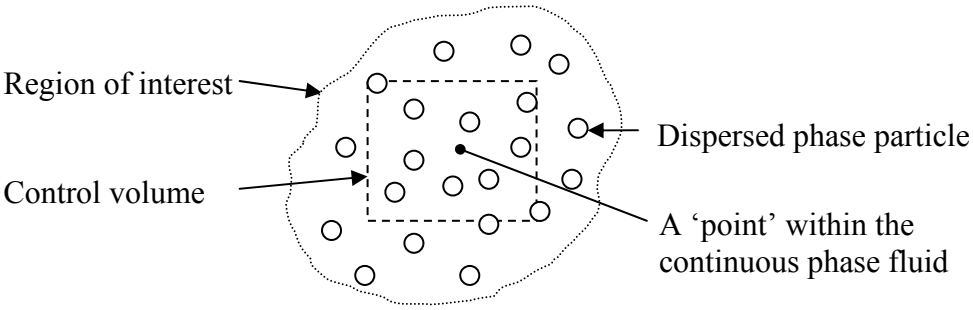

Figure 1.2: A qualitative example of particles within a fluid. Here it is illustrated that the additional force due to particle(s) – F_i – is not valid at a point within the continuous phase, but rather valid over a control volume that is larger than the limiting volume of the continuous phase and contains enough particles to obtain a stationary average. Unless the particle surfaces are treated as boundary conditions, a temporal averaging approach does not include the effect of neighboring particles at a point in the flow.

CHAPTER TWO

A REVIEW OF VOLUME AVERAGING AND ITS RELATION TO TURBULENCE

Although the volume averaged momentum equations have been developed (Crowe et al. 1998), an alternative approach to obtaining the volume averaged momentum equations for single phase and particle laden flows is presented. When considering volume averaged momentum equations, it is not obvious that these are used quite frequently in fluid dynamics research.

Let's reconsider the momentum equations derived from Newton's second law ($\vec{F} = m\vec{a}$). Using the Reynolds transport theorem (RTT), the acceleration is transformed from a Lagrangian reference frame to an Eulerian reference frame. If the forces are continuous, then they can be converted from a surface integral to a volume integral using Gauss's theorem. Assuming that the fluid is Newtonian and incompressible, the result is

$$\int_V \frac{\partial}{\partial t}(\rho u_i)dV + \int_V \frac{\partial}{\partial x_j}(\rho u_j u_i)dV = -\int_V \frac{\partial P}{\partial x_i}dV + \int_V \frac{\partial}{\partial x_j}\left(\mu \frac{\partial u_i}{\partial x_j}\right)dV + \int_V \rho g_i dV \qquad (2.1)$$

Traditionally, the terms are gathered on one side and collected within the volume integral and equated to zero. In order to ensure that the resultant equation can be applied to an arbitrary volume of fluid requires the integrand to be zero, yielding the well known incompressible Navier Stokes equations.

Now consider an alternative approach. The definition of the volume average of a property (B) is

$$\overline{B} = \frac{1}{V}\int_V B dV \tag{2.2}$$

Multiplying Eq. (2.1) by $1/V$ and applying Eq. (2.2), Eq. (2.1) can be rewritten according to the form

$$\overline{\frac{\partial}{\partial t}(\rho u_i)} + \overline{\frac{\partial}{\partial x_j}(\rho u_j u_i)} = -\overline{\frac{\partial P}{\partial x_i}} + \overline{\frac{\partial}{\partial x_j}\mu\frac{\partial u_i}{\partial x_j}} + \overline{\rho g_i} \tag{2.3}$$

The relationship between the volume average of a spatial gradient and the gradient of the volume average in a single phase fluid is

$$\overline{\frac{\partial B}{\partial x_i}} = \frac{1}{V}\int_V \frac{\partial B}{\partial x_i} dV = \frac{1}{V}\frac{\partial}{\partial x_i}\int_V B dV = \frac{\partial \overline{B}}{\partial x_i} \tag{2.4}$$

Also, the volume average of the time rate of change is related to the time rate of change of the volume average for a single phase fluid

$$\overline{\frac{\partial B}{\partial t}} = \frac{1}{V}\int_V \frac{\partial B}{\partial t} dV = \frac{1}{V}\frac{\partial}{\partial t}\int_V B dV = \frac{\partial \overline{B}}{\partial t} \tag{2.5}$$

Applying Eqs. (2.4) and (2.5) to Eq. (2.3) reveals

$$\frac{\partial}{\partial t}\overline{(\rho u_i)} + \frac{\partial}{\partial x_j}\overline{(\rho u_j u_i)} = -\frac{\partial \overline{P}}{\partial x_i} + \frac{\partial}{\partial x_j}\mu\overline{\frac{\partial u_i}{\partial x_j}} + \overline{\rho g_i} \tag{2.6}$$

The above equation can also be viewed as an alternative form of the Navier-Stokes equations, albeit the volume averaged form.

The rationale comes from considering a number of molecules within a limiting volume. In a continuum, the volume must be large enough to obtain an average of molecular effects. The properties of pressure and velocity of a single molecule do not make sense from a continuum point of view, but the average bulk motion of many

molecules produces macroscopic properties and in order for a continuum to be defined these macroscopic properties must be related to the molecular properties averaged over the limiting volume. Thus properties at a 'point' have no meaning and the form of Eq. (2.6) must be equivalent to the momentum equations defined at a 'point', Eq. (1.57), when the control volume is shrunk to the limiting volume of the fluid.

Now consider a volume larger than the limiting volume of the continuous phase that is laden with particles (shown in Figure 2.1). The additional forces arising from the particle surfaces are now accounted for. The volume average of a spatial gradient can be obtained from Leibniz rule and is shown to be (see Appendix A, Crowe et al. 1998, or Slattery 1972 for details)

$$\overline{\frac{\partial B}{\partial x_i}} = \frac{\partial \overline{B}}{\partial x_i} - \frac{1}{V}\int_{S_d} B n_i \, dS \tag{2.7}$$

where the integration is carried out over the particle surfaces, S_d, inside the control volume. In addition, the volume average of the time rate of change of a property is known as (see Appendix A, or Crowe et al. 1998 for additional details)

$$\overline{\frac{\partial B}{\partial t}} = \frac{\partial \overline{B}}{\partial t} + \frac{1}{V}\int_{S_d} B(v_i n_i) dS \tag{2.8}$$

where v_i is the translational velocity of the particle (rotational effects and mass transfer are neglected). The volume averaged Navier-Stokes equations (shown in Eq. (2.3)) are applicable to a continuous phase. If particles are included, the volume over which the terms are integrated becomes the continuous phase volume (i.e. $\int_{V \to V_c}$). Applying Eq. (2.7) and (2.8) to (2.3) results in a new form of the incompressible momentum equations that is applicable to particle laden flows, namely

$$\frac{\partial}{\partial t}\overline{(\rho u_i)}+\frac{\partial}{\partial x_i}\overline{(\rho u_j u_i)}=-\frac{\partial \overline{P}}{\partial x_i}+\frac{\partial}{\partial x_j}\overline{\left[\mu\frac{\partial u_i}{\partial x_j}\right]}+\overline{\rho g_i}+\frac{1}{V}\int_{S_d}Pn_i\,dS-\frac{1}{V}\int_{S_d}\mu\frac{\partial u_i}{\partial x_j}n_j\,dS$$
$$+\frac{1}{V}\int_{S_d}\rho u_j u_i n_j\,dS-\frac{1}{V}\int_{S_d}\rho u_i\left(v_j n_j\right)dS \qquad (2.9)$$

The above equation accounts for all the forces due to particles within the continuous phase. At the particle surface, it is assumed that the 'no slip' condition applies, then the velocity of the continuous phase at any point on the particle surface is the velocity of the particle at that point; thus Eq. (2.9) results in

$$\frac{\partial}{\partial t}\overline{(\rho u_i)}+\frac{\partial}{\partial x_i}\overline{(\rho u_j u_i)}=-\frac{\partial \overline{P}}{\partial x_i}+\frac{\partial}{\partial x_j}\overline{\left[\mu\frac{\partial u_i}{\partial x_j}\right]}+\overline{\rho g_i}+\frac{1}{V}\int_{S_d}Pn_i\,dS-\frac{1}{V}\int_{S_d}\tau_{ij}n_j\,dS \qquad (2.10)$$

where an additional pressure and shear term due to the particle surfaces arises. The remaining terms are those associated with single phase flow; in fact Eq. (2.10) reduces to Eq. (2.6) when no particles are present. Evaluating the surface integrals, Eq. (2.10) becomes of the form

$$\frac{\partial}{\partial t}\alpha_c\langle\rho u_i\rangle+\frac{\partial}{\partial x_i}\alpha_c\langle\rho u_j u_i\rangle=-\alpha_c\frac{\partial\langle P\rangle}{\partial x_i}+\alpha_c\mu\frac{\partial^2\langle u_i\rangle}{\partial x_j^2}+\alpha_c\langle\rho g_i\rangle-\frac{3\pi\mu_c}{V}\sum_n\left[f\,D(u_i-v_i)\right]_n \qquad (2.11)$$

where the pressure and shear terms integrated over all the particle surfaces within the control volume yield the sum of the hydrodynamic drag force of each particle, and the pressure and shear contribution of the particles sum with the continuous phase pressure and shear terms to form the void fraction (see Crowe et al. 1998 for additional details).

At this point, some researchers have used Reynolds averaging procedures to obtain the turbulent kinetic energy and dissipation equations. However, the average velocities in the volume averaged equations do not represent the local (point wise) instantaneous velocity of a given flow and thereby are not amenable to the Reynolds averaging procedures used in single phase flows. In other words, the temporal

fluctuations of the averaged velocities do not reflect the flow turbulence. Aside from temporal averaging, another way of defining turbulence is by the velocity deviation from the volume averaged velocity at a point in time (Crowe and Gillandt 1998), such as

$$u_i = \langle u_i \rangle + \delta u_i \tag{2.12}$$

where u_i is the instantaneous velocity or the velocity at an instance in time and a 'point' in space, $<u_i>$ is the volume averaged velocity and δu_i is the velocity deviation as illustrated in Figure 2.2. At this point, it is worthwhile to discuss this hypothesis, since it has been presumed that volume averaging processes average out important turbulent scales within the flow (Eaton, 2006). Hinze (1975) defines turbulence flow as, "…*an irregular condition of flow in which the various quantities show a random variation with time and space coordinates, so that statistically distinct average values can be discerned*." To explore this concept more, consider a volume averaged property, such as velocity. In order for statistically distinct average values to be discerned, N number of particles must be present, and for sake of simplicity tracer particles are considered. If the volume fraction of the particles is low, then this would imply that a large volume would be needed in order to obtain an average (since a volume average is obtained at an instance in time). However, the averaging volume must be large enough to maintain a stationary average yet small compared to system dimensions to enable the use of differential operators. So consider shrinking the large volume with N tracer particles (at an instance in time) down to a smaller volume associated with a diameter that is on the order of the tracer particles within the continuous phase. In this scenario, N number of particles is still needed to obtain a statistical average, so time is allowed to pass until N number of particles is obtained. This scenario is representative of the non-intrusive laser Doppler

velocimetry (LDV) measurement system, where the volume average is analogous to the time average and the volume deviation is analogous to the fluctuations. This concept is basically viewed as taking a long thin strip of flow frozen in time (that would provide statistically distinct volume average and deviation properties) and passing it through a measurement window at an arbitrary speed (e.g. the speed of the flow) and is similar to Taylor's hypothesis or the frozen turbulence theory. In this simple scenario, the time average and the volume average cannot change if more samples are taken; thus there is no need to "temporal average" when by shrinking the volume of a volume averaged process, a time average is inevitable.

Substituting Eq. (2.12) into (2.11) reveals a volume deviation stress (analogous to the Reynolds stress found by Reynolds averaging procedures). Assuming that the material properties of the continuous phase are constant over the volume of interest, Eq. (2.11) becomes

$$\frac{\partial}{\partial t}\alpha_c\langle u_i\rangle+\frac{\partial}{\partial x_i}\alpha_c\langle u_i u_j\rangle=-\frac{\alpha_c}{\rho}\frac{\partial\langle P\rangle}{\partial x_i}-\frac{\partial}{\partial x_i}\alpha_c\langle\delta u_i\delta u_j\rangle+\alpha_c g_i+\alpha_c\nu\frac{\partial^2\langle u_i\rangle}{\partial x_j^2}$$
$$-\frac{3\pi\mu_c}{\rho V}\sum_n\left[f\,D\left(\langle u_i\rangle-\langle v_i\rangle\right)\right]_n \tag{2.13}$$

where α_c is the volume fraction of the continuous phase, ρ is the density of the continuous phase, ν is the kinematic viscosity, V is the mixture volume, f is the drag factor, D is the particle diameter and n represents the particle number. The above equation describes the momentum of the continuous phase in particle laden turbulent flows, but it requires a closure model to evaluate the volume deviation stress.

To close the equation set, the turbulent-viscosity hypothesis (Pope 2000) is assumed to apply. The volume deviation stress is then modeled as

$$\left\langle \delta u_i \delta u_j \right\rangle = \frac{2}{3}\delta_{ij}k - \nu_T\left(\frac{\partial\langle u_i\rangle}{\partial x_j} + \frac{\partial\langle u_j\rangle}{\partial x_i}\right) \tag{2.14}$$

where ν_T is the turbulence viscosity defined as

$$\nu_T = C_\mu \frac{k^2}{\varepsilon} \tag{2.15}$$

where C_μ is a constant (0.09) and k is the volume averaged turbulent kinetic energy (TKE) defined as

$$k = \frac{1}{V_c}\int_{V_c}\frac{\delta u_i \delta u_i}{2}dV = \left\langle \frac{\delta u_i \delta u_i}{2} \right\rangle \tag{2.16}$$

and ε is the volume averaged dissipation defined as

$$\varepsilon = \frac{1}{V_c}\int_{V_c}\nu\frac{\partial \delta u_i}{\partial x_j}\frac{\partial \delta u_i}{\partial x_j}dV = \nu\left\langle \frac{\partial \delta u_i}{\partial x_j}\frac{\partial \delta u_i}{\partial x_j} \right\rangle \tag{2.17}$$

Thus a transport equation for the volume averaged TKE and dissipation is needed.

A volume averaged TKE transport equation was derived by Crowe and Gillandt (1998). The transport equation for TKE was found to be

$$\begin{aligned}\alpha_c\frac{Dk}{Dt} = &\overbrace{-\alpha_c\left\langle \delta u_i \delta u_j \right\rangle\frac{\partial\langle u_i\rangle}{\partial x_j}}^{\text{Production}} \overbrace{-\frac{\partial}{\partial x_j}\left[\alpha_c\left\langle \delta u_j k \right\rangle\right]}^{\text{Transport}} \overbrace{-\frac{1}{\rho_c}\frac{\partial}{\partial x_i}\left(\alpha_c\left\langle \delta P \delta u_i \right\rangle\right)}^{\text{Pressure Strain}} \\ &\underbrace{-\frac{\beta_V}{\rho_c}\left[\left\langle \delta u_i \delta v_i \right\rangle - \left\langle \delta v_i \delta v_i \right\rangle\right]}_{\text{Redistribution}} \underbrace{+\frac{\beta_V}{\rho_c}\left[\langle u_i\rangle - \langle v_i\rangle\right]^2}_{\text{Generation}} \underbrace{+\alpha_c\left\langle \frac{\partial}{\partial x_j}\left(\nu\frac{\partial k}{\partial x_j}\right)\right\rangle}_{\text{Diffusion}} \underbrace{-\alpha_c\varepsilon}_{\text{Dissipation}}\end{aligned} \tag{2.18}$$

where β_V is the hydrodynamic drag coefficient, described as

$$\beta_V = \frac{\alpha_d \rho_d f}{\tau_p} \tag{2.19}$$

and α_d is the volume fraction of the dispersed phase, ρ_d is the material density of the dispersed phase particles, and τ_p is the particle response time. The above equation describes the turbulent kinetic energy within the carrier phase of a particle-laden turbulent flow. Using the same procedure as single phase flow, the pressure strain and transport terms are modeled as a gradient diffusion and a model of the TKE equation is proposed of the form

$$\alpha_c \frac{Dk}{Dt} = -\alpha_c \left\langle \delta u_i \delta u_j \right\rangle \frac{\partial \langle u_i \rangle}{\partial x_j} - \frac{\beta_V}{\rho_c}\left[\left\langle \delta u_i \delta v_i \right\rangle - \left\langle \delta v_i \delta v_i \right\rangle\right] + \frac{\beta_V}{\rho_c}\left[\langle u_i \rangle - \langle v_i \rangle\right]^2 + \frac{\partial}{\partial x_j}\left(\alpha_c\left(\nu + \frac{\nu_T}{\sigma_k}\right)\frac{\partial k}{\partial x_j}\right) - \alpha_c \varepsilon \tag{2.20}$$

The above equation describes the TKE within the carrier phase of a particle-laden turbulent flow. It is noted that an additional generation term due to the presence of particles is presented along with a redistribution term. These terms are not *ad hoc* but rather appear fundamentally through volume averaging.

At this point, it should be noted that the turbulence length scales associated with multi-phase flow can be reflected through the volume deviation term. The well known Kolmogorov and Taylor length scales are defined by the time averaged dissipation. But this does not deny the fact that turbulent scales associated with volume averaging (i.e. volume deviation properties) are still present within the flow. For example, the Kolmogorov length scale based on volume averaged dissipation would be defined as

$$\eta = \left(\frac{\nu^3}{\varepsilon}\right)^{1/4} \tag{2.21}$$

where the volume averaged dissipation is defined by Eq. (2.17). Likewise, other turbulent scales, such as time and velocity, can be defined in terms of volume averaged properties.

The advantage of using volume averaging is that the effects of the surfaces are easily distinguished from the effects of the fluid. Another very important advantage in applying the volume average concept to dispersed phase flows is that moving meshes are not needed as would be in a point wise flow analysis (such as the RANS equations). In the presence of millions of particles, this approach would become computationally expensive. An interim solution to this complex problem is volume averaging.

The difficulty with the application of volume averaging to multi-phase turbulence equations is in the comparison to experiments. Typical experiments are set up for point wise measurements, however with newly developed instrumentation such as particle image velocimetry (PIV) there is potential to perform volume averaged measurements.

The volume averaged momentum and turbulent kinetic energy equations are shown in this chapter. However, to close the equation set, a dissipation equation is needed.

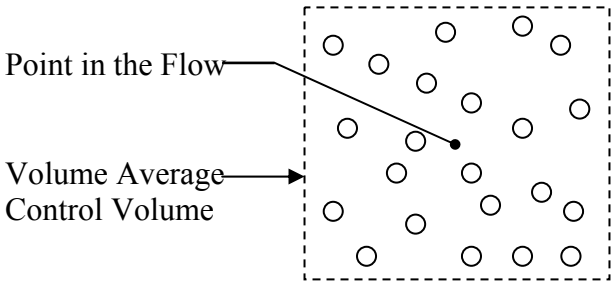

Figure 2.1: A volume containing N number of particles such that a statistical average can be discerned.

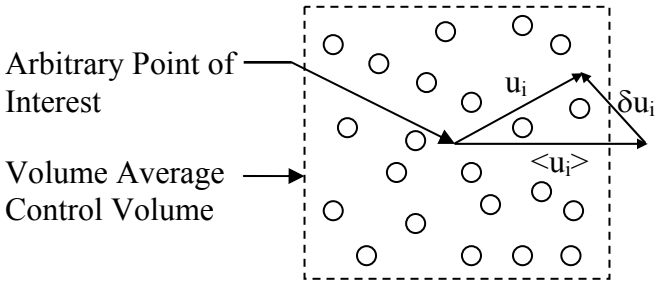

Figure 2.2: An illustration of the volume deviation velocity used to define turbulence in a volume averaged setting. The instantaneous velocity, at any point in the flow, is the sum of the volume average and the volume deviation velocity at an instance in time.

CHAPTER THREE

THE DISSIPATION TRANSPORT EQUATION

The development of the equation for dissipation is not as straight forward as the turbulent kinetic energy equation. Before the volume averaged dissipation transport equation is described, a review of the time averaged dissipation transport equation is presented.

The time averaged dissipation is defined as

$$\varepsilon \equiv \nu \overline{\left(\frac{\partial u'_i}{\partial x_j} \frac{\partial u'_i}{\partial x_j} \right)} \tag{3.1}$$

A rate equation for dissipation is developed by taking the gradient of the momentum equation, multiplying it by twice the kinematic viscosity and by the gradient of the fluctuating velocity and then time averaging the entire equation, which is mathematically represented by

$$\overline{\left(\frac{\partial}{\partial x_j} [NS_i] \right) * 2\nu \left(\frac{\partial u_i'}{\partial x_j} \right)}$$

The instantaneous velocity, pressure, and shear stress are decomposed into the sum of a time averaged and a fluctuating property to obtain

$$\frac{D\varepsilon}{Dt} = -2\nu\frac{\partial\overline{\overline{u_k}}}{\partial x_j}\left[\overline{\overline{\frac{\partial u'_i}{\partial x_j}\frac{\partial u'_i}{\partial x_k}}}\right] - \varepsilon_{ik}\frac{\partial\overline{\overline{u_i}}}{\partial x_k} - 2\nu\left[\overline{\overline{u'_k\frac{\partial u'_i}{\partial x_j}}}\right]\frac{\partial^2\overline{\overline{u_i}}}{\partial x_j\partial x_k} - 2\nu\left[\overline{\overline{\frac{\partial u'_i}{\partial x_j}\frac{\partial \delta u'_k}{\partial x_j}\frac{\partial u'_i}{\partial x_k}}}\right]$$
$$-\nu\frac{\partial}{\partial x_k}\left[\overline{\overline{u'_k\frac{\partial u'_i}{\partial x_j}\frac{\partial u'_i}{\partial x_j}}}\right] - 2\frac{\nu}{\rho}\frac{\partial}{\partial x_i}\left[\overline{\overline{\frac{\partial u'_i}{\partial x_j}\frac{\partial P'}{\partial x_j}}}\right] + \nu\frac{\partial^2\varepsilon}{\partial x_k^2} - 2\nu^2\left(\overline{\overline{\frac{\partial^2 u'_i}{\partial x_j\partial x_k}}}\right)^2 \tag{3.2}$$

where ε_{ik} is the dissipation tensor. A discussion of each of the terms is presented in Bernard and Wallace (2002). They make arguments for grouping terms together and modeling of other terms to yield the equation for dissipation, namely

$$\frac{D\varepsilon}{Dt} = C_{\varepsilon 1}\frac{P_\varepsilon\varepsilon}{k} - C_{\varepsilon 2}\frac{\varepsilon^2}{k} + \frac{\partial}{\partial x_i}\left[\left(\nu + \frac{\nu_T}{\sigma_\varepsilon}\right)\frac{\partial\varepsilon}{\partial x_i}\right] \tag{3.3}$$

where P_ε is the production of dissipation due to the mean velocity gradients, ν_T is the turbulent viscosity and $C_{\varepsilon 1}$, $C_{\varepsilon 2}$ are empirical constants and σ_ε is the turbulent Schmidt number for diffusion of dissipation. The dissipation is affected by diffusion of dissipation, production of dissipation and dissipation of dissipation.

3.1 Derivation by Volume Averaging

To close the volume averaged turbulence equation set, an equation for the transport of dissipation is needed. The following derivation is analogous to the derivation of the time average dissipation equation, provided by Bernard and Wallace (2002). The definition of volume average dissipation introduced by Crowe and Gillant (1998) is

$$\varepsilon = \nu\left\langle\frac{\partial\delta u_i}{\partial x_j}\frac{\partial\delta u_i}{\partial x_j}\right\rangle \tag{3.4}$$

To begin, a spatial gradient of the Navier-Stokes equation is taken. This is multiplied by the volume deviation velocity gradient ($\partial\delta u_i/\partial x_j$) and twice the kinematic viscosity. Finally the result is volume averaged, which is represented mathematically by

$$\overline{\left(\frac{\partial}{\partial x_j}\left[NS_i\right]\right) * 2\nu\left(\frac{\partial \delta u_i}{\partial x_j}\right)}$$

which can also be expressed as

$$\overline{2\nu\frac{\partial \delta u_i}{\partial x_j}\frac{\partial}{\partial x_j}\left(\rho\frac{\partial u_i}{\partial t}\right)} + \overline{2\nu\frac{\partial \delta u_i}{\partial x_j}\frac{\partial}{\partial x_j}\left(\rho u_k\frac{\partial u_i}{\partial x_k}\right)} = \overline{-2\nu\frac{\partial \delta u_i}{\partial x_j}\frac{\partial}{\partial x_j}\frac{\partial P}{\partial x_i}} + \overline{2\nu\frac{\partial \delta u_i}{\partial x_j}\frac{\partial^2 \tau_{ik}}{\partial x_j \partial x_k}} \tag{3.5}$$

Decomposing the instantaneous terms in Eq. (3.5) into volume average and deviation terms, Eq. (2.12), and assuming the flow is incompressible, the above equation can be rewritten as

$$\begin{aligned}
&\overline{2\nu\frac{\partial \delta u_i}{\partial x_j}\frac{\partial}{\partial x_j}\left(\frac{\partial \langle u_i\rangle}{\partial t}\right)} + \overline{2\nu\frac{\partial \delta u_i}{\partial x_j}\frac{\partial}{\partial x_j}\left(\frac{\partial \delta u_i}{\partial t}\right)} + \overline{2\nu\frac{\partial \delta u_i}{\partial x_j}\frac{\partial \langle u_k\rangle}{\partial x_j}\frac{\partial \langle u_i\rangle}{\partial x_k}} + \overline{2\nu\langle u_k\rangle\frac{\partial \delta u_i}{\partial x_j}\frac{\partial^2 \langle u_i\rangle}{\partial x_j \partial x_k}} + \\
&\overline{2\nu\frac{\partial \delta u_i}{\partial x_j}\frac{\partial \langle u_k\rangle}{\partial x_j}\frac{\partial \delta u_i}{\partial x_k}} + \overline{2\nu\langle u_k\rangle\frac{\partial \delta u_i}{\partial x_j}\frac{\partial^2 \delta u_i}{\partial x_j \partial x_k}} + \overline{2\nu\frac{\partial \delta u_i}{\partial x_j}\frac{\partial \delta u_k}{\partial x_j}\frac{\partial \langle u_i\rangle}{\partial x_k}} + \overline{2\nu\delta u_k\frac{\partial \delta u_i}{\partial x_j}\frac{\partial^2 \langle u_i\rangle}{\partial x_j \partial x_k}} + \\
&\overline{2\nu\frac{\partial \delta u_i}{\partial x_j}\frac{\partial \delta u_k}{\partial x_j}\frac{\partial \delta u_i}{\partial x_k}} + \overline{2\nu\delta u_k\frac{\partial \delta u_i}{\partial x_j}\frac{\partial^2 \delta u_i}{\partial x_j \partial x_k}} = \overline{-2\frac{\nu}{\rho}\frac{\partial \delta u_i}{\partial x_j}\frac{\partial}{\partial x_j}\frac{\partial \langle P\rangle + \delta P}{\partial x_i}} + \\
&\overline{2\frac{\nu}{\rho}\frac{\partial \delta u_i}{\partial x_j}\frac{\partial^2}{\partial x_j \partial x_k}\left(\langle \tau_{ik}\rangle + \delta\tau_{ik}\right)}
\end{aligned} \tag{3.6}$$

The volume average of each term in Eq. (3.6) must be taken to obtain the effects of particle surfaces by utilizing Eqs. (2.7) and (2.8). Applying volume averaging techniques to each term in Eq. (3.6) is the purpose of the next sections.

3.1.1 Volume average of the first term of Eq. (3.6):

The definition of the volume average is applied to the first term of Eq. (3.6)

$$\overline{2\nu\frac{\partial \delta u_i}{\partial x_j}\frac{\partial}{\partial x_j}\left(\frac{\partial \langle u_i\rangle}{\partial t}\right)} = \frac{1}{V}\int_{V_c} 2\nu\frac{\partial \delta u_i}{\partial x_j}\frac{\partial}{\partial x_j}\left(\frac{\partial \langle u_i\rangle}{\partial t}\right)dV \tag{3.7}$$

Assuming that the kinematic viscosity is constant over the control volume, then the above equation can be simplified to

$$\overline{2\nu\frac{\partial\delta u_i}{\partial x_j}\frac{\partial}{\partial x_j}\left(\frac{\partial\langle u_i\rangle}{\partial t}\right)}=\frac{2\nu}{V}\frac{\partial}{\partial x_j}\left(\frac{\partial\langle u_i\rangle}{\partial t}\right)\int_{V_c}\frac{\partial\delta u_i}{\partial x_j}dV \tag{3.8}$$

Applying the identity shown in Eq. (2.7), the above equation can be represented as

$$\overline{2\nu\frac{\partial\delta u_i}{\partial x_j}\frac{\partial}{\partial x_j}\left(\frac{\partial\langle u_i\rangle}{\partial t}\right)}=\frac{2\nu}{V}\frac{\partial}{\partial x_j}\left(\frac{\partial\langle u_i\rangle}{\partial t}\right)\left[\frac{\partial}{\partial x_j}\int_{V_c}\delta u_i dV-\int_{S_d}\delta u_i n_j dS\right] \tag{3.9}$$

By definition the volume average of the volume deviation property is zero

$$\int_{V_c}\delta u_i dV=0 \tag{3.10}$$

Substituting in the definition of the velocity deviation, Eq. (2.12), into the surface integral shows

$$\int_{S_d}\delta u_i n_j dS=\int_{S_d}u_i n_j dS-\int_{S_d}\langle u_i\rangle n_j dS \tag{3.11}$$

The instantaneous velocity of the fluid at the surface of the particle is equal to the velocity of the particle and the volume averaged velocity is constant within the control volume (i.e. over all the surfaces of the particles within the volume of interest). Neglecting particle rotation and mass transfer, the above equation is reduced to

$$\int_{S_d}\delta u_i n_j dS=v_i\int_{S_d}n_j dS-\langle u_i\rangle\int_{S_d}n_j dS=0 \tag{3.12}$$

The integral of the unit vector (outward normal) over the surface of the particle is zero. Substituting Eq. (3.12) and (3.10) into Eq. (3.9), it can be concluded that the volume average of the first term is zero

$$\overline{2\nu\frac{\partial\delta u_i}{\partial x_j}\frac{\partial}{\partial x_j}\left(\frac{\partial\langle u_i\rangle}{\partial t}\right)}=0 \tag{3.13}$$

3.1.2 Volume average of the second term in Eq. (3.6):

Assuming no mass transfer between the phases ($\dot{r}=0$) and neglecting particle rotation, then the volume average of the 2nd term in Eq. (3.6) is shown to be

$$\begin{aligned}\overline{2\nu\frac{\partial\delta u_i}{\partial x_j}\frac{\partial}{\partial x_j}\left(\frac{\partial\delta u_i}{\partial t}\right)} &= \nu\overline{\frac{\partial}{\partial t}\left[\frac{\partial\delta u_i}{\partial x_j}\frac{\partial\delta u_i}{\partial x_j}\right]} = \nu\frac{\partial}{\partial t}\left[\overline{\frac{\partial\delta u_i}{\partial x_j}\frac{\partial\delta u_i}{\partial x_j}}\right]+\frac{\nu}{V}\int_{S_d}\frac{\partial\delta u_i}{\partial x_j}\frac{\partial\delta u_i}{\partial x_j}(v_k n_k)dS \\ &= \nu\frac{\partial}{\partial t}\left[\alpha_c\left\langle\frac{\partial\delta u_i}{\partial x_j}\frac{\partial\delta u_i}{\partial x_j}\right\rangle\right]+\frac{\nu}{V}\int_{S_d}\frac{\partial\delta u_i}{\partial x_j}\frac{\partial\delta u_i}{\partial x_j}(v_k n_k)dS\end{aligned} \tag{3.14}$$

3.1.3 Volume average of the third term in Eq. (3.6):

The volume average of the 3rd term in Eq. (3.6) is shown to be zero

$$\overline{2\nu\frac{\partial\delta u_i}{\partial x_j}\frac{\partial\langle u_k\rangle}{\partial x_j}\frac{\partial\langle u_i\rangle}{\partial x_k}} = 2\nu\frac{\partial\langle u_k\rangle}{\partial x_j}\frac{\partial\langle u_i\rangle}{\partial x_k}\overline{\frac{\partial\delta u_i}{\partial x_j}} = 0 \tag{3.15}$$

3.1.4 Volume average of the fourth term in Eq. (3.6):

The volume average of the 4th term in Eq. (3.6) is also shown to be zero

$$\overline{2\nu\langle u_k\rangle\frac{\partial\delta u_i}{\partial x_j}\frac{\partial^2\langle u_i\rangle}{\partial x_j\partial x_k}} = 2\nu\langle u_k\rangle\frac{\partial^2\langle u_i\rangle}{\partial x_j\partial x_k}\overline{\frac{\partial\delta u_i}{\partial x_j}} = 0 \tag{3.16}$$

3.1.5 Volume average of the fifth term in Eq. (3.6):

The volume average of the 5th term in Eq. (3.6) is simply

$$\overline{2\nu\frac{\partial\delta u_i}{\partial x_j}\frac{\partial\langle u_k\rangle}{\partial x_j}\frac{\partial\delta u_i}{\partial x_k}} = 2\nu\alpha_c\frac{\partial\langle u_k\rangle}{\partial x_j}\left\langle\frac{\partial\delta u_i}{\partial x_j}\frac{\partial\delta u_i}{\partial x_k}\right\rangle \tag{3.17}$$

3.1.6 Volume average of the sixth term in Eq. (3.6):

The volume average of the 6th term in Eq. (3.6) includes the surface effects of particles

$$\overline{2\nu\langle u_k\rangle\frac{\partial\delta u_i}{\partial x_j}\frac{\partial^2\delta u_i}{\partial x_j\partial x_k}} = \nu\langle u_k\rangle\overline{\frac{\partial}{\partial x_k}\left[\frac{\partial\delta u_i}{\partial x_j}\frac{\partial\delta u_i}{\partial x_j}\right]}$$
$$= \nu\langle u_k\rangle\frac{\partial}{\partial x_k}\left[\alpha_c\left\langle\frac{\partial\delta u_i}{\partial x_j}\frac{\partial\delta u_i}{\partial x_j}\right\rangle\right] - \frac{\nu}{V}\langle u_k\rangle\int_{S_d}\frac{\partial\delta u_i}{\partial x_j}\frac{\partial\delta u_i}{\partial x_j}n_k dS \tag{3.18}$$

3.1.7 Volume average of the seventh term in Eq. (3.6):

The volume average of the 7th term in Eq. (3.6) becomes

$$\overline{2\nu\frac{\partial\delta u_i}{\partial x_j}\frac{\partial\delta u_k}{\partial x_j}\frac{\partial\langle u_i\rangle}{\partial x_k}} = 2\nu\alpha_c\frac{\partial\langle u_i\rangle}{\partial x_k}\left\langle\frac{\partial\delta u_i}{\partial x_j}\frac{\partial\delta u_k}{\partial x_j}\right\rangle \tag{3.19}$$

3.1.8 Volume average of the eighth term in Eq. (3.6):

The volume average of the 8th term in Eq. (3.6) is found to be

$$\overline{2\nu\delta u_k\frac{\partial\delta u_i}{\partial x_j}\frac{\partial^2\langle u_i\rangle}{\partial x_j\partial x_k}} = 2\nu\alpha_c\frac{\partial^2\langle u_i\rangle}{\partial x_j\partial x_k}\left\langle\delta u_k\frac{\partial\delta u_i}{\partial x_j}\right\rangle \tag{3.20}$$

3.1.9 Volume average of the ninth term in Eq. (3.6):

The volume average of the 9th term in Eq. (3.6) is simply

$$\overline{2\nu\frac{\partial\delta u_i}{\partial x_j}\frac{\partial\delta u_k}{\partial x_j}\frac{\partial\delta u_i}{\partial x_k}} = 2\nu\alpha_c\left\langle\frac{\partial\delta u_i}{\partial x_j}\frac{\partial\delta u_k}{\partial x_j}\frac{\partial\delta u_i}{\partial x_k}\right\rangle \tag{3.21}$$

3.1.10 Volume average of the tenth term in Eq. (3.6):

The volume average of the 10th term in Eq. (3.6) includes the effects of particle surfaces and assumes the form

$$\overline{2\nu\delta u_k\frac{\partial\delta u_i}{\partial x_j}\frac{\partial^2\delta u_i}{\partial x_j\partial x_k}} = \overline{\nu\delta u_k\frac{\partial}{\partial x_k}\left[\frac{\partial\delta u_i}{\partial x_j}\frac{\partial\delta u_i}{\partial x_j}\right]}$$
$$= \overline{\nu u_k\frac{\partial}{\partial x_k}\left[\frac{\partial\delta u_i}{\partial x_j}\frac{\partial\delta u_i}{\partial x_j}\right]} - \overline{\nu\langle u_k\rangle\frac{\partial}{\partial x_k}\left[\frac{\partial\delta u_i}{\partial x_j}\frac{\partial\delta u_i}{\partial x_j}\right]} \tag{3.22}$$

The continuity equation for an incompressible flow is

$$\frac{\partial u_k}{\partial x_k} = 0 \tag{3.23}$$

where u_k is the instantaneous velocity, defined as the velocity at an instance in time and a 'point' in space. Substituting Eq. (3.23) into Eq. (3.22) shows

$$\begin{aligned}2\nu\overline{\delta u_k\frac{\partial\delta u_i}{\partial x_j}\frac{\partial^2\delta u_i}{\partial x_j\partial x_k}} &= \nu\overline{\frac{\partial}{\partial x_k}\left[u_k\frac{\partial\delta u_i}{\partial x_j}\frac{\partial\delta u_i}{\partial x_j}\right]}-\nu\langle u_k\rangle\overline{\frac{\partial}{\partial x_k}\left[\frac{\partial\delta u_i}{\partial x_j}\frac{\partial\delta u_i}{\partial x_j}\right]}\\ &= \nu\frac{\partial}{\partial x_k}\left[\alpha_c\left\langle u_k\frac{\partial\delta u_i}{\partial x_j}\frac{\partial\delta u_i}{\partial x_j}\right\rangle\right]-\frac{\nu}{V}\int_{S_d}u_k\frac{\partial\delta u_i}{\partial x_j}\frac{\partial\delta u_i}{\partial x_j}n_k dS\\ &\quad-\nu\langle u_k\rangle\frac{\partial}{\partial x_k}\left[\alpha_c\left\langle\frac{\partial\delta u_i}{\partial x_j}\frac{\partial\delta u_i}{\partial x_j}\right\rangle\right]+\frac{\nu}{V}\langle u_k\rangle\int_{S_d}\frac{\partial\delta u_i}{\partial x_j}\frac{\partial\delta u_i}{\partial x_j}n_k dS\end{aligned} \tag{3.24}$$

At the surface of the dispersed phase, the instantaneous continuous phase velocity is equal to the dispersed phase velocity, and if the instantaneous velocity is decomposed, Eq. (2.12), the above equation is reduced to

$$\begin{aligned}2\nu\overline{\delta u_k\frac{\partial\delta u_i}{\partial x_j}\frac{\partial^2\delta u_i}{\partial x_j\partial x_k}} &= \nu\frac{\partial}{\partial x_k}\left[\alpha_c\langle u_k\rangle\left\langle\frac{\partial\delta u_i}{\partial x_j}\frac{\partial\delta u_i}{\partial x_j}\right\rangle\right]+\nu\frac{\partial}{\partial x_k}\left[\alpha_c\left\langle\delta u_k\frac{\partial\delta u_i}{\partial x_j}\frac{\partial\delta u_i}{\partial x_j}\right\rangle\right]\\ &\quad-\frac{\nu}{V}\int_{S_d}v_k\frac{\partial\delta u_i}{\partial x_j}\frac{\partial\delta u_i}{\partial x_j}n_k dS-\nu\langle u_k\rangle\frac{\partial}{\partial x_k}\left[\alpha_c\left\langle\frac{\partial\delta u_i}{\partial x_j}\frac{\partial\delta u_i}{\partial x_j}\right\rangle\right]\\ &\quad+\frac{\nu}{V}\langle u_k\rangle\int_{S_d}\frac{\partial\delta u_i}{\partial x_j}\frac{\partial\delta u_i}{\partial x_j}n_k dS\end{aligned} \tag{3.25}$$

3.1.11 Volume average of the eleventh (pressure) term in Eq. (3.6):

The eleventh term in Eq. (3.6), or the pressure term, is split into two terms

$$-2\overline{\frac{\nu}{\rho}\frac{\partial\delta u_i}{\partial x_j}\frac{\partial}{\partial x_j}\frac{\partial\langle P\rangle+\delta P}{\partial x_i}}=-\frac{2\nu}{V\rho}\frac{\partial^2\langle P\rangle}{\partial x_j\partial x_i}\int_{V_c}\frac{\partial\delta u_i}{\partial x_j}dV-\frac{2\nu}{V\rho}\int_{V_c}\frac{\partial\delta u_i}{\partial x_j}\frac{\partial^2\delta P}{\partial x_j\partial x_i}dV \tag{3.26}$$

Substituting in the deviation velocity, Eq. (2.12), and neglecting particle rotation shows that the first term on the RHS of the above equation is zero, thus Eq. (3.26) is reduced to

$$-2\overline{\frac{\nu}{\rho}\frac{\partial\delta u_i}{\partial x_j}\frac{\partial}{\partial x_j}\frac{\partial\langle P\rangle+\delta P}{\partial x_i}}=-\frac{2\nu}{V\rho}\int_{V_c}\frac{\partial u_i}{\partial x_j}\frac{\partial^2\delta P}{\partial x_j\partial x_i}dV+\frac{2\nu}{V\rho}\int_{V_c}\frac{\partial\langle u_i\rangle}{\partial x_j}\frac{\partial^2\delta P}{\partial x_j\partial x_i}dV \tag{3.27}$$

Applying the product rule, the first term on the RHS of Eq. (3.27) can be represented as

$$-\frac{2\nu}{V\rho}\int_{V_c}\frac{\partial u_i}{\partial x_j}\frac{\partial^2\delta P}{\partial x_j\partial x_i}dV=-\frac{2\nu}{V\rho}\int_{V_c}\frac{\partial}{\partial x_i}\left[\frac{\partial u_i}{\partial x_j}\frac{\partial\delta P}{\partial x_j}\right]dV+\frac{2\nu}{V\rho}\int_{V_c}\frac{\partial\delta P}{\partial x_j}\frac{\partial^2 u_i}{\partial x_j\partial x_i}dV \tag{3.28}$$

Applying the continuity equation (Eq. 3.23) for incompressible flow to the last term in Eq. (3.28) results in

$$-\frac{2\nu}{V\rho}\int_{V_c}\frac{\partial}{\partial x_i}\left[\frac{\partial u_i}{\partial x_j}\frac{\partial\delta P}{\partial x_j}\right]dV=-\frac{2\nu}{V\rho}\int_{V_c}\frac{\partial u_i}{\partial x_j}\frac{\partial^2\delta P}{\partial x_j\partial x_i}dV \tag{3.29}$$

Substituting Eq. (3.29) into Eq. (3.27) leads to

$$-\overline{2\frac{\nu}{\rho}\frac{\partial\delta u_i}{\partial x_j}\frac{\partial}{\partial x_j}\frac{\partial\langle P\rangle+\delta P}{\partial x_i}}=-\frac{2\nu}{V\rho}\int_{V_c}\frac{\partial}{\partial x_i}\left[\frac{\partial u_i}{\partial x_j}\frac{\partial\delta P}{\partial x_j}\right]dV+\frac{2\nu}{V\rho}\int_{V_c}\frac{\partial\langle u_i\rangle}{\partial x_j}\frac{\partial^2\delta P}{\partial x_j\partial x_i}dV \tag{3.30}$$

Converting the instantaneous velocity into the sum of the volume average and deviation shows

$$\begin{aligned}-\overline{2\frac{\nu}{\rho}\frac{\partial\delta u_i}{\partial x_j}\frac{\partial}{\partial x_j}\frac{\partial\langle P\rangle+\delta P}{\partial x_i}}=&\\-\frac{2\nu}{V\rho}\int_{V_c}\frac{\partial}{\partial x_i}\left[\frac{\partial\langle u_i\rangle}{\partial x_j}\frac{\partial\delta P}{\partial x_j}\right]dV-\frac{2\nu}{V\rho}\int_{V_c}\frac{\partial}{\partial x_i}\left[\frac{\partial\delta u_i}{\partial x_j}\frac{\partial\delta P}{\partial x_j}\right]dV+\frac{2\nu}{V\rho}\int_{V_c}\frac{\partial\langle u_i\rangle}{\partial x_j}\frac{\partial^2\delta P}{\partial x_j\partial x_i}dV&\end{aligned} \tag{3.31}$$

The above equation then reduces to

$$-\overline{2\frac{\nu}{\rho}\frac{\partial\delta u_i}{\partial x_j}\frac{\partial}{\partial x_j}\frac{\partial\langle P\rangle+\delta P}{\partial x_i}}=-\frac{2\nu}{V\rho}\int_{V_c}\frac{\partial^2\langle u_i\rangle}{\partial x_i\partial x_j}\frac{\partial\delta P}{\partial x_j}dV-\frac{2\nu}{V\rho}\int_{V_c}\frac{\partial}{\partial x_i}\left[\frac{\partial\delta u_i}{\partial x_j}\frac{\partial\delta P}{\partial x_j}\right]dV \tag{3.32}$$

The last term on the RHS of Eq. (3.32) can be represented as

$$-\frac{2\nu}{V\rho}\int_{V_c}\frac{\partial}{\partial x_i}\left[\frac{\partial\delta u_i}{\partial x_j}\frac{\partial\delta P}{\partial x_j}\right]dV=-\frac{2\nu}{V\rho}\frac{\partial}{\partial x_i}\int_{V_c}\left[\frac{\partial\delta u_i}{\partial x_j}\frac{\partial\delta P}{\partial x_j}\right]dV+\frac{2\nu}{V\rho}\int_{S_d}\frac{\partial\delta u_i}{\partial x_j}\frac{\partial\delta P}{\partial x_j}n_i dS \tag{3.33}$$

Substituting Eq. (3.33) into Eq. (3.32) and converting to a phase average results in

$$-2\overline{\frac{\nu}{\rho}\frac{\partial \delta u_i}{\partial x_j}\frac{\partial}{\partial x_j}\frac{\partial \langle P\rangle + \delta P}{\partial x_i}} = -\alpha_c \frac{2\nu}{\rho}\frac{\partial^2 \langle u_i\rangle}{\partial x_i \partial x_j}\left\langle \frac{\partial \delta P}{\partial x_j}\right\rangle - \alpha_c \frac{2\nu}{\rho}\frac{\partial}{\partial x_i}\left\langle \frac{\partial \delta u_i}{\partial x_j}\frac{\partial \delta P}{\partial x_j}\right\rangle + \frac{2\nu}{V\rho}\int_{S_d}\frac{\partial \delta u_i}{\partial x_j}\frac{\partial \delta P}{\partial x_j}n_i dS \tag{3.34}$$

The first term on the right hand side remains because the volume average continuity equation is different than the time averaged continuity equation. The volume averaged continuity equation is

$$\frac{\partial \langle u_i\rangle}{\partial x_i} = -\frac{1}{\alpha_c}\frac{\partial \alpha_c}{\partial t} - \frac{\langle u_i\rangle}{\alpha_c}\frac{\partial \alpha_c}{\partial x_i} = -\frac{1}{\alpha_c}\frac{D\alpha_c}{Dt} \tag{3.35}$$

This equation suggests that the first term on the RHS of Eq. (3.34) could be important in particle laden compressible flow. In order to avoid the complications of determining a transport equation for the void fraction, an order of magnitude analysis is used to simplify the above equation. Taking a spatial gradient of Eq. (2.12) and applying continuity for the instantaneous velocity in incompressible flow yields

$$\frac{\partial \langle u_i\rangle}{\partial x_i} = \frac{\partial \delta u_i}{\partial x_i} \tag{3.36}$$

Substituting Eq. (3.36) into Eq. (3.34) yields a direct comparison of the properties

$$-2\overline{\frac{\nu}{\rho}\frac{\partial \delta u_i}{\partial x_j}\frac{\partial}{\partial x_j}\frac{\partial \langle P\rangle + \delta P}{\partial x_i}} = -\alpha_c \frac{2\nu}{\rho}\frac{\partial^2 \delta u_i}{\partial x_i \partial x_j}\left\langle \frac{\partial \delta P}{\partial x_j}\right\rangle - \alpha_c \frac{2\nu}{\rho}\frac{\partial}{\partial x_i}\left\langle \frac{\partial \delta u_i}{\partial x_j}\frac{\partial \delta P}{\partial x_j}\right\rangle + \frac{2\nu}{V\rho}\int_{S_d}\frac{\partial \delta u_i}{\partial x_j}\frac{\partial \delta P}{\partial x_j}n_i dS \tag{3.37}$$

Approximating the length scale of the spatial derivative of a volume average property as L and the spatial derivative of a volume deviation property as l, where $L >> l$ shows

$$\frac{\partial^2 \delta u_i}{\partial x_i \partial x_j}\left\langle \frac{\partial \delta P}{\partial x_j}\right\rangle \approx \frac{\delta u_i}{L^2}\frac{\delta P}{l} \quad \text{and} \quad \frac{\partial}{\partial x_i}\left\langle \frac{\partial \delta u_i}{\partial x_j}\frac{\partial \delta P}{\partial x_j}\right\rangle \approx \frac{1}{L}\frac{\delta u_i \delta P}{l^2} \tag{3.38}$$

Therefore the first term on the right hand side of Eq. (3.37) can be neglected. Thus the volume average of the pressure term is approximated as

$$-\overline{2\frac{\nu}{\rho}\frac{\partial\delta u_i}{\partial x_j}\frac{\partial}{\partial x_j}\frac{\partial\langle P\rangle+\delta P}{\partial x_i}} \cong -\alpha_c\frac{2\nu}{\rho}\frac{\partial}{\partial x_i}\left\langle\frac{\partial\delta u_i}{\partial x_j}\frac{\partial\delta P}{\partial x_j}\right\rangle+\frac{2\nu}{V\rho}\int_{S_d}\frac{\partial\delta u_i}{\partial x_j}\frac{\partial\delta P}{\partial x_j}n_i dS \tag{3.39}$$

3.1.12 Volume average of the twelfth (shear) term in Eq. (3.6):

The shear term in Eq. (3.6) is simplified for incompressible flow

$$\overline{2\frac{\nu}{\rho}\frac{\partial\delta u_i}{\partial x_j}\frac{\partial^2\tau_{ik}}{\partial x_j\partial x_k}}=\overline{2\nu^2\frac{\partial\delta u_i}{\partial x_j}\frac{\partial}{\partial x_j}\frac{\partial}{\partial x_k}\left(\frac{\partial u_i}{\partial x_k}+\frac{\partial u_k}{\partial x_i}\right)}=\overline{2\nu^2\frac{\partial\delta u_i}{\partial x_j}\frac{\partial}{\partial x_j}\frac{\partial^2 u_i}{\partial x_k^2}} \tag{3.40}$$

Decomposing the instantaneous velocity into volume average and volume deviation components results in

$$\overline{2\nu^2\frac{\partial\delta u_i}{\partial x_j}\frac{\partial}{\partial x_j}\frac{\partial^2 u_i}{\partial x_k^2}}=\overline{2\nu^2\frac{\partial\delta u_i}{\partial x_j}\frac{\partial^2}{\partial x_j\partial x_k}\left(\frac{\partial\langle u_i\rangle}{\partial x_k}\right)}+\overline{2\nu^2\frac{\partial\delta u_i}{\partial x_j}\frac{\partial^2}{\partial x_j\partial x_k}\left(\frac{\partial\delta u_i}{\partial x_k}\right)} \tag{3.41}$$

Applying the volume average to the first term on the right hand side of the above equation

$$\overline{2\nu^2\frac{\partial\delta u_i}{\partial x_j}\frac{\partial^2}{\partial x_j\partial x_k}\left(\frac{\partial\langle u_i\rangle}{\partial x_k}\right)}=\frac{2\nu^2}{V}\frac{\partial^3\langle u_i\rangle}{\partial x_j\partial x_k^2}\int_{V_c}\frac{\partial\delta u_i}{\partial x_j}dV=0 \tag{3.42}$$

Before applying the volume average to the second term on the right hand side of Eq. (3.41), it is advantageous to rearrange this term to be of the form

$$\overline{2\nu^2\frac{\partial\delta u_i}{\partial x_j}\frac{\partial^2}{\partial x_j\partial x_k}\left(\frac{\partial\delta u_i}{\partial x_k}\right)}=\nu^2\overline{\frac{\partial^2}{\partial x_k^2}\left[\frac{\partial\delta u_i}{\partial x_j}\frac{\partial\delta u_i}{\partial x_j}\right]}-\overline{2\nu^2\left(\frac{\partial^2\delta u_i}{\partial x_j\partial x_k}\frac{\partial^2\delta u_i}{\partial x_j\partial x_k}\right)} \tag{3.43}$$

The last term in the above equation is the volume averaged dissipation of dissipation. Converting the last term in Eq. (3.43) to a phase volume average shows

$$\overline{2\nu^2\left(\frac{\partial^2\delta u_i}{\partial x_j\partial x_k}\frac{\partial^2\delta u_i}{\partial x_j\partial x_k}\right)} = 2\alpha_c\nu^2\left\langle\left(\frac{\partial^2\delta u_i}{\partial x_j\partial x_k}\right)^2\right\rangle \tag{3.44}$$

Volume averaging the first term on the RHS of Eq. (3.43) shows

$$\overline{\nu^2\frac{\partial^2}{\partial x_k^2}\left[\frac{\partial\delta u_i}{\partial x_j}\frac{\partial\delta u_i}{\partial x_j}\right]} = \nu^2\frac{\partial}{\partial x_k}\left[\overline{\frac{\partial}{\partial x_k}\left(\frac{\partial\delta u_i}{\partial x_j}\frac{\partial\delta u_i}{\partial x_j}\right)}\right] - \frac{\nu^2}{V}\int_{S_d}\frac{\partial}{\partial x_k}\left(\frac{\partial\delta u_i}{\partial x_j}\frac{\partial\delta u_i}{\partial x_j}\right)n_k dS \tag{3.45}$$

Applying the volume average to the first term in Eq. (3.45) shows

$$\nu^2\frac{\partial}{\partial x_k}\left[\overline{\frac{\partial}{\partial x_k}\left(\frac{\partial\delta u_i}{\partial x_j}\frac{\partial\delta u_i}{\partial x_j}\right)}\right] = \nu^2\frac{\partial^2}{\partial x_k^2}\left[\alpha_c\left\langle\frac{\partial\delta u_i}{\partial x_j}\frac{\partial\delta u_i}{\partial x_j}\right\rangle\right] - \frac{\nu^2}{V}\frac{\partial}{\partial x_k}\int_{S_d}\frac{\partial\delta u_i}{\partial x_j}\frac{\partial\delta u_i}{\partial x_j}n_k dS \tag{3.46}$$

Substituting Eq. (3.46) into Eq. (3.45) and the resultant equation with Eq. (3.44) into Eq. (3.43), and then substituting the resultant equation along with Eq. (3.42) into Eq. (3.41), and the resultant equation into Eq. (3.40) yields the volume average of the shear term as

$$\begin{aligned}\overline{2\nu^2\frac{\partial\delta u_i}{\partial x_j}\frac{\partial^2\tau_{ik}}{\partial x_j\partial x_k}} = {} & \nu^2\frac{\partial^2}{\partial x_k^2}\left[\alpha_c\left\langle\frac{\partial\delta u_i}{\partial x_j}\frac{\partial\delta u_i}{\partial x_j}\right\rangle\right] - \frac{\nu^2}{V}\frac{\partial}{\partial x_k}\int_{S_d}\frac{\partial\delta u_i}{\partial x_j}\frac{\partial\delta u_i}{\partial x_j}n_k dS \\ & - 2\nu^2\alpha_c\left\langle\left(\frac{\partial^2\delta u_i}{\partial x_j\partial x_k}\right)^2\right\rangle - \frac{2\nu^2}{V}\int_{S_d}\frac{\partial\delta u_i}{\partial x_j}\frac{\partial}{\partial x_j}\frac{\partial\delta u_i}{\partial x_k}n_k dS\end{aligned} \tag{3.47}$$

3.1.13 Formulation of the Dissipation Transport Equation:

Substituting Eqs. (3.13 – 3.21), Eq. (3.25), Eq. (3.39), and Eq. (3.47) into Eq. (3.6) results in

$$
\begin{aligned}
&0+\nu\frac{\partial}{\partial t}\left[\alpha_c\left\langle\frac{\partial\delta u_i}{\partial x_j}\frac{\partial\delta u_i}{\partial x_j}\right\rangle\right]+\frac{\nu}{V}\int_{S_d}\frac{\partial\delta u_i}{\partial x_j}\frac{\partial\delta u_i}{\partial x_j}(v_k n_k)dS+0+0+2\nu\alpha_c\frac{\partial\langle u_k\rangle}{\partial x_j}\left\langle\frac{\partial\delta u_i}{\partial x_j}\frac{\partial\delta u_i}{\partial x_k}\right\rangle\\
&+\nu\langle u_k\rangle\frac{\partial}{\partial x_k}\left[\alpha_c\left\langle\frac{\partial\delta u_i}{\partial x_j}\frac{\partial\delta u_i}{\partial x_j}\right\rangle\right]-\frac{\nu}{V}\langle u_k\rangle\int_{S_d}\frac{\partial\delta u_i}{\partial x_j}\frac{\partial\delta u_i}{\partial x_j}n_k dS+2\nu\alpha_c\frac{\partial\langle u_i\rangle}{\partial x_k}\left\langle\frac{\partial\delta u_i}{\partial x_j}\frac{\partial\delta u_k}{\partial x_j}\right\rangle\\
&+2\nu\alpha_c\frac{\partial^2\langle u_i\rangle}{\partial x_j\partial x_k}\left\langle\delta u_k\frac{\partial\delta u_i}{\partial x_j}\right\rangle+2\nu\alpha_c\left\langle\frac{\partial\delta u_i}{\partial x_j}\frac{\partial\delta u_k}{\partial x_j}\frac{\partial\delta u_i}{\partial x_k}\right\rangle+\nu\frac{\partial}{\partial x_k}\left[\alpha_c\langle u_k\rangle\left\langle\frac{\partial\delta u_i}{\partial x_j}\frac{\partial\delta u_i}{\partial x_j}\right\rangle\right]\\
&+\nu\frac{\partial}{\partial x_k}\left[\alpha_c\left\langle\delta u_k\frac{\partial\delta u_i}{\partial x_j}\frac{\partial\delta u_i}{\partial x_j}\right\rangle\right]-\frac{\nu}{V}\int_{S_d}v_k\frac{\partial\delta u_i}{\partial x_j}\frac{\partial\delta u_i}{\partial x_j}n_k dS-\nu\langle u_k\rangle\frac{\partial}{\partial x_k}\left[\alpha_c\left\langle\frac{\partial\delta u_i}{\partial x_j}\frac{\partial\delta u_i}{\partial x_j}\right\rangle\right]\\
&+\frac{\nu}{V}\langle u_k\rangle\int_{S_d}\frac{\partial\delta u_i}{\partial x_j}\frac{\partial\delta u_i}{\partial x_j}n_k dS=-\alpha_c\frac{2\nu}{\rho}\frac{\partial}{\partial x_i}\left\langle\frac{\partial\delta u_i}{\partial x_j}\frac{\partial\delta P}{\partial x_j}\right\rangle+\frac{2\nu}{V\rho}\int_{S_d}\frac{\partial\delta u_i}{\partial x_j}\frac{\partial\delta P}{\partial x_j}n_i dS+\nu^2\frac{\partial^2}{\partial x_k^2}\left[\alpha_c\left\langle\frac{\partial\delta u_i}{\partial x_j}\frac{\partial\delta u_i}{\partial x_j}\right\rangle\right]\\
&-\frac{\nu^2}{V}\frac{\partial}{\partial x_k}\int_{S_d}\frac{\partial\delta u_i}{\partial x_j}\frac{\partial\delta u_i}{\partial x_j}n_k dS-2\nu^2\alpha_c\left\langle\left(\frac{\partial^2\delta u_i}{\partial x_j\partial x_k}\right)^2\right\rangle-\frac{2\nu^2}{V}\int_{S_d}\frac{\partial\delta u_i}{\partial x_j}\frac{\partial}{\partial x_j}\frac{\partial\delta u_i}{\partial x_k}n_k dS
\end{aligned}
\tag{3.48}
$$

Canceling terms and rearranging reduces Eq. (3.48) of the form

$$
\begin{aligned}
&\nu\frac{\partial}{\partial t}\left[\alpha_c\left\langle\frac{\partial\delta u_i}{\partial x_j}\frac{\partial\delta u_i}{\partial x_j}\right\rangle\right]+\nu\frac{\partial}{\partial x_k}\left[\alpha_c\langle u_k\rangle\left\langle\frac{\partial\delta u_i}{\partial x_j}\frac{\partial\delta u_i}{\partial x_j}\right\rangle\right]=-2\nu\alpha_c\frac{\partial\langle u_k\rangle}{\partial x_j}\left\langle\frac{\partial\delta u_i}{\partial x_j}\frac{\partial\delta u_i}{\partial x_k}\right\rangle-2\nu\alpha_c\frac{\partial\langle u_i\rangle}{\partial x_k}\left\langle\frac{\partial\delta u_i}{\partial x_j}\frac{\partial\delta u_k}{\partial x_j}\right\rangle\\
&-2\nu\alpha_c\frac{\partial^2\langle u_i\rangle}{\partial x_j\partial x_k}\left\langle\delta u_k\frac{\partial\delta u_i}{\partial x_j}\right\rangle-2\nu\alpha_c\left\langle\frac{\partial\delta u_i}{\partial x_j}\frac{\partial\delta u_k}{\partial x_j}\frac{\partial\delta u_i}{\partial x_k}\right\rangle-\nu\frac{\partial}{\partial x_k}\left[\alpha_c\delta u_k\left\langle\frac{\partial\delta u_i}{\partial x_j}\frac{\partial\delta u_i}{\partial x_j}\right\rangle\right]\\
&-2\frac{\nu}{\rho}\frac{\partial}{\partial x_i}\left[\alpha_c\left\langle\frac{\partial\delta u_i}{\partial x_j}\frac{\partial\delta P}{\partial x_j}\right\rangle\right]+\nu^2\frac{\partial^2}{\partial x_k^2}\left[\alpha_c\left\langle\frac{\partial\delta u_i}{\partial x_j}\frac{\partial\delta u_i}{\partial x_j}\right\rangle\right]-2\nu^2\alpha_c\left\langle\left(\frac{\partial^2\delta u_i}{\partial x_j\partial x_k}\right)^2\right\rangle\\
&-\frac{\nu^2}{V}\frac{\partial}{\partial x_k}\int_{S_d}\frac{\partial\delta u_i}{\partial x_j}\frac{\partial\delta u_i}{\partial x_j}n_k dS+\frac{2\nu}{\rho V}\int_{S_d}\frac{\partial\delta u_i}{\partial x_j}\frac{\partial\delta P}{\partial x_j}n_i dS-\frac{2\nu^2}{V}\int_{S_d}\frac{\partial\delta u_i}{\partial x_j}\frac{\partial}{\partial x_j}\frac{\partial\delta u_i}{\partial x_k}n_k dS
\end{aligned}
\tag{3.49}
$$

Identifying the volume averaged dissipation tensor as $\varepsilon_{ik}=2\nu\left\langle\frac{\partial\delta u_i}{\partial x_j}\frac{\partial\delta u_k}{\partial x_j}\right\rangle$ and noting that the volume averaged continuity equation for incompressible flow is $\frac{\partial\alpha_c}{\partial t}+\frac{\partial\left(\alpha_c\langle u_k\rangle\right)}{\partial x_k}=0$, allows Eq. (3.49) to be rewritten in the form

$$
\begin{aligned}
&\alpha_c\frac{D\varepsilon}{Dt}=-2\nu\alpha_c\frac{\partial\langle u_k\rangle}{\partial x_j}\left\langle\frac{\partial\delta u_i}{\partial x_j}\frac{\partial\delta u_i}{\partial x_k}\right\rangle-\alpha_c\varepsilon_{ik}\frac{\partial\langle u_i\rangle}{\partial x_k}-2\nu\alpha_c\left\langle\delta u_k\frac{\partial\delta u_i}{\partial x_j}\right\rangle\frac{\partial^2\langle u_i\rangle}{\partial x_j\partial x_k}-\\
&2\nu\alpha_c\left\langle\frac{\partial\delta u_i}{\partial x_j}\frac{\partial\delta u_k}{\partial x_j}\frac{\partial\delta u_i}{\partial x_k}\right\rangle-\nu\frac{\partial}{\partial x_k}\left[\alpha_c\left\langle\delta u_k\frac{\partial\delta u_i}{\partial x_j}\frac{\partial\delta u_i}{\partial x_j}\right\rangle\right]-2\frac{\nu}{\rho}\frac{\partial}{\partial x_i}\left[\alpha_c\left\langle\frac{\partial\delta u_i}{\partial x_j}\frac{\partial\delta P}{\partial x_j}\right\rangle\right]+\nu\frac{\partial^2}{\partial x_k^2}[\alpha_c\varepsilon]-\\
&2\nu^2\alpha_c\left\langle\left(\frac{\partial^2\delta u_i}{\partial x_j\partial x_k}\right)^2\right\rangle-\frac{\nu^2}{V}\frac{\partial}{\partial x_k}\int_{S_d}\frac{\partial\delta u_i}{\partial x_j}\frac{\partial\delta u_i}{\partial x_j}n_k dS+\frac{2\nu}{\rho V}\int_{S_d}\frac{\partial\delta u_i}{\partial x_j}\frac{\partial\delta P}{\partial x_j}n_i dS-\frac{\nu^2}{V}\int_{S_d}\frac{\partial}{\partial x_k}\left[\frac{\partial\delta u_i}{\partial x_j}\frac{\partial\delta u_i}{\partial x_j}\right]n_k dS
\end{aligned}
\tag{3.50}
$$

The above equation is the general dissipation equation for two-way coupled particle laden flows. The assumptions associated with Eq. (3.50) are incompressible flow and no mass transfer between the dispersed and continuous phase. If the void fraction is unity and no dispersed phase surfaces are present Eq. (3.50) reduces to the single-phase flow dissipation equation

$$\overbrace{\frac{D\varepsilon}{Dt} = -2\nu\frac{\partial\langle u_i\rangle}{\partial x_k}\left\langle\frac{\partial\delta u_j}{\partial x_k}\frac{\partial\delta u_j}{\partial x_i}\right\rangle - \varepsilon_{ik}\frac{\partial\langle u_i\rangle}{\partial x_k} - 2\nu\left\langle\delta u_k\frac{\partial\delta u_i}{\partial x_j}\right\rangle\frac{\partial^2\langle u_i\rangle}{\partial x_j\partial x_k} - 2\nu\left\langle\frac{\partial\delta u_i}{\partial x_j}\frac{\partial\delta u_k}{\partial x_j}\frac{\partial\delta u_i}{\partial x_k}\right\rangle}^{\text{Production of Dissipation}}$$
$$\underbrace{-\nu\frac{\partial}{\partial x_k}\left[\left\langle\delta u_k\frac{\partial\delta u_i}{\partial x_j}\frac{\partial\delta u_i}{\partial x_j}\right\rangle\right]}_{\text{Transport of Dissipation}} \underbrace{-2\frac{\nu}{\rho}\frac{\partial}{\partial x_i}\left[\left\langle\frac{\partial\delta u_i}{\partial x_j}\frac{\partial\delta P}{\partial x_j}\right\rangle\right]}_{\text{Pressure Diffusion of Dissipation}} \underbrace{+\nu\frac{\partial^2}{\partial x_k^2}[\varepsilon]}_{\text{Viscous Diffusion of Dissipation}} \underbrace{-2\nu^2\left\langle\left(\frac{\partial^2\delta u_i}{\partial x_j\partial x_k}\right)^2\right\rangle}_{\text{Dissipation of Dissipation}} \tag{3.51}$$

which is the volume average equivalent to time average dissipation equation presented by Bernard and Wallace (2002). It is now apparent that the effects of the surfaces of the dispersed phase are associated with the following terms

$$\underbrace{-\frac{\nu^2}{V}\frac{\partial}{\partial x_k}\int_{S_d}\frac{\partial\delta u_i}{\partial x_j}\frac{\partial\delta u_i}{\partial x_j}n_k dS}_{\text{Diffusion of dissipation due to the presence of particles}} + \underbrace{\frac{2\nu}{\rho V}\int_{S_d}\frac{\partial\delta u_i}{\partial x_j}\frac{\partial\delta P}{\partial x_j}n_i dS}_{\text{Pressure-strain due to the presence of particles}} - \underbrace{\frac{\nu^2}{V}\int_{S_d}\frac{\partial}{\partial x_k}\left[\frac{\partial\delta u_i}{\partial x_j}\frac{\partial\delta u_i}{\partial x_j}\right]n_k dS}_{\text{Production of dissipation due to the presence of particles}} \tag{3.52}$$

3.2 Evaluation of the Surface Integrals:

The integrals in Eq. (3.52) represent the dissipation effects caused by surfaces of the particles. Within these integrals are spatial gradients of volume deviation properties. In order to evaluate the integrals, the coupled gradients must be captured. A first attempt

to evaluate these terms is based on the assumption that the particles are much smaller than the equivalent Kolmogorov length scale and that Stokes drag is valid around the particles. The relative velocity (U_i) can be expressed as the instantaneous velocity between the particle and the surrounding fluid as

$$U_i = u_i - v_i \tag{3.53}$$

which is the same as taking a particle at rest in a flow field with velocity U_i. Substituting Eq. (2.12) into Eq. (3.53) shows a relationship between the local velocity deviation and the relative velocity in the form

$$\delta u_i = U_i + v_i - \langle u_i \rangle \tag{3.54}$$

The spatial velocity gradients shown in Eq. (3.52) are evaluated at the surfaces of the particles. Taking a spatial gradient of the above equation shows

$$\left.\frac{\partial \delta u_i}{\partial x_j}\right|_{S_d} = \left.\frac{\partial U_i}{\partial x_j}\right|_{S_d} + \left.\frac{\partial v_i}{\partial x_j}\right|_{S_d} - \left.\frac{\partial \langle u_i \rangle}{\partial x_j}\right|_{S_d} \tag{3.55}$$

where S_d represents the surface of the dispersed phase. If the particle is rigid and rotational effects are neglected, then the velocity of the particle is assumed to be constant along the surface of the particle. Therefore the last two terms on the right hand side of Eq. (3.55) are zero when evaluated along the particle surface, reducing Eq. (3.55) to

$$\left.\frac{\partial \delta u_i}{\partial x_j}\right|_{S_d} = \left.\frac{\partial U_i}{\partial x_j}\right|_{S_d} \tag{3.56}$$

3.2.1 Coordinate Transformation

The relative velocity in Stokes flow is typically solved using spherical polar coordinates with the particle velocity set to zero. Simplifying Eq. (3.56) for the case of

Stokes flow shows that the gradient of the volume deviation velocity is equal to the gradient of the instantaneous velocity of the continuous phase, such as

$$\left.\frac{\partial \delta u_i}{\partial x_j}\right|_{S_d} = \left.\frac{\partial u_i}{\partial x_j}\right|_{S_d} \tag{3.57}$$

The components of the instantaneous velocity in Stokes flow is represented in spherical polar coordinates by

$$\vec{u}(r,\theta) = U\left[\cos\theta\left(1+\frac{a^3}{2r^3}-\frac{3a}{2r}\right)\hat{r} - \sin\theta\left(1-\frac{a^3}{4r^3}-\frac{3a}{4r}\right)\hat{\theta}\right] \tag{3.58}$$

where a is the radius of the particle. Converting the volume deviation velocity gradient from the Cartesian coordinate system to the spherical polar coordinate system yields

$$\frac{\partial \delta u_i}{\partial x_j} = \begin{pmatrix} \dfrac{\partial u_r}{\partial r} & \dfrac{\partial u_\theta}{\partial r} & \dfrac{\partial u_\varphi}{\partial r} \\ \dfrac{1}{r}\dfrac{\partial u_r}{\partial \theta} - \dfrac{u_\theta}{r} & \dfrac{u_r}{r} + \dfrac{1}{r}\dfrac{\partial u_\theta}{\partial \theta} & \dfrac{1}{r}\dfrac{\partial u_\varphi}{\partial \theta} \\ \dfrac{1}{r\sin\theta}\dfrac{\partial u_r}{\partial \varphi} - \dfrac{u_\varphi}{r} & \dfrac{1}{r\sin\theta}\dfrac{\partial u_\theta}{\partial \varphi} - \dfrac{u_\varphi}{r}\cot\theta & \dfrac{1}{r\sin\theta}\dfrac{\partial u_\varphi}{\partial \varphi} + \dfrac{u_r}{r} + \dfrac{u_\theta}{r}\cot\theta \end{pmatrix} \tag{3.59}$$

In Stokes flow, the velocity in the φ direction is zero. Thus for the case of Stokes flow, the above equation is further reduced to

$$\frac{\partial \delta u_i}{\partial x_j} = \begin{pmatrix} \dfrac{\partial u_r}{\partial r} & \dfrac{\partial u_\theta}{\partial r} & 0 \\ \dfrac{1}{r}\dfrac{\partial u_r}{\partial \theta} - \dfrac{u_\theta}{r} & \dfrac{u_r}{r} + \dfrac{1}{r}\dfrac{\partial u_\theta}{\partial \theta} & 0 \\ 0 & 0 & \dfrac{u_r}{r} + \dfrac{u_\theta}{r}\cot\theta \end{pmatrix}_{Stokes\ Condition} \tag{3.60}$$

At the particle surface, the velocities in the radial and tangential directions are both zero. Evaluating the above equation at the particle surface leaves only the velocity gradients in the radial and tangential directions of the form

$$\left.\frac{\partial \delta u_i}{\partial x_j}\right|_{r=a} = \begin{pmatrix} \frac{\partial u_r}{\partial r} & \frac{\partial u_\theta}{\partial r} & 0 \\ \frac{1}{r}\frac{\partial u_r}{\partial \theta} & \frac{1}{r}\frac{\partial u_\theta}{\partial \theta} & 0 \\ 0 & 0 & 0 \end{pmatrix}_{Stokes\ Condition} \tag{3.61}$$

The square of the volume deviation velocity gradient evaluated at the surface is

$$\left.\frac{\partial \delta u_i}{\partial x_j}\frac{\partial \delta u_i}{\partial x_j}\right|_{r=a} = \begin{pmatrix} \frac{\partial u_r}{\partial r}\frac{\partial u_r}{\partial r} & \frac{\partial u_\theta}{\partial r}\frac{\partial u_\theta}{\partial r} & 0 \\ \frac{1}{r^2}\frac{\partial u_r}{\partial \theta}\frac{\partial u_r}{\partial \theta} & \frac{1}{r^2}\frac{\partial u_\theta}{\partial \theta}\frac{\partial u_\theta}{\partial \theta} & 0 \\ 0 & 0 & 0 \end{pmatrix}_{Stokes\ Condition} \tag{3.62}$$

Taking spatial gradients of the Stokes velocity and evaluating them at the surface of the particle shows that there is only one contributing spatial gradient

$$\left.\frac{\partial \delta u_i}{\partial x_j}\right|_{r=a} = \left.\frac{\partial \delta u_2}{\partial x_1}\right|_{r=a} = \left.\frac{\partial u_\theta}{\partial r}\right|_{r=a} = -\frac{3U\sin\theta}{2a} \tag{3.63}$$

so the deviation velocity gradient squared is then represented by

$$\left.\frac{\partial \delta u_i}{\partial x_j}\frac{\partial \delta u_i}{\partial x_j}\right|_{r=a} = \left.\frac{\partial \delta u_2}{\partial x_1}\frac{\partial \delta u_2}{\partial x_1}\right|_{r=a} = \left.\frac{\partial u_\theta}{\partial r}\frac{\partial u_\theta}{\partial r}\right|_{r=a} = \frac{9U^2\sin^2\theta}{4a^2} \tag{3.64}$$

The unit vector within the surface integrals of Eq. (3.52) is the unit vector outward normal to the surface. Assuming the particles are spherical, then the unit vector is related to the radial component

$$n_k = e_r \tag{3.65}$$

The integral over the surface area of the particles within the domain is expressed as

$$\int_{S_d} B dS = \sum_n \int_0^{2\pi}\int_0^{\pi} B r^2 \sin\theta\, d\theta\, d\varphi \tag{3.66}$$

where n is the number of particles within the domain. This expression integrates the effects of a single particle but through the summation allows for the effects of different particle diameters, friction factors, etc.

By transforming the gradients and unit normal vectors between Cartesian and spherical polar coordinate systems, the terms in Eq. (3.52) can be obtained directly.

3.2.2 Diffusion of Dissipation at the Particle Surface

To evaluate the diffusion of dissipation at the particle surface, the derivative on the outside of the integral is left in Cartesian coordinates. The gradients of the deviation velocity are transformed into spherical polar coordinates and evaluated at the surface. The unit normal vector in Cartesian coordinates is

$$n_k = e_r = \sin\theta\cos\varphi\,\hat{i} + \sin\theta\sin\varphi\,\hat{j} + \cos\theta\,\hat{k} \tag{3.67}$$

Substituting Eqs. (3.64), (3.66) and (3.67) into the first term in Eq. (3.52) results in

$$\begin{aligned} &-\frac{\nu^2}{V}\frac{\partial}{\partial x_k}\int_{S_d}\frac{\partial \delta u_i}{\partial x_j}\frac{\partial \delta u_i}{\partial x_j}n_k\,dS = \\ &\quad -\frac{\nu^2}{V}\frac{\partial}{\partial x_k}\sum_n\int_0^{2\pi}\int_0^{\pi}\frac{9U^2\sin^2\theta}{4a^2}\left[\sin\theta\cos\varphi\,\hat{i} + \sin\theta\sin\varphi\,\hat{j} + \cos\theta\,\hat{k}\right]r^2\sin\theta\,d\theta\,d\varphi \end{aligned} \tag{3.68}$$

At the surface, $r = a$, the free-stream velocity (U) is constant and independent of the position along the particle surface, thus the above equation is simplified to

$$\begin{aligned} &-\frac{\nu^2}{V}\frac{\partial}{\partial x_k}\int_{S_d}\frac{\partial \delta u_i}{\partial x_j}\frac{\partial \delta u_i}{\partial x_j}n_k\,dS = \\ &\quad -\frac{9\nu^2}{4V}\frac{\partial}{\partial x_k}\sum_n U^2\int_0^{2\pi}\int_0^{\pi}\left[\sin^4\theta\cos\varphi\,\hat{i} + \sin^4\theta\sin\varphi\,\hat{j} + \sin^2\theta\cos\theta\,\hat{k}\right]d\theta\,d\varphi \end{aligned} \tag{3.69}$$

Each term within the brackets integrates to zero. Although this is the case for the assumption of Stokes flow, this may not be the case if the particle is larger than the

Kolmogorov length scale and in the presence of mean velocity gradients that would cause the particle to rotate.

3.2.3 Pressure Strain at the Particle Surface

The second term in Eq. (3.52) is shown to be

$$\frac{2\nu}{\rho V}\int_{S_d}\frac{\partial \delta u_i}{\partial x_j}\frac{\partial \delta P}{\partial x_j}n_i dS \tag{3.70}$$

Evaluation of the second term in Eq. (3.52) begins with defining the volume deviation pressure within a Stokes drag regime. In Stokes flow, the instantaneous pressure is given by (White 1974)

$$P = P_o - \frac{3\mu a U}{2r^2}\cos\theta \tag{3.71}$$

where P_o is the uniform free-stream pressure. Decomposing the instantaneous pressure into a volume average and a volume deviation pressure and comparing it to Stokes pressure shows that the deviation pressure is represented by

$$\delta P = -\frac{3\mu a U}{2r^2}\cos\theta \tag{3.72}$$

The spatial gradient of the deviation pressure is converted from Cartesian to spherical polar coordinates

$$\frac{\partial \delta P}{\partial x_j} = e_r\frac{\partial \delta P}{\partial r},\quad e_\theta\frac{1}{r}\frac{\partial \delta P}{\partial \theta},\quad e_\varphi\frac{1}{r\sin\theta}\frac{\partial \delta P}{\partial \varphi} \tag{3.73}$$

The gradients of the deviation pressure are found by taking derivatives of Eq. (3.72)

$$\frac{\partial \delta P}{\partial r} = \frac{3\mu a U}{r^3}\cos\theta,\quad \frac{\partial \delta P}{\partial \theta} = \frac{3\mu a U}{2r^2}\sin\theta,\ \text{and}\ \frac{\partial \delta P}{\partial \varphi} = 0 \tag{3.74}$$

In order to couple the correct terms, the unit normal vector is evaluated. Since both the deviation velocity gradient and the deviation pressure gradient are converted to spherical

polar coordinates, the unit vector is also converted. The unit vector is the unit normal vector, thus it is required that

$$n_i = n_1 = e_r \tag{3.75}$$

Substituting Eqs. (3.63), (3.66), (3.74) and (3.75) into Eq. (3.70) results in

$$\frac{2\nu}{\rho V}\int_{S_d}\frac{\partial \delta u_i}{\partial x_j}\frac{\partial \delta P}{\partial x_j}n_i dS = \frac{2\nu}{\rho V}\sum_n\int_0^{2\pi}\int_0^{\pi}\frac{\partial u_r}{\partial r}\frac{\partial \delta P}{\partial r}r^2\sin\theta\, d\theta\, d\varphi + \frac{2\nu}{\rho V}\sum_n\int_0^{2\pi}\int_0^{\pi}\left[\frac{1}{r}\frac{\partial u_r}{\partial \theta}-\frac{u_\theta}{r}\right]\frac{1}{r}\frac{\partial \delta P}{\partial \theta}r^2\sin\theta\, d\theta\, d\varphi \tag{3.76}$$

where u_r and u_θ are the radial and tangential components of the instantaneous velocity and δP is the deviation of the volume pressure or Stokes pressure. Evaluation of the velocity gradients in Eq. (3.76) at the surface of the particle shows that they are zero. Thus the pressure strain at the surface of the particle is shown to be zero for Stokes conditions

$$\frac{2\nu}{\rho V}\int_{S_d}\frac{\partial \delta u_i}{\partial x_j}\frac{\partial \delta P}{\partial x_j}n_i dS = 0 \tag{3.77}$$

Again, this is based on the assumption of Stokes flow and may not be the case for particles larger than the Kolmogorov length scale.

3.2.4 Production of Dissipation at the Particle Surface

The last term in Eq. (3.52) is

$$-\frac{\nu^2}{V}\int_{S_d}\frac{\partial}{\partial x_k}\left[\frac{\partial \delta u_i}{\partial x_j}\frac{\partial \delta u_i}{\partial x_j}\right]n_k dS \tag{3.78}$$

The terms within the integral represent a scalar, thus the gradient is represented in spherical polar coordinates as

$$\frac{\partial}{\partial x_k} = e_r \frac{\partial}{\partial r}, e_\theta \frac{1}{r}\frac{\partial}{\partial \theta}, e_\varphi \frac{1}{r\sin\theta}\frac{\partial}{\partial \varphi} \tag{3.79}$$

The unit vector is the unit normal vector and is represented in spherical polar coordinates by

$$n_k = n_1 = e_r \tag{3.80}$$

Then Eq. (3.78) is reduced to

$$-\frac{\nu^2}{V}\int_{S_d}\frac{\partial}{\partial x_k}\left[\frac{\partial \delta u_i}{\partial x_j}\frac{\partial \delta u_i}{\partial x_j}\right]n_k dS = -\frac{\nu^2}{V}\int_{S_d}\frac{\partial}{\partial r}\left[\frac{\partial \delta u_i}{\partial x_j}\frac{\partial \delta u_i}{\partial x_j}\right]dS \tag{3.81}$$

The square of the velocity deviation gradient is found in Eq. (3.64). Evaluating the terms at the surface shows that the only non-zero gradient is $\partial u_\theta / \partial r$. Taking a spatial gradient of Eq. (3.64) with respect to the radius results in

$$\frac{\partial}{\partial r}\left\{\frac{\partial \delta u_i}{\partial x_j}\frac{\partial \delta u_i}{\partial x_j}\bigg|_{r=a}\right\} = 2\frac{\partial u_\theta}{\partial r}\frac{\partial^2 u_\theta}{\partial r^2} \tag{3.82}$$

Substituting in the velocity gradients found from evaluating Stokes velocities at the surface of the particle results in

$$\frac{\partial}{\partial r}\left\{\frac{\partial \delta u_i}{\partial x_j}\frac{\partial \delta u_i}{\partial x_j}\bigg|_{r=a}\right\} = -\frac{27U^2}{2a^3}\sin^2\theta \tag{3.83}$$

where U is the free stream velocity in Stokes flow. Substituting Eq. (3.66) and Eq. (3.83) into Eq. (3.81) shows

$$-\frac{\nu^2}{V}\int_{S_d}\frac{\partial}{\partial x_k}\left[\frac{\partial \delta u_i}{\partial x_j}\frac{\partial \delta u_i}{\partial x_j}\right]n_k dS = -\frac{\nu^2}{V}\sum_n\int_0^{2\pi}\int_0^{\pi}\left(-\frac{27U_n^2}{2a^3}\sin^2\theta\right)r^2\sin\theta\, d\theta\, d\varphi \tag{3.84}$$

Evaluating at the surface by setting r = a and noting that the free-stream velocity (U) is constant over the particle surface, Eq. (3.84) is simplified to

$$-\frac{\nu^2}{V}\int_{S_d}\frac{\partial}{\partial x_k}\left[\frac{\partial \delta u_i}{\partial x_j}\frac{\partial \delta u_i}{\partial x_j}\right]n_k dS = \frac{\nu^2}{V}\sum_n \frac{27U_n^2}{D_n}\int_0^{2\pi}\int_0^{\pi}\sin^3\theta\, d\theta d\varphi \tag{3.85}$$

where the summation represents the effects of the all the particles within the control volume and *n* represents each particle within the control volume. Evaluating the integral yields

$$-\frac{\nu^2}{V}\int_{S_d}\frac{\partial}{\partial x_k}\left[\frac{\partial \delta u_i}{\partial x_j}\frac{\partial \delta u_i}{\partial x_j}\right]n_k dS = 72\pi\frac{\nu^2}{V}\sum_n \frac{\left|u_i - v_i\right|_n^2}{D_n} \tag{3.86}$$

Thus the last term in Eq. (3.52) can be identified as a production of dissipation term. The deviation from Stokes drag may be approximated by multiplying by the drag factor, *f*, which is the ratio of the drag coefficient for a sphere to Stokes drag. In order to apply this equation to particles that are larger than the Kolmogorov length scale, it is assumed that the coefficient 72π can be replaced by an empirical coefficient so Eq. (3.86) can be represented by

$$-\frac{\nu^2}{V}\int_{S_d}\frac{\partial}{\partial x_k}\left[\frac{\partial \delta u_i}{\partial x_j}\frac{\partial \delta u_i}{\partial x_j}\right]n_k dS = C_{\varepsilon 3}\frac{\nu^2}{V}\sum_n f_n\frac{\left|u_i - v_i\right|_n^2}{D_n} \tag{3.87}$$

where $C_{\varepsilon 3}$ would be determined by experiments.

To summarize, the terms in Eq. (3.52) were analyzed by assuming that the particles were much smaller than the Kolmogorov length scale of the flow. This assumption allowed the terms in Eq. (3.52) to be evaluated analytically. However, this assumption does not apply to turbulent particle laden flows where the wake effect is important. Thus once the form of the terms within Eq. (3.52) was found, it was then assumed that a coefficient could be applied along with the drag factor to account for the wake effects in turbulent flows. The coefficient can be calibrated for homogeneous turbulence generation by particles (discussed further in Chapter 4). Although the

assumption of Stokes flow to analyze the terms within Eq. (3.52) by assuming that the particles are smaller than the Kolmogorov length scale could be argued, this assumption resulted in a simple term that can be easily calibrated and modeled.

3.3 The Modified Dissipation Model

Evaluating the surface integrals using Stokes flow, the volume averaged dissipation transport equation assumes the form

$$\begin{aligned}\alpha_c \frac{D\varepsilon}{Dt} = &-2\nu\alpha_c \frac{\partial\langle u_k\rangle}{\partial x_j}\left\langle \frac{\partial\delta u_i}{\partial x_j}\frac{\partial\delta u_i}{\partial x_k}\right\rangle - \alpha_c\varepsilon_{ik}\frac{\partial\langle u_i\rangle}{\partial x_k} - 2\nu\alpha_c\left\langle \delta u_k \frac{\partial\delta u_i}{\partial x_j}\right\rangle\frac{\partial^2\langle u_i\rangle}{\partial x_j\partial x_k} - 2\nu\alpha_c\left\langle \frac{\partial\delta u_i}{\partial x_j}\frac{\partial\delta u_k}{\partial x_j}\frac{\partial\delta u_i}{\partial x_k}\right\rangle \\ &-\nu\frac{\partial}{\partial x_k}\left[\alpha_c\left\langle \delta u_k\frac{\partial\delta u_i}{\partial x_j}\frac{\partial\delta u_i}{\partial x_j}\right\rangle\right] - 2\frac{\nu}{\rho}\frac{\partial}{\partial x_i}\left[\alpha_c\left\langle \frac{\partial\delta u_i}{\partial x_j}\frac{\partial\delta P}{\partial x_j}\right\rangle\right] + \nu\frac{\partial^2}{\partial x_k^2}[\alpha_c\varepsilon] \\ &-2\nu^2\alpha_c\left\langle\left(\frac{\partial^2\delta u_i}{\partial x_j\partial x_k}\right)^2\right\rangle - \frac{\nu^2}{V}\int_{S_d}\frac{\partial}{\partial x_k}\left[\frac{\partial\delta u_i}{\partial x_j}\frac{\partial\delta u_i}{\partial x_j}\right]n_k dS\end{aligned} \tag{3.88}$$

The above equation is difficult to model directly, thus a simple model is proposed using similar arguments for the development of the time averaged dissipation model, i.e. obtaining Eq. (3.3) from Eq. (3.2). Using these techniques (Bernard and Wallace 2002, Pope 2000) the terms representing the production of dissipation (characterized by mean velocity gradients) can be represented by

$$-2\nu\alpha_c \frac{\partial\langle u_k\rangle}{\partial x_j}\left\langle \frac{\partial\delta u_i}{\partial x_j}\frac{\partial\delta u_i}{\partial x_k}\right\rangle - \alpha_c\varepsilon_{ik}\frac{\partial\langle u_i\rangle}{\partial x_k} - 2\nu\alpha_c\left\langle \delta u_k \frac{\partial\delta u_i}{\partial x_j}\right\rangle\frac{\partial^2\langle u_i\rangle}{\partial x_j\partial x_k} - 2\nu\alpha_c\left\langle \frac{\partial\delta u_i}{\partial x_j}\frac{\partial\delta u_k}{\partial x_j}\frac{\partial\delta u_i}{\partial x_k}\right\rangle \approx \alpha_c C'_{\varepsilon 1}\frac{P_\varepsilon\varepsilon}{k} \tag{3.89}$$

where P_ε is modeled as $\upsilon_T \frac{\partial\langle u_i\rangle}{\partial x_j}\frac{\partial\langle u_i\rangle}{\partial x_j}$ and $C'_{\varepsilon 1}$ is not necessarily equal to 1.44 but rather a combination of single and dispersed phase effects (discussed further in Chapter 6). The terms representing the diffusion of dissipation (characterized by the spatial gradients) can be represented by

$$-\nu\frac{\partial}{\partial x_k}\left[\alpha_c\left\langle\delta u_k\frac{\partial\delta u_i}{\partial x_j}\frac{\partial\delta u_i}{\partial x_j}\right\rangle\right]-2\frac{\nu}{\rho}\frac{\partial}{\partial x_i}\left[\alpha_c\left\langle\frac{\partial\delta u_i}{\partial x_j}\frac{\partial\delta P}{\partial x_j}\right\rangle\right]+\nu\frac{\partial^2}{\partial x_k^2}[\alpha_c\varepsilon]\approx\frac{\partial}{\partial x_i}\left[\alpha_c\left(\nu+\frac{\nu_T}{\sigma_\varepsilon}\right)\frac{\partial\varepsilon}{\partial x_i}\right] \tag{3.90}$$

The terms representing dissipation of dissipation can be modeled as

$$-2\nu^2\alpha_c\left\langle\left(\frac{\partial^2\delta u_i}{\partial x_j\partial x_k}\right)^2\right\rangle\approx-C'_{\varepsilon 2}\alpha_c\frac{\varepsilon^2}{k} \tag{3.91}$$

where $C'_{\varepsilon 2}$ is not necessarily equal to 1.92 (the coefficient for the dissipation of dissipation in the time averaged dissipation model) but rather a combination of single and dispersed phase effects (discussed further in Chapter 5). The effects of the particle surfaces constitute a production of dissipation term and can be modeled as

$$-\frac{\nu^2}{V}\int_{S_d}\frac{\partial}{\partial x_k}\left[\frac{\partial\delta u_i}{\partial x_j}\frac{\partial\delta u_i}{\partial x_j}\right]n_k dS\approx C_{\varepsilon 3}\frac{\nu^2}{V}\sum_n f_n\frac{|u_i-v_i|_n^2}{D_n} \tag{3.92}$$

Substituting Eqs. (3.89 – 3.92) into Eq. (3.88) yields a model for the volume averaged dissipation transport in the form

$$\alpha_c\frac{D\varepsilon}{Dt}=C'_{\varepsilon 1}\alpha_c\frac{P_\varepsilon\varepsilon}{k}-C'_{\varepsilon 2}\alpha_c\frac{\varepsilon^2}{k}+C_{\varepsilon 3}\frac{\nu^2}{V}\sum_n f_n\frac{|u_i-v_i|_n^2}{D_n}+\frac{\partial}{\partial x_i}\left[\alpha_c\left(\nu+\frac{\nu_T}{\sigma_\varepsilon}\right)\frac{\partial\varepsilon}{\partial x_i}\right] \tag{3.93}$$

where α_c is the void fraction, P_ε is the production of dissipation, $C'_{\varepsilon 1}$ and $C'_{\varepsilon 2}$ are the combined single and dispersed phase production and dissipation of dissipation coefficients respectively, $C_{\varepsilon 3}$ is the production of dissipation coefficient (due to particles), V is the mixture volume, ν is the kinematic viscosity, f is the drag factor, u_i and v_i are the instantaneous fluid and particle velocities respectively, D is the particle diameter, n is the particle number within the mixture volume, ν_T is the turbulent viscosity, σ_ε is the effective Schmidt number for turbulent diffusion, and k and ε are the volume averaged turbulent kinetic energy and dissipation defined in Eqs. (2.16) and (2.17) respectively. Applying Eq. (3.93) to the fundamental case of particle laden turbulent flows described

above where the particles are stationary and the flow is steady and homogeneous (with no wall effects) reduces to

$$C_{\varepsilon 3}\frac{v^2}{V}\sum_n f_n\frac{|u_i|_n^2}{D_n}=C'_{\varepsilon 2}\alpha_c\frac{\varepsilon^2}{k} \tag{3.94}$$

which shows that the production of dissipation due to the presence of particles must balance the dissipation of dissipation of the fluid.

According to the experimental data reviewed by of Gore and Crowe (1989), the turbulence intensity for particle-laden flows is increased (relative to a single phase flow) for D/L > 0.1 and decreased for D/L < 0.1, where D is the particle diameter and L is the characteristic length of the most energetic eddy. Although the magnitude of the ratio of particle diameter to the fluid length scale at which this transition occurs is arguable (Eaton 2006), clearly there is a transition. Non-dimensionalizing Eq. (3.94) by a mean velocity (U) and a characteristic length scale in the flow (L), a measure of the most energetic eddy, shows

$$C_{\varepsilon 3}\frac{1}{\mathrm{Re}_L^2}\frac{1}{\widetilde{V}}\sum_n f_n\frac{|\widetilde{u}_i|_n^2}{(D/L)_n}=C'_{\varepsilon 2}\alpha_c\frac{\widetilde{\varepsilon}^2}{\widetilde{k}} \tag{3.95}$$

where the tilde is the non-dimensional form and Re_L is the Reynolds number based on the mean velocity and a characteristic length scale of the flow, a measure of the most energetic eddy. The ratio D/L appears as a fundamental parameter. For this idealized case, it can be shown that the turbulence intensity ($\sigma=\sqrt{2\widetilde{k}}$) is a function of D/L which corresponds to the findings of Gore and Crowe (1989).

CHAPTER FOUR

THE PRODUCTION OF DISSIPATION COEFFICIENT DUE TO THE PRESENCE OF PARTICLES

In the dissipation model, Eq. (3.93), a production of dissipation term due to the presence of particles was obtained. This term was modeled using Stokes analysis. However, the wake effect must be accounted for, so the coefficient must be determined from experimental data involving the production of homogeneous turbulence by particles.

4.1 Determining the Particle Production of Dissipation Coefficient ($C_{\varepsilon 3}$)

Since the fundamental case cannot be obtained experimentally, the next most basic flow configuration is dropping particles into an initially quiescent fluid, i.e. homogeneous turbulence generation by particles. There are several data sets associated with this type of experiment.

The volume averaged turbulent kinetic energy equation developed by Crowe and Gillandt (1998) reduces to

$$\varepsilon = \frac{\beta_V}{\alpha_c \rho} \left| \langle v_i \rangle \right|^2 = \frac{\alpha_d \rho_d}{\alpha_c \rho} \frac{f}{\tau_p} \left| \langle v_i \rangle \right|^2 \tag{4.1}$$

for $\sqrt{k} \big/ \left| \langle v_i \rangle \right| << 1$. Simplifying Eq. (3.93) for the case of falling particles through an initially quiescent fluid results in

$$C_{\varepsilon 3}\frac{v^2}{V}\sum_n f_n\frac{\left|(v_i)_n\right|^2}{D_n}=C'_{\varepsilon 2}\alpha_c\frac{\varepsilon^2}{k} \tag{4.2}$$

The left hand side of the above equation represents the production of dissipation rate due to the relative velocity gradients at the particle surface while the right hand side is the dissipation of dissipation rate of the viscous fluid. For the case of particles, of the same diameter, uniformly falling in an initially quiescent fluid, Eq. (4.2) reduces to

$$C'_{\varepsilon 2}\alpha_c\frac{\varepsilon^2}{k}=C_{\varepsilon 3}nv^2 f\frac{\left|\langle v_i\rangle\right|^2}{D} \tag{4.3}$$

There is in-sufficient information at this point to evaluate both empirical coefficients. The value of $C'_{\varepsilon 2}$ for the standard single phase k-ε model is 1.92. However, it is assumed that this coefficient contains a contribution due to the presence of particles. For this reason, the ratio of coefficients will be evaluated. By substituting Eq. (4.1) into Eq. (4.3) a relationship between the coefficients associated with the production of dissipation due to presence of particles and the dissipation of dissipation within the fluid is obtained

$$\frac{C_{\varepsilon 3}}{C'_{\varepsilon 2}}=\frac{\alpha_c\left[\frac{\alpha_d\rho_d}{\alpha_c\rho_c}\frac{f}{\tau_p}\left|\langle v_i\rangle\right|^2\right]^2}{knv^2 f\frac{\left|\langle v_i\rangle\right|^2}{D}}\approx\left(\frac{\pi 18^2}{6}\right)\frac{\alpha_d}{\alpha_c}\frac{f\left|\langle v_i\rangle\right|^2}{k} \tag{4.4}$$

Crowe and Wang (2000) compiled data from several different authors and showed a correlation between the relative Reynolds number and the ratio of Taylor length scale to particle diameter. Most of the data fit remarkably well, however a few sets of data seemed to deviate. Crowe and Wang (2000) report that the data of Kenning and Crowe (1997) may be low compared to the rest of the data due to analyzing the turbulence after the particle cloud passed. There does not seem to be enough data with varying volume

fractions that confirm this conclusion. The volume fractions associated with Kenning and Crowe's data are on the order of 10^{-2}, and those associated with the data of Mizukami et al. (1992) and Parthasarathy et al. (1990) are on the order of 10^{-6} and 10^{-4} respectively. The volume fractions of Lance and Bataille (1982) were on the order of Kenning and Crowe's data. According to Elghobashi (1994), volume fractions less than 10^{-6} have negligible effect on the turbulence of the carrier phase (one-way coupling), volume fractions in the range of 10^{-6}–10^{-3} alter the turbulence of the carrier phase (two-way coupling), and volume fractions greater than 10^{-3} further alter the turbulence of the carrier phase due to particle-particle collisions (four way coupling). The data of Kenning and Crowe (1997) and Lance and Bataille (1982) showed volume fractions on the order of 10^{-2}; which appears to fall into a four-way coupling category.

The correlation presented by Crowe and Wang (2000) for two-way coupling is

$$\frac{\lambda}{D} \propto \left[\frac{\alpha_c}{\alpha_d} \frac{1}{18f} \frac{k}{\Delta u^2} \right]^{1/2} \tag{4.5}$$

where, λ is the Taylor length scale, D is the particle diameter, α_c and α_d are the volume fractions of the continuous and dispersed phase respectively, k is the turbulent kinetic energy of the carrier phase, f is the drag factor, and Δu is the velocity difference between the phases. Comparing equations (4.4) and (4.5), it is clearly noted that the ratio of the particle production of dissipation coefficient to the total dissipation of dissipation coefficient is proportional to the square of the ratio of the particle diameter to the Taylor length scale of the fluid

$$\frac{C_{\varepsilon 3}}{C'_{\varepsilon 2}} \propto \left[\frac{D}{\lambda} \right]^2 \tag{4.6}$$

In order to evaluate the ratio of coefficients, data from experiments of particles falling in an initially quiescent fluid with volume fractions between 10^{-6} and 10^{-2} were considered along with useful data at the centerline of pipe flow experiments. The data of Parthasarathy et al. (1990), Mizukami, et al. (1992), Hosokawa, et al. (1998), Varaksin et al. (1998), and Chen, et al. (2000) provided enough information to determine the coefficient over a wide range of relative Reynolds numbers (1 – 1000), volume fractions (10^{-6} – 10^{-2}), particle density (900 – 3600 kg/m^3), carrier phase density (1 – 1000kg/m^3). Mizukami et al. (1992) and Parthasarathy et al. (1990) performed experiments to determine the production of dissipation due to particles falling in an initially quiescent fluid, representing the conditions for Eqs. (4.1) and (4.2). In their data, the particle diameters exhibited minimal deviations and particle velocities were nearly uniform. The data of Hosokawa et al. (1998), Varaksin et al. (1998) and Chen et al. (2000) involved particles in pipe flow, of which only the data at the centerline of the pipe was taken. These data sets were chosen due to the necessary information needed to compute the ratio of coefficients over a wide range of relative Reynolds numbers (shown in Figure 4.1) within an environment containing homogeneous turbulence generation by particles. The data reduced for the ratio of coefficients as a function of relative Reynolds number, defined as

$$\mathrm{Re}_r = \frac{|u_i - v_i|D}{\nu_c} \tag{4.7}$$

are shown in Figure 4.1. The data do appear to correlate well for relative Reynolds numbers ranging from 100 - 1000. The data of Mizukami et al. (1992) and Parthasarathy et al. (1990) involve high particle Reynolds numbers over a wide range of particle mass loadings; at high particle Reynolds numbers, the correlation does not appear to be

affected by the particle mass loading. However, at low relative Reynolds numbers, the data of Varaksin et al. (1998) shows that the particle mass loading (0.12 – 0.39) must contribute to the coefficient. The fact that there is a correlation lends credence to the model, yet more data is needed at low relative Reynolds numbers to understand the effect of particle mass loading.

Fitting the data shown in Figure 4.1 using the least squares method with the equation

$$\frac{C_{\varepsilon 3}}{C'_{\varepsilon 2}} \approx C_{\varepsilon p}\left(\mathrm{Re}_r\right)^m \tag{4.8}$$

where $C_{\varepsilon p}$ is the fit coefficient equal to 0.058, and m is the exponent found to be 1.416. Substituting Eq. (4.8) into Eq. (3.93) results in a general dissipation transport equation for incompressible flow with no mass transfer between the phases of the form

$$\alpha_c \frac{D\varepsilon}{Dt} = C'_{\varepsilon 1}\alpha_c \frac{P\varepsilon}{k} + C'_{\varepsilon 2}\left[C_{\varepsilon p}\alpha_d \frac{v^2}{V_d}\sum_n \left(\mathrm{Re}_r^m\right)_n f_n \frac{\left|u_i - v_i\right|_n^2}{D_n} - \alpha_c \frac{\varepsilon^2}{k}\right] + \frac{\partial}{\partial x_i}\left[\alpha_c \frac{\nu_T}{\sigma_\varepsilon}\frac{\partial \varepsilon}{\partial x_i}\right] \tag{4.9}$$

where V_d is the total volume of the dispersed phase particles within the mixture volume. For steady state dispersed phase systems with no diffusion or mean carrier phase velocity gradients, Eq. (4.9) reduces to

$$\varepsilon = \left[0.0587\mathrm{Re}_r^{\,1.4169}\frac{\alpha_d}{\alpha_c}\frac{kv^2}{V_d}\sum_n f_n \frac{\left|u_i - \left(v_i\right)_n\right|^2}{D_n}\right]^{1/2} \tag{4.10}$$

A comparison of the model prediction of the dissipation found from experimental data is shown in Figure 4.2. The data of Hosokawa and Varaksin did not include results for the dissipation.

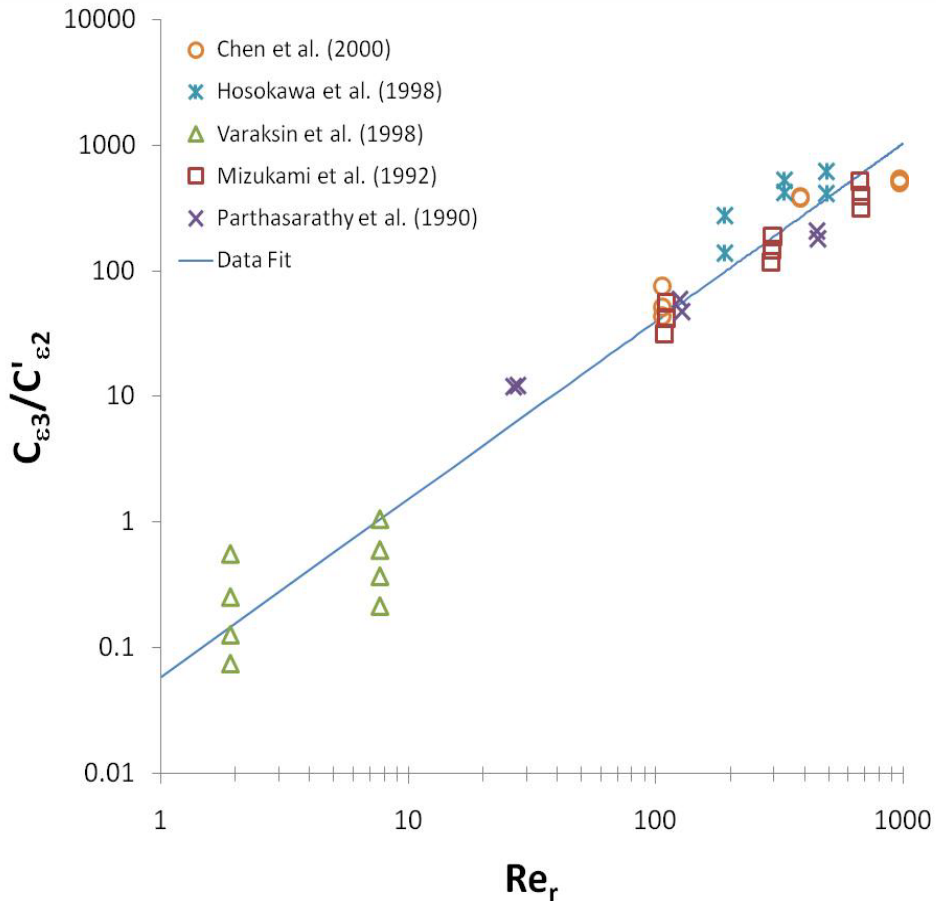

Figure 4.1: Variation of the ratio of the production of dissipation coefficient ($C_{\varepsilon 3}$) to the dissipation of dissipation coefficient ($C'_{\varepsilon 2}$) over a wide range of relative Reynolds numbers for various types of particle laden flows. For low relative Reynolds numbers, the data of Varaksin et al. (1998) shows that the ratio of coefficients depends on the particle mass loading – for increased loading, the ratio of coefficients is increased.

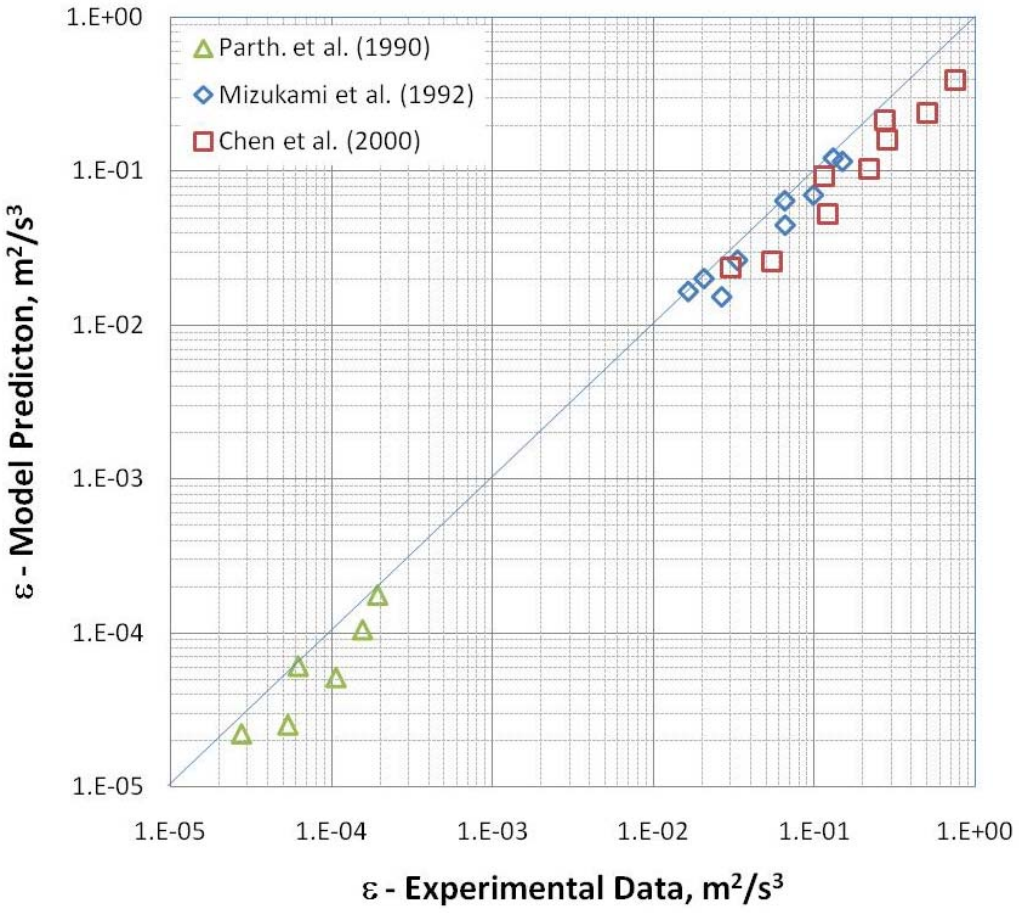

Figure 4.2: Comparison of the dissipation predicted by the model to the experimental data of Parthasarathy et al. (1990), Mizukami et al. (1992), and Chen et al. (2000).

CHAPTER FIVE

THE DISSIPATION OF DISSIPATION COEFFICIENT

In the recent decade, direct numerical solution has been used to study the effects of particles on the modulation of turbulence within the carrier phase. Squires and Eaton (1990) simulated a large number of particles using direct numerical simulation. The turbulence was forced at low wave numbers and the governing equations were solved using pseudo-spectral methods. The Reynolds number was ~37 and the solution was shown to be grid independent by increasing the number of grid points from 32^3 to 64^3. The particles were modeled as point forces using the particle-source-in-cell (PSIC) method. To account for interactions between cells, the overall force was interpolated back to the surrounding eight grid points using volume-weighted averaging. Their results showed that the presence of particles (for a mass loading from 0 – 1) tend to decrease the turbulent kinetic energy and dissipation relative to un-laden flows. If the response time of the particle is increased, the dissipation and turbulent kinetic energy is further reduced. Ferrante and Elghobashi (2003) also used DNS techniques to study the effect of a large number of particles in the flow. They used second order finite differencing rather than pseudo-spectral methods on a 256^3 grid and tracked upwards of $8 \cdot 10^7$ particles.

The results of the work of Ferrante and Elghobashi show decreased kinetic energy with certain particle properties, but they also show increased kinetic energy and no change in kinetic energy all relative to un-laden flow. In other words, there appears to be combined particle and fluid properties that would produce dissipation, destroy dissipation or yield no net dissipation such that the particle-laden flow behaves as though it did not have any particles. The particles that produced no net change in turbulent kinetic energy relative to an un-laden flow were referred to as "ghost particles". The parameter used by Ferrante and Elghobashi to distinguish between these three regimes is the ratio of the particle response time to the Kolmogorov time scale (τ_p / τ_k).

Burton and Eaton (2005) used an overset grid technique to directly resolve the flow around a single particle in a turbulent field. Their simulations focused on a Reynolds number around 30 with a 192^3 and 384^3 grid. By comparing laden simulations to un-laden, they found that within 1.5 particle diameters from the surface the dissipation was enhanced and beyond 5 particle diameters the level of turbulence was not affected. They concluded that the drag force was the dominate force of all the forces acting on the particle. They also determined that the volume fraction and the formation of the boundary layer on the particle appeared to modify the turbulence in a local region.

Schreck and Kleis (1993) studied how particles modify grid-generated turbulence. They uniformly dispersed glass and plastic particles ranging in diameter from 0.6 mm to 0.71 mm into a stream of water. Their results show that the presence of particles attenuated the carrier phase turbulent kinetic energy. The attenuation was more pronounced at higher particle volume concentrations and larger particle densities. The particle volume concentrations varied from 0.4% to 1.5%. Geiss et al. (2001, 2004) also

studied the modulation of carrier phase turbulent kinetic energy by particles. The particles were glass having a nominal diameter of 110 - 480 μm. The experimental setup of Geiss et al. (2001) was a modified version of the setup used by Kulick et al. (1993). They report attenuation of turbulent kinetic energy with particles in the axial flow direction.

The dissipation of dissipation coefficient is typically calibrated for homogeneous, isotropic turbulence decay. This involves data from flow behind a grid or direct numerical simulation (DNS). The dissipation of dissipation coefficient for particle laden flows is assumed to be of the form

$$C'_{\varepsilon 2} = C_{\varepsilon 2} + C_{\varepsilon 2p} \tag{5.1}$$

where $C_{\varepsilon 2}$ is the single phase coefficient (1.92) and $C_{\varepsilon 2p}$ is the contribution of the particles to the dissipation of dissipation. It is a requirement that $C_{\varepsilon 2p}$ goes to zero as the flow transitions to single phase, thus $C_{\varepsilon 2p}$ must be a function of one or more of the four fundamental non-dimensional variables found in particle laden flows

$$C_{\varepsilon 2p} = f(\mathrm{Re}, \mathrm{Re}_r, C, St) \tag{5.2}$$

where Re is the Reynolds number of the fluid, Re_r is the relative Reynolds number, C is the particle mass concentration and St is the Stokes number. The experimental data needed to calibrate the dissipation of dissipation coefficient ($C'_{\varepsilon 2}$) are insufficient; however, direct numerical simulations (DNS) can be used to find the particle contribution to the dissipation of dissipation coefficient.

The current research differs from previous studies by modeling the decay of homogeneous turbulence in a field of stationary particles. The rationale for the use of stationary particles is to minimize the production of dissipation by particles by assuming

that the particles are traveling at the same speed as the decaying fluid. A comparison between DNS simulations with no particles (i.e. single phase) and with stationary particles applied at discrete grid points is used to understand the effect of the particles on the dissipation of dissipation coefficient. The purpose of this study is to determine how the presence of particles alters the dissipation of dissipation coefficient $(C'_{\varepsilon 2})$ in the volume averaged k-ε model.

5.1 Governing Equations for DNS

A spectral based code was used to simulate all the length scales of an isotropic homogeneous turbulent decay. The benefit is that no closure model is needed as the length and time scales within the flow are directly resolved. Orzag and Patterson (1972) and Rogallo (1981) developed and used this method to study isotropic, homogeneous turbulence.

In a DNS environment, the Navier-Stokes equations are non-dimesionalized and solved for in Fourier space due to the accuracy in determining the spatial gradients. The physical velocity is expressed using a Fourier series of the form

$$u_i(x_j,t) = \sum_k e^{ik_j x_j} \hat{u}_i(k_j,t) \tag{5.3}$$

and the orthogonality condition is applied to solve for the velocity coefficients. Within the Fourier domain, a point force is applied at distinct grid points to simulate a stationary particle. For incompressible flow, the non-dimensional Navier-Stokes equations with a point force due to stationary particles are shown to be

$$\frac{\partial \tilde{u}_i}{\partial \tilde{t}} + \tilde{u}_j \frac{\partial \tilde{u}_i}{\partial \tilde{x}_j} = -\frac{\partial \tilde{P}}{\partial \tilde{x}_j} + \mathrm{Re}_L^{-1} \frac{\partial^2 \tilde{u}_i}{\partial \tilde{x}_j^2} - \frac{3\pi \tilde{D}}{\Delta \tilde{V}} \mathrm{Re}_L^{-1} f \tilde{u}_i \tag{5.4}$$

where the equation was non-dimensionalized by the mean fluid velocity (U) and the domain length scale (L). The tilde represents the non-dimensional form of each term, where $\tilde{t}$ is the non-dimensional time, $\tilde{D}$ is the non-dimensional particle diameter, $\Delta\tilde{V}$ is the non-dimensional volume of the computational cell, f is the drag factor, and Re_L is the Reynolds number. The energy spectrum used to initialize the domain was the form

$$E(\kappa) = \lambda\left(\frac{\kappa/c}{1+(\kappa/c)^2}\right)^4 \tag{5.5}$$

where λ and c are constants and κ is the wavenumber (McMurtry, 1987, de Bruyn Kops et al. 1989). To ensure that the smallest scales are being modeled, the grid was set to be smaller than the Kolmogorov length scale ($\eta\kappa_{max} > 1$). To avoid aliasing effects, the 2/3 rule was applied to determine the maximum wave number based on the number of grid points chosen and spherical truncation was applied to the domain. All spatial derivatives were computed using pseudo-spectral methods. The length of the domain was set at 2π and the boundary conditions were periodic. The time stepping routine was a second order Adam-Bashforth algorithm. Additional details on the development of the code can be found in McMurtry, 1987.

The non-dimensional Navier Stokes equation (5.4) can be represented in Fourier space as

$$\frac{\partial\hat{\tilde{u}}_i}{\partial\tilde{t}} = \left[\delta_{ij} - \frac{\kappa_i\kappa_j}{\kappa^2}\right] T\left[\varepsilon_{jkl}\tilde{u}_k\tilde{\omega}_l\right] - \tilde{\nu}\kappa^2\hat{\tilde{u}}_i - \frac{3\pi\tilde{\nu}}{\Delta\tilde{V}} N\tilde{D}f\,\hat{\tilde{u}}_i \tag{5.6}$$

where $\hat{\tilde{u}}_i$ are the non-dimensional Fourier velocity coefficients, N is the number of particles, δ_{ij} is the Kronecker delta, ε_{jkl} is the permutation tensor, $\tilde{\omega}_l$ is the non-dimensional vorticity and κ_i is wavnumber vector in the Fourier domain. From the above

equation, it is clear that the presence of particles appear to behave as an increase in non-dimensional viscosity. Thus the non-dimensional force due to particles can be solved in Fourier space rather than physical space and the above equation takes the form

$$\frac{\partial \hat{\tilde{u}}_i}{\partial \tilde{t}} = \left[\delta_{ij} - \frac{\kappa_i \kappa_j}{\kappa^2}\right] T\left[\varepsilon_{jkl}\tilde{u}_k\tilde{\omega}_l\right] - \frac{1}{\mathrm{Re}_L}\left(\kappa^2 + \frac{3\pi}{\Delta\tilde{V}} N\tilde{D}f\right)\hat{\tilde{u}}_i \tag{5.7}$$

5.2 Validating the single phase DNS Results

To validate the code, the non-dimensional viscosity was set to 0.08 (Re_L = 12.5) and the results of a 64^3 domain were compared to 128^3 (shown in Figure 5.1). In addition, the decay rate predicted by the DNS model was compared to the decay power law [$k/k_o = (t/t_o)^{-n}$] (Pope, 2000). For the case of Re_L = 12.5 and an exponent of n = 1.56, the slope of the decay model closely matches the slope of the DNS results (Figure 5.1). The literature shows values for decay exponent in the range of $1.15 < n < 1.45$ (Pope, 2000).

5.3 Non-dimensionalization of the Dissipation Equation

To determine the effect of particles on the dissipation of dissipation coefficient, stationary particles are placed at various grid points within a DNS domain. The flow is isotropic and homogeneous with stationary forces representing the particles at each grid point within the flow. For this case, the dissipation rate model, Eq. (3.93), reduces to the form

$$\alpha_c \frac{\partial \varepsilon}{\partial t} = -C'_{\varepsilon 2}\alpha_c \frac{\varepsilon^2}{k} + C_{\varepsilon 3}\frac{v^2}{V}\sum_n f_n \frac{\left|\delta u_i\right|_n^2}{D_n} \tag{5.8}$$

Defining the non-dimensional terms in the dissipation equation

$$
\begin{aligned}
\tilde{\varepsilon} &= \frac{L}{U^3}\varepsilon \\
\tilde{k} &= \frac{1}{U^2}k \\
\tilde{t} &= \frac{L}{U}t \\
\tilde{D} &= \frac{D}{L} \\
\tilde{v} &= \frac{1}{UL}v \\
\tilde{V} &= \frac{1}{L^3}V \\
\delta\tilde{u}_i &= \frac{\delta u_i}{U}
\end{aligned}
\tag{5.9}
$$

Substituting Eq. (5.9) into Eq. (5.8), the dissipation rate equation can be represented in non-dimensional form as

$$
\alpha_c \frac{U^4}{L^2}\frac{\partial\tilde{\varepsilon}}{\partial\tilde{t}} = -C'_{\varepsilon 2}\alpha_c \frac{U^4}{L^2}\frac{\tilde{\varepsilon}^2}{\tilde{k}} + C_{\varepsilon 3}\frac{U^4}{L^2}\frac{\tilde{v}^2}{\tilde{V}}\sum_n f_n \frac{\left|\delta\tilde{u}_i\right|_n^2}{\tilde{D}_n} \tag{5.10}
$$

The above equation is then reduced to

$$
\alpha_c \frac{\partial\tilde{\varepsilon}}{\partial\tilde{t}} = -C'_{\varepsilon 2}\alpha_c \frac{\tilde{\varepsilon}^2}{\tilde{k}} + C_{\varepsilon 3}\frac{\tilde{v}^2}{\tilde{V}}\sum_n f_n \frac{\left|\delta\tilde{u}_i\right|_n^2}{\tilde{D}_n} \tag{5.11}
$$

Assuming that a particle is placed at every grid point within the DNS domain and that the particle diameter is the same, the non-dimensional velocity deviations can be represented by the non-dimensional turbulent kinetic energy ($\tilde{k}$), and Eq. (5.11) can be further reduced to

$$
\alpha_c \frac{\partial\tilde{\varepsilon}}{\partial\tilde{t}} = -C'_{\varepsilon 2}\alpha_c \frac{\tilde{\varepsilon}^2}{\tilde{k}} + C_{\varepsilon 3}\frac{\tilde{v}^2}{\tilde{V}} N_p f_n \frac{2\tilde{k}}{\tilde{D}_n} \tag{5.12}
$$

where N_p represents the number of particles (or grid points for a single particle placed at every grid point). Substituting Eq. (4.8) for $C_{\varepsilon 3}$ into Eq. (5.12) shows

$$
\frac{\partial\tilde{\varepsilon}}{\partial\tilde{t}} = C'_{\varepsilon 2}\left[-\frac{\tilde{\varepsilon}^2}{\tilde{k}} + 2C_{\varepsilon p}\,\mathrm{Re}_r^m\, N_p \frac{\tilde{v}^2 f \tilde{k}}{\alpha_c \tilde{V}\tilde{D}}\right] \tag{5.13}
$$

where $C_{\varepsilon p} = 0.058$ and $m = 1.416$.

5.4 Method for Determining the Dissipation of Dissipation Coefficient ($C'_{\varepsilon 2}$)

From the DNS results, the volume averaged dissipation and kinetic energy are computed for each time step. The time rate of change of dissipation is computed using a central differencing scheme. The terms in brackets on the right hand side (RHS) of Eq. (5.13) are easily computed and compared to the non-dimensional time rate of change of dissipation. The coefficient is adjusted such that the square of the difference between both sides of the equation is minimized. This is defined as

$$\left[\sum_{1}^{N_t}\left\{\frac{\partial\widetilde{\varepsilon}}{\partial\widetilde{t}} - C'_{\varepsilon 2}\left[-\frac{\widetilde{\varepsilon}^2}{\widetilde{k}} + 2C_{\varepsilon p}\,\mathrm{Re}_r^m\,N_p\,\frac{\widetilde{v}^2 f\widetilde{k}}{\alpha_c\widetilde{V}\widetilde{D}}\right]\right\}^2\right]^{1/2} \approx 0 \tag{5.14}$$

where N_t is the number of time steps over which the equation is applied.

The dissipation of dissipation coefficient for particle laden flows is shown in Eq. (5.1). It is a requirement that $C_{\varepsilon 2p}$ approaches zero as the flow transitions to single phase. Therefore $C_{\varepsilon 2p}$ must be a function of one or more of the four fundamental non-dimensional parameters related to the particulate phase (shown in Eq. (5.2)). An analysis of Eq. (5.4) shows that the non-dimensional form of the coefficient for the force due to the presence of particles is related to the ratio of particle concentration to the Stokes number (C/St) – where the Stokes number is defined as the ratio of the particle response time to the fluid time scale (defined in terms of the free stream velocity and a length scale based on the size of the domain). Therefore, it is proposed that the dissipation of dissipation coefficient due to the presence of particles, within Eq. (5.1), can be modeled as a function of

$$C_{\varepsilon 2p} \approx f\left(\frac{C}{St}\right) \tag{5.15}$$

A comparison between DNS simulations with and without stationary particles is used to assess the effect of the particles on the overall dissipation of dissipation coefficient.

The effect of particle loading is shown in Figures 5.2(a) and 5.2(b). As the ratio of concentration over Stokes number is increased, the particles rapidly attenuate the turbulent kinetic energy (Figure 5.2(a)) and dissipation (Figure 5.2(b)). The notion of decreased turbulent kinetic energy for increased loading is in agreement with the DNS work of Squires and Eaton (1990) and also the experimental work of Schreck and Kleis (1993). The trends for dissipation show that the slope is becoming more negative as the concentration is increased; from Eq. (5.13) it can be seen that the additional production of dissipation term (due to particles) does not account for this case. Therefore, the dissipation of dissipation must balance with the production of dissipation due to particles and the time rate of change of dissipation due to turbulent decay. Based on the trends, it is hypothesized that the particle contribution to the dissipation of dissipation coefficient can be modeled of the form described in Eq. (5.15).

In order to validate this hypothesis, two different Reynolds numbers were used, Re_L = 12.5 and 3.3. The Reynolds number of 12.5 is close to the turbulent decay region found in literature (n = 1.56) and the Reynolds number of 3.3 is close to the final decay region (n = 2.5). An iterative method was used to determine the dissipation of dissipation coefficient $C'_{\varepsilon 2}$. The time rate of change of dissipation in Eq. (5.14) was computed from DNS results for dissipation using a central difference scheme. The comparison was based on the range of Taylor scale Reynolds numbers (~4.5 – 0.01) that agreed with the results from the power decay law. The DNS results for k and ε were substituted into Eq.

(5.14) and $C'_{\varepsilon 2}$ was iterated until Eq. (5.14) was minimized. It was found that the additional production of dissipation term was negligible due to the low relative Reynolds number. Based on the results, it is clearly seen that the slopes are captured for each C/St (ranging from 1 – 10) by merely increasing the coefficient – $C'_{\varepsilon 2}$, shown in Figures 5.3(a) and 5.3(b).

With this method, the contribution to the coefficient of dissipation of dissipation due to the presence of particles can be isolated. The dissipation coefficient for the single phase ($C_{\varepsilon 2}$) was determined from the DNS results with no particles. The effect of $C_{\varepsilon 2p}$ is determined from Eq. (5.1) and plotted against the ratio of concentration to Stokes number, as proposed in Eq. (5.15) and shown in Figure 5.4. The results show that the effect of the particles on the dissipation of dissipation coefficient $\left(C_{\varepsilon 2p}\right)$ correlated well to the ratio of the particle concentration to the Stokes number. From the data, it is clear that for particle laden flows involving low concentrations and high Stokes numbers, the effect of the particles on the dissipation of dissipation term is negligible, thus the single phase coefficient is adequate. However, for particle laden flows involving high concentrations and low Stokes numbers (e.g. dusty gas conditions) the presence of particles can have a significant effect on the dissipation of dissipation term when compared to single phase. The above results were fit using the least squares method. The fit is found to be of the form

$$C_{\varepsilon 2p} = \xi\left(\frac{C}{St}\right)^m \tag{5.16}$$

where ξ is 0.362 and m is 0.76. It can also be seen that the effects of the fluid Reynolds number may not be important at the lower C/St values, however this may not be the case

at higher C/St. The results, plotted as a function of $\frac{C}{St}\cdot \mathrm{Re}$, are shown in Figure 5.5 and seem to collapse rather nicely. The values were fit using a least squares method and found to be of the form

$$C_{\varepsilon 2p} = 0.062\left(\frac{C}{St}\mathrm{Re}\right)^{0.83} \tag{5.17}$$

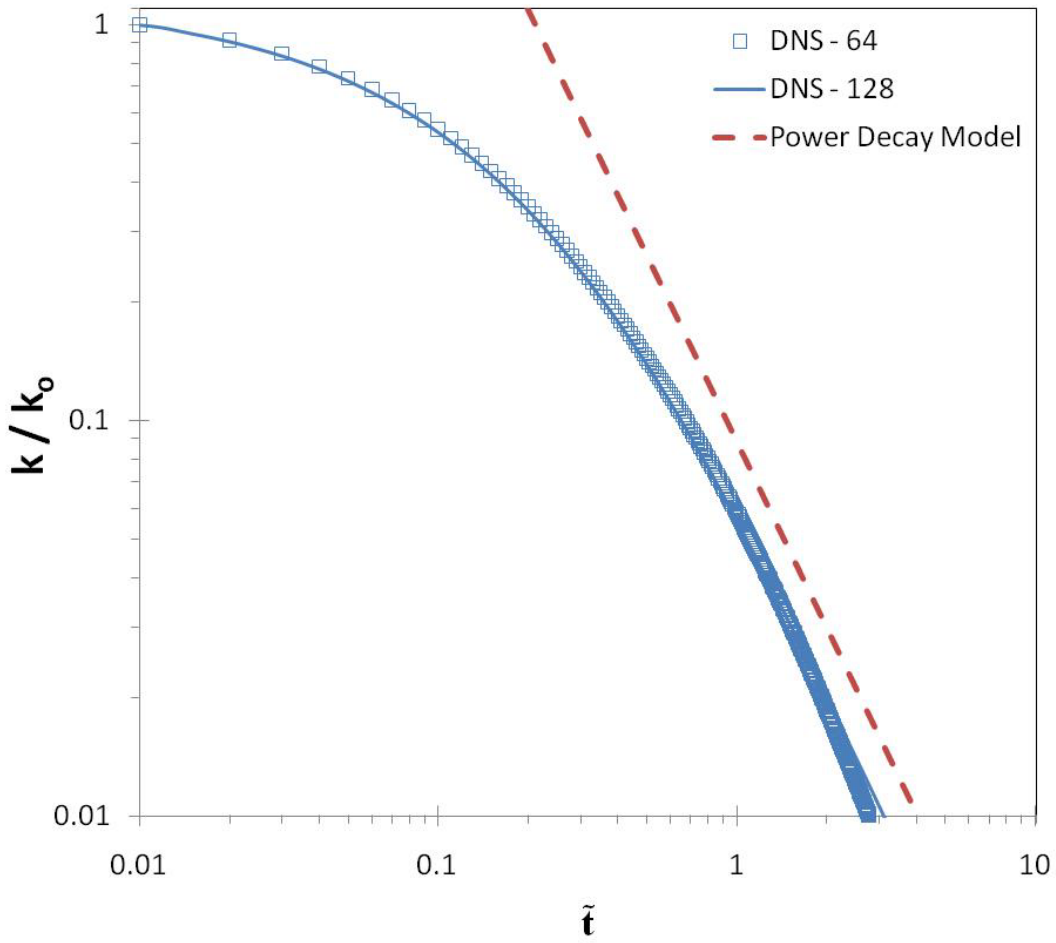

Figure 5.1: Comparison of DNS results with the power decay model (Pope, 2000) for n = 1.56 over the non-dimensional time ($\tilde{t}$) for Re_L = 12.5: the power decay model is offset intentionally for clarity.

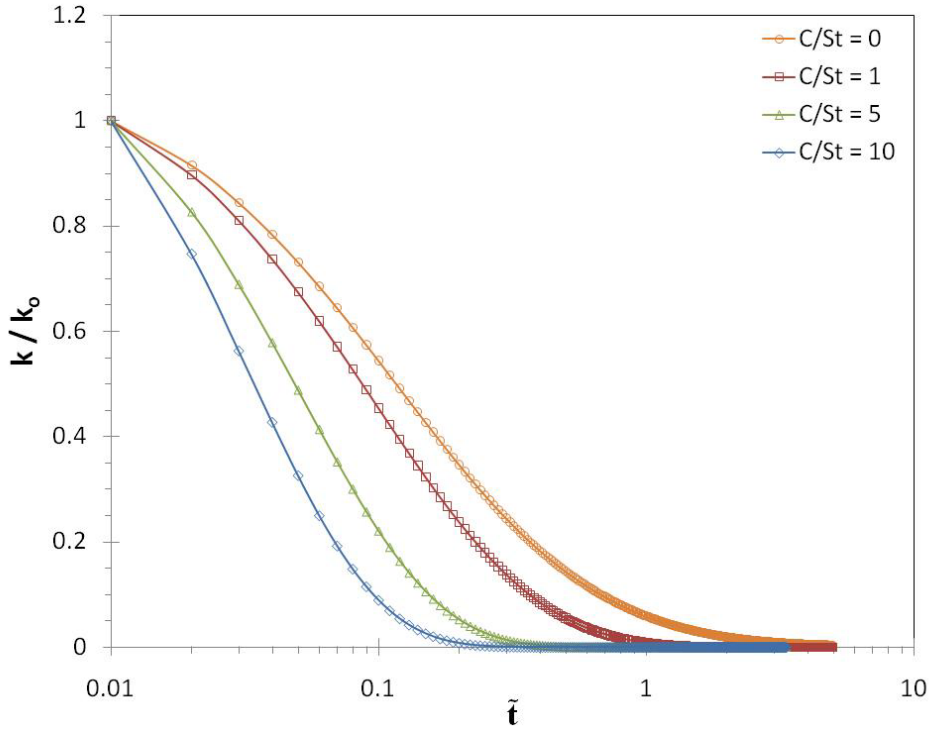

(a)

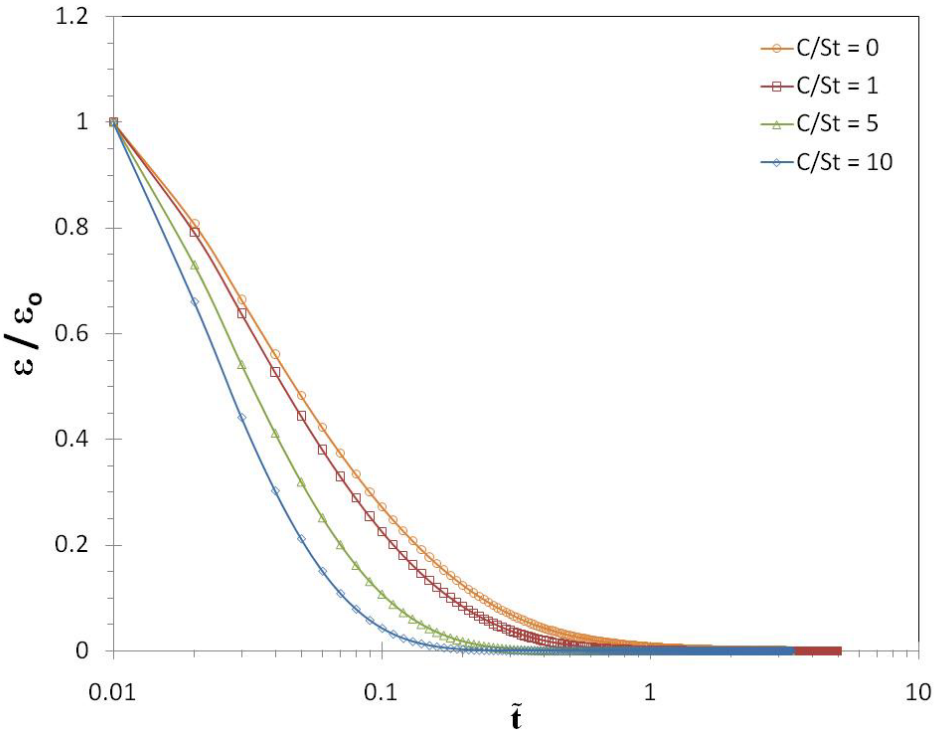

(b)

Figure 5.2: DNS comparison of various particle loadings over the non-dimensional time ($\tilde{t}$) for Re_L = 12.5: (a) effect of particle loading on normalized TKE, (b) effect of particle loading on normalized dissipation (the TKE and dissipation are normalized by the initial value).

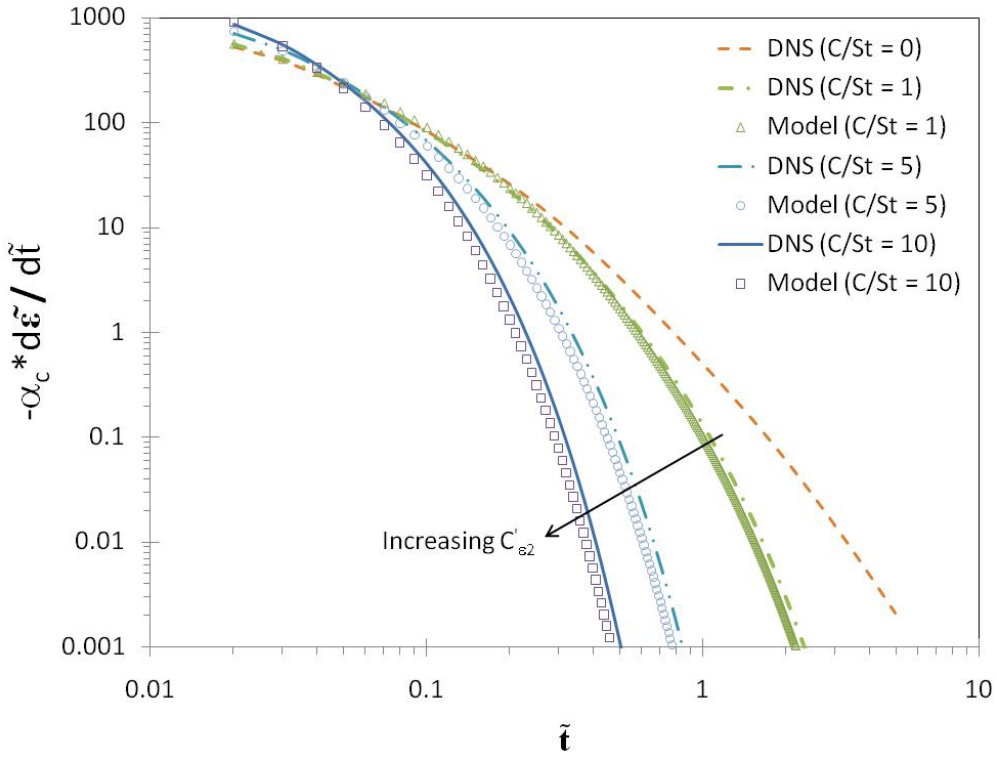

(a)

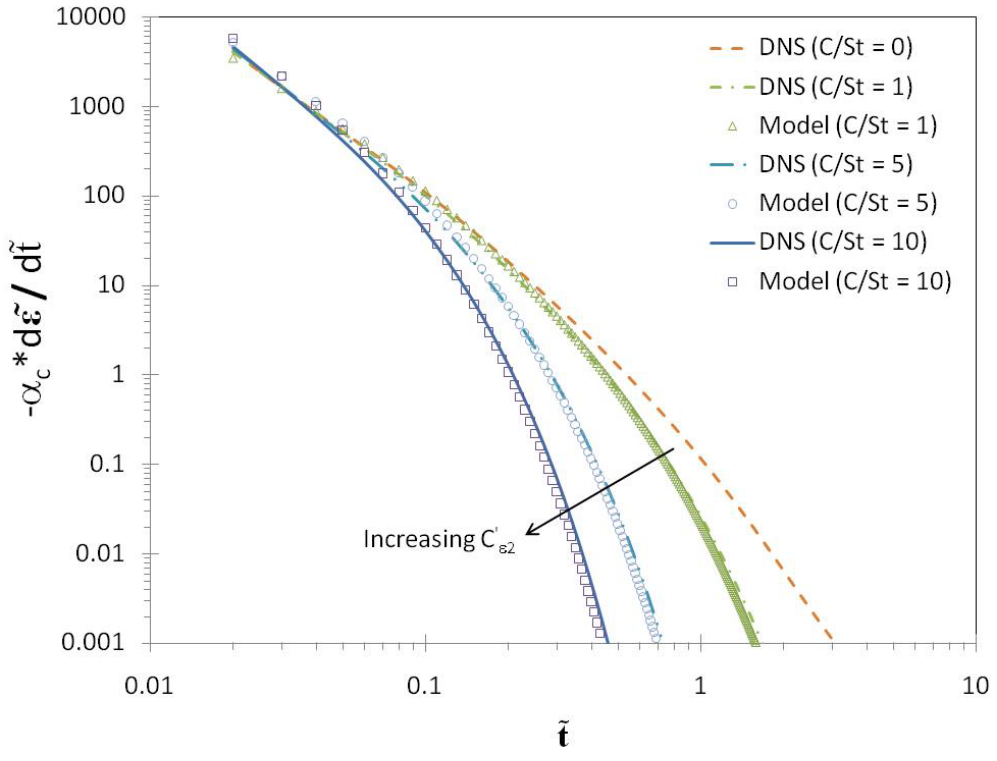

(b)

Figure 5.3: Comparison of the dissipation with $C'_{\varepsilon 2}$ to the DNS results over the non-dimensional time ($\tilde{t}$): (a) Re_L = 12.5, (b) Re_L = 3.3. These results show that by increasing $C'_{\varepsilon 2}$ with C/St, the trends can be modeled accurately.

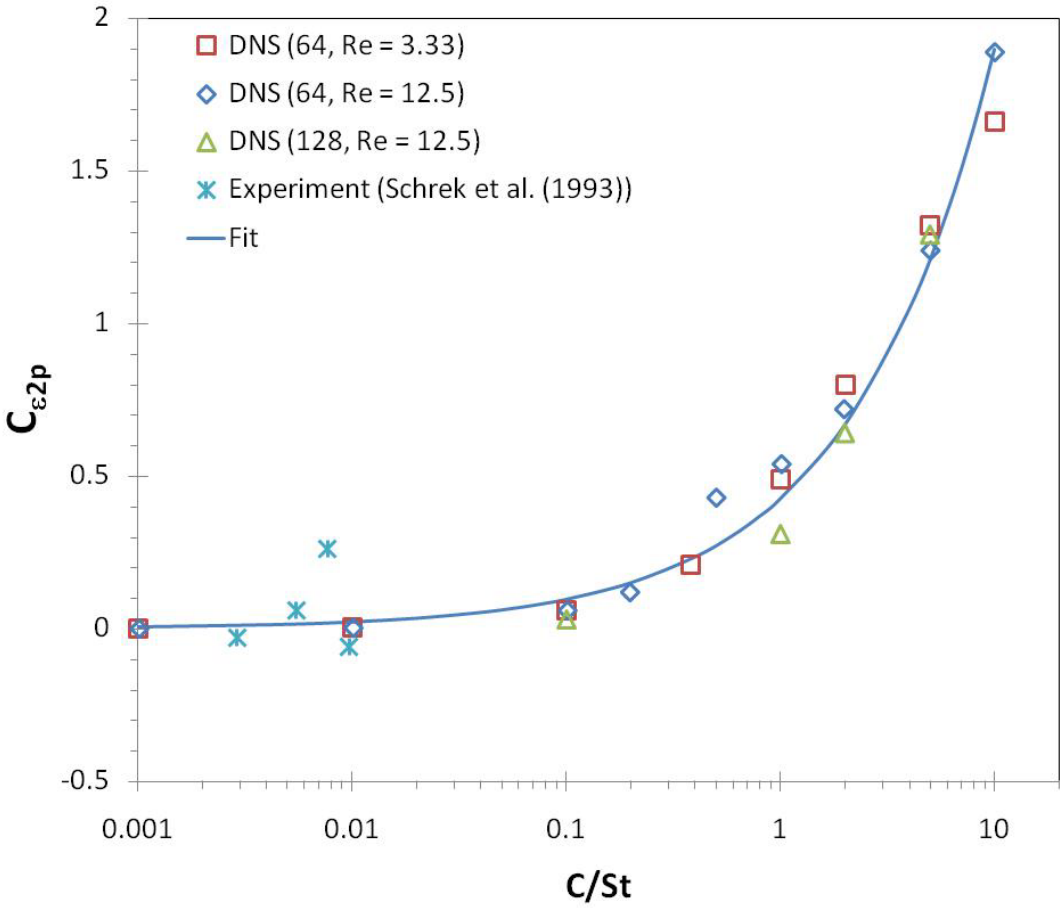

Figure 5.4: The contribution of particles to the dissipation of dissipation coefficient ($C_{\varepsilon 2p}$) correlated with the particle concentration over the Stokes number (C/St). The legend shows the number of grid points in each direction along with the Reynolds number.

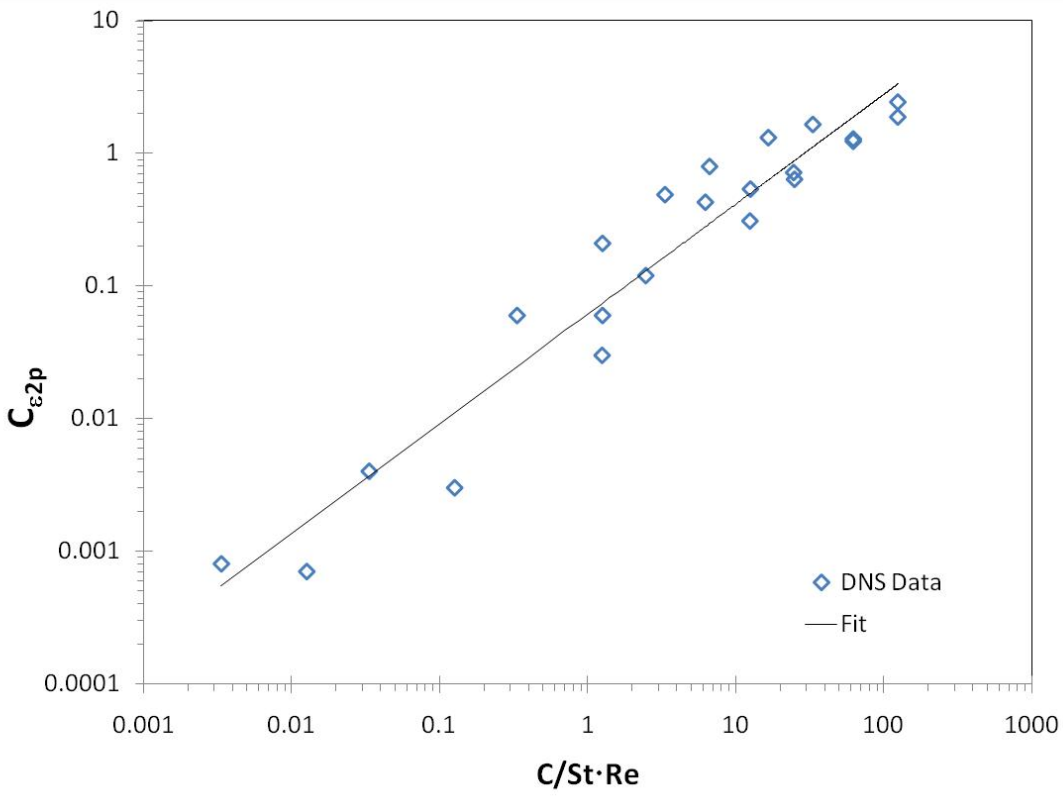

Figure 5.5: The contribution of particles to the dissipation of dissipation coefficient ($C_{\varepsilon 2p}$) correlated with the Reynolds number (Re_L) and the particle concentration over the Stokes number (C/St).

CHAPTER SIX

THE PRODUCTION OF DISSIPATION COEFFICIENT DUE TO MEAN VELOCITY GRADIENTS

In the dissipation transport model, Eq. (3.93), a production of dissipation term due to the mean velocity gradients was modeled. It was not assumed that the coefficient for the production of dissipation due to mean velocity gradients is equal to 1.44, as used for single phase flows, but rather assumed that the presence of particles may alter this coefficient. In this chapter, the additional effect of particles on the production of dissipation coefficient (due to mean velocity gradients) is evaluated.

6.1 Determining the Production of Dissipation Coefficient ($C'_{\varepsilon 1}$)

The production of dissipation coefficient due to mean velocity gradients is equal to 1.44 for single phase flows. In order to validate this coefficient, the flow of particles in a turbulent channel flow is evaluated. Assuming the diffusion of kinetic energy near the wall in a fully developed channel flow with particles is negligible, the volume averaged turbulent kinetic energy equation presented by Crowe and Gillandt (1998) is reduced to

$$0 = -\alpha_c P_k - \alpha_c \varepsilon + \frac{1}{N}\sum_n \frac{\beta_V}{\rho_c}\left[u_i - v_i\right]_n\left[\langle u_i\rangle - v_i\right]_n \tag{6.1}$$

Assuming that the shear near the wall is constant, the production can be modeled as

$$P_k = -\upsilon_T \left(\frac{d\langle u \rangle}{dy} \right)^2 \tag{6.2}$$

Kulick et al. (1993) showed that the law of the wall profile is valid with particles; with this assumption the dissipation near the wall is found to be

$$\varepsilon = \frac{u_\tau^3}{\kappa y} + \frac{1}{N} \sum_n \frac{\beta_V}{\alpha_c \rho_c} [u_i - v_i]_n [\langle u_i \rangle - v_i]_n \tag{6.3}$$

The above equation is the general form of dissipation near the wall. For many cases, this can be simplified by neglecting the redistribution terms. For such a case, the dissipation near the wall can be represented by

$$\varepsilon = \frac{u_\tau^3}{\kappa y} + \frac{\beta_V}{\alpha_c \rho_c} [\langle u_i \rangle - \langle v_i \rangle]^2 \tag{6.4}$$

The kinetic energy is also found by assuming a constant shear layer near the wall. The shear at the wall is related to the friction velocity by

$$C_\mu \frac{k^2}{\varepsilon} \frac{d\langle u \rangle}{dy} = u_\tau^2 \tag{6.5}$$

Again, assuming the law of the wall is valid and substituting in the dissipation near the wall shows a relation for the particle laden turbulent kinetic energy near the wall of the form

$$k = \frac{u_\tau^2}{\sqrt{C_\mu}} \sqrt{\left(1 + \frac{\beta_V \kappa y}{\alpha_c \rho_c u_\tau^3} \left([\langle u_i \rangle - \langle v_i \rangle]^2 + \langle \delta v_i \delta v_i \rangle - \langle \delta u_i \delta v_i \rangle \right) \right)} \tag{6.6}$$

Equations (6.3) and (6.6) assure that production of turbulent kinetic energy due to particles and mean velocity gradients is balanced by dissipation near the wall. In most cases the re-distribution terms can be neglected and Eq. (6.6) can be simplified to

$$k = \frac{u_\tau^2}{\sqrt{C_\mu}} \sqrt{\left(1 + \frac{\beta_V \kappa y}{\alpha_c \rho_c u_\tau^3} \left([\langle u_i \rangle - \langle v_i \rangle]^2 \right) \right)} \tag{6.7}$$

6.1.1 Calibrating the production coefficient ($C'_{\varepsilon 1}$)

To calibrate the production of dissipation coefficient, the volume averaged turbulent dissipation equation, Eq. (3.93), is reduced for steady, fully developed flow conditions

$$0 = C'_{\varepsilon 1}\alpha_c\mu_T\left(\frac{\partial\langle u\rangle}{\partial y}\right)^2\frac{\varepsilon}{k} - C'_{\varepsilon 2}\alpha_c\rho_c\frac{\varepsilon^2}{k} + C_{\varepsilon 3}\rho_c\frac{v^2}{V}\sum_n f_n\frac{|u-v|_n^2}{D_n} + \alpha_c\frac{\partial}{\partial y}\left[\left(\mu+\frac{\mu_T}{\sigma_\varepsilon}\right)\frac{\partial\varepsilon}{\partial y}\right] \tag{6.8}$$

Carrying out the derivative in the last term shows

$$\begin{aligned} 0 = {} & C'_{\varepsilon 1}\alpha_c\mu_T\left(\frac{\partial\langle u\rangle}{\partial y}\right)^2\frac{\varepsilon}{k} - C'_{\varepsilon 2}\alpha_c\rho_c\frac{\varepsilon^2}{k} + C_{\varepsilon 3}\rho_c\frac{v^2}{V}\sum_n f_n\frac{|u-v|_n^2}{D_n} + \alpha_c\left(\mu+\frac{\mu_T}{\sigma_\varepsilon}\right)\frac{\partial^2\varepsilon}{\partial y^2} \\ & + \alpha_c\frac{\rho C_\mu}{\sigma_\varepsilon}\frac{\partial\varepsilon}{\partial y}\left[\frac{2k}{\varepsilon}\frac{\partial k}{\partial y} - \frac{k^2}{\varepsilon^2}\frac{\partial\varepsilon}{\partial y}\right] \end{aligned} \tag{6.9}$$

Near the wall, the gradient of dissipation is

$$\frac{\partial\varepsilon}{\partial y} = -\frac{u_\tau^3}{\kappa y^2} + \left[\langle u\rangle - \langle v\rangle\right]^2\frac{\partial}{\partial y}\left(\frac{\beta_V}{\alpha_c\rho_c}\right) + 2\frac{\beta_V}{\alpha_c\rho_c}\left[\langle u\rangle - \langle v\rangle\right]\left(\frac{\partial\langle u\rangle}{\partial y} - \frac{\partial\langle v\rangle}{\partial y}\right) \tag{6.10}$$

Based on the experimental work of Tsuji et al. (1984), Sheen et al. (1993), Kulick et al. (1993) and Paris et al. (2001), the variation in the particle velocity across the channel is minimal. To simplify, the particle velocity and the particle properties are assumed to be constant. Substituting in the velocity gradient based on the law of the wall profile shows

$$\frac{\partial\varepsilon}{\partial y} = -\frac{u_\tau^3}{\kappa y^2} + 2\frac{\beta_V}{\alpha_c\rho_c}\left[\langle u\rangle - \langle v\rangle\right]\frac{u_\tau}{\kappa y} \tag{6.11}$$

Taking a second derivative yields

$$\frac{\partial^2\varepsilon}{\partial y^2} = 2\frac{u_\tau^3}{\kappa y^3} + 2\frac{\beta_V}{\alpha_c\rho_c}\left(\frac{u_\tau}{\kappa y}\right)^2 - 2\frac{\beta_V}{\alpha_c\rho_c}\left[\langle u\rangle - \langle v\rangle\right]\frac{u_\tau}{\kappa y^2} \tag{6.12}$$

Near the wall the gradient of turbulent kinetic energy is

$$\frac{\partial k}{\partial y} = \frac{\partial}{\partial y}\left[\frac{u_\tau^2}{\sqrt{C_\mu}}\left[1+\frac{\beta_V}{\alpha_c\rho_c}\frac{\kappa y}{u_\tau^3}\left[\langle u\rangle-\langle v\rangle\right]^2\right]^{1/2}\right] \tag{6.13}$$

or

$$\begin{aligned}\frac{\partial k}{\partial y} &= \frac{u_\tau^2}{2\sqrt{C_\mu}}\left[1+\frac{\beta_V}{\alpha_c\rho_c}\frac{\kappa y}{u_\tau^3}\left[\langle u\rangle-\langle v\rangle\right]^2\right]^{-1/2} * \\ &\left[\left[\langle u\rangle-\langle v\rangle\right]^2\frac{\kappa y}{u_\tau^3}\frac{\partial}{\partial y}\left(\frac{\beta_V}{\alpha_c\rho_c}\right)+\frac{\beta_V}{\alpha_c\rho_c}\frac{\kappa}{u_\tau^3}\left[\langle u\rangle-\langle v\rangle\right]^2+2\frac{\beta_V}{\alpha_c\rho_c}\frac{\kappa y}{u_\tau^3}\left[\langle u\rangle-\langle v\rangle\right]\left(\frac{\partial\langle u\rangle}{\partial y}-\frac{\partial\langle v\rangle}{\partial y}\right)\right]\end{aligned} \tag{6.14}$$

Again, to simplify, the particle velocity and the particle properties are assumed to be constant across the channel. Substituting in the velocity gradient based on the law of the wall profile shows

$$\frac{\partial k}{\partial y} = \frac{u_\tau^2}{2\sqrt{C_\mu}}\left[1+\frac{\beta_V}{\alpha_c\rho_c}\frac{\kappa y}{u_\tau^3}\left[\langle u\rangle-\langle v\rangle\right]^2\right]^{-1/2}\left[\frac{\beta_V}{\alpha_c\rho_c}\frac{\kappa}{u_\tau^3}\left[\langle u\rangle-\langle v\rangle\right]^2+\frac{2\beta_V}{\alpha_c\rho_c u_\tau^2}\left[\langle u\rangle-\langle v\rangle\right]\right] \tag{6.15}$$

Substituting equation (6.15), (6.12), and (6.11) into equation (6.9) results in

$$\begin{aligned}0 &= C'_{\varepsilon 1}\alpha_c\mu_T\left(\frac{\partial\langle u\rangle}{\partial y}\right)^2\frac{\varepsilon}{k}-C'_{\varepsilon 2}\alpha_c\rho_c\frac{\varepsilon^2}{k}+C_{\varepsilon 3}\rho_c\frac{v^2}{V}\sum_n f_n\frac{|u-v|_n^2}{D_n} \\ &+\alpha_c\left(\mu+\frac{\mu_T}{\sigma_\varepsilon}\right)\left(2\frac{u_\tau^3}{\kappa y^3}+2\frac{\beta_V}{\alpha_c\rho_c}\left(\frac{u_\tau}{\kappa y}\right)^2-2\frac{\beta_V}{\alpha_c\rho_c}\left[\langle u\rangle-\langle v\rangle\right]\frac{u_\tau}{\kappa y^2}\right) \\ &+\alpha_c\frac{\rho C_\mu}{\sigma_\varepsilon}\frac{2k}{\varepsilon}\frac{u_\tau^2}{2\sqrt{C_\mu}}\left[1+\frac{\beta_V}{\alpha_c\rho_c}\frac{\kappa y}{u_\tau^3}\left[\langle u\rangle-\langle v\rangle\right]^2\right]^{-1/2}\left[\frac{\beta_V}{\alpha_c\rho_c}\frac{\kappa}{u_\tau^3}\left[\langle u\rangle-\langle v\rangle\right]^2+\frac{2\beta_V}{\alpha_c\rho_c u_\tau^2}\left[\langle u\rangle-\langle v\rangle\right]\right]* \\ &\left(-\frac{u_\tau^3}{\kappa y^2}+2\frac{\beta_V}{\alpha_c\rho_c}\left[\langle u\rangle-\langle v\rangle\right]\frac{u_\tau}{\kappa y}\right)-\alpha_c\frac{\rho C_\mu}{\sigma_\varepsilon}\frac{k^2}{\varepsilon^2}\left(-\frac{u_\tau^3}{\kappa y^2}+2\frac{\beta_V}{\alpha_c\rho_c}\left[\langle u\rangle-\langle v\rangle\right]\frac{u_\tau}{\kappa y}\right)^2\end{aligned} \tag{6.16}$$

Substituting in the equations for k and ε near the wall, Eq. (6.7) and (6.4) respectively, gives

$$
\begin{aligned}
0 = & \left(C'_{\varepsilon 1}\alpha_c\rho_c\frac{u_\tau^3}{\kappa y} - C'_{\varepsilon 2}\alpha_c\rho_c\left(\frac{u_\tau^3}{\kappa y}+\frac{\beta_V}{\alpha_c\rho_c}\left[\langle u_i\rangle-\langle v_i\rangle\right]^2\right)\right)\frac{\frac{u_\tau^3}{\kappa y}+\frac{\beta_V}{\alpha_c\rho_c}\left[\langle u_i\rangle-\langle v_i\rangle\right]^2}{\frac{u_\tau^2}{\sqrt{C_\mu}}\sqrt{\left(1+\frac{\beta_V\kappa y}{\alpha_c\rho_c u_\tau^3}\left(\left[\langle u_i\rangle-\langle v_i\rangle\right]^2\right)\right)}} \\
& + C_{\varepsilon 3}\rho_c\frac{v^2}{V}\sum_n f_n\frac{|u-v|_n^2}{D_n} + \alpha_c\left(\mu+\frac{\mu_T}{\sigma_\varepsilon}\right)\left(2\frac{u_\tau^3}{\kappa y^3}+2\frac{\beta_V}{\alpha_c\rho_c}\left(\left(\frac{u_\tau}{\kappa y}\right)^2-\left[\langle u\rangle-\langle v\rangle\right]\frac{u_\tau}{\kappa y^2}\right)\right) \\
& + \alpha_c\frac{\rho u_\tau^4}{\sigma_\varepsilon}\frac{\beta_V}{\alpha_c\rho_c}\left[\frac{\kappa}{u_\tau^3}\left[\langle u\rangle-\langle v\rangle\right]^2+\frac{2}{u_\tau^2}\left[\langle u\rangle-\langle v\rangle\right]\right]\frac{\left(-\frac{u_\tau^3}{\kappa y^2}+2\frac{\beta_V}{\alpha_c\rho_c}\left[\langle u\rangle-\langle v\rangle\right]\frac{u_\tau}{\kappa y}\right)}{\frac{u_\tau^3}{\kappa y}+\frac{\beta_V}{\alpha_c\rho_c}\left[\langle u_i\rangle-\langle v_i\rangle\right]^2} \\
& - \alpha_c\frac{\rho u_\tau^4}{\sigma_\varepsilon}\left(1+\frac{\beta_V\kappa y}{\alpha_c\rho_c u_\tau^3}\left(\left[\langle u_i\rangle-\langle v_i\rangle\right]^2\right)\right)\left[\frac{\left(-\frac{u_\tau^3}{\kappa y^2}+2\frac{\beta_V}{\alpha_c\rho_c}\left[\langle u\rangle-\langle v\rangle\right]\frac{u_\tau}{\kappa y}\right)}{\left(\frac{u_\tau^3}{\kappa y}+\frac{\beta_V}{\alpha_c\rho_c}\left[\langle u_i\rangle-\langle v_i\rangle\right]^2\right)}\right]^2
\end{aligned}
\tag{6.17}
$$

The above equation can be used to determine the production coefficient due to mean velocity gradients. However, from the experimental data, the shear at the wall is not given and the von Karman constant (0.4) is questionable in particle laden turbulent flows. Additional experimentation is needed to determine these parameters, which are necessary to calibrate the coefficient $C'_{\varepsilon 1}$. However, from the above equation, it is clear that the coefficient must be a function of the mass concentration, the Stokes number, and the relative Reynolds number of the particle. Since the data is lacking, a model is developed to understand the effects of the volume averaged equation set with the determined coefficients and the assumption that $C'_{\varepsilon 1}$ can be treated as a constant (similar to the single phase coefficient).

6.2 Modeling with the Production Coefficients

To validate the volume averaged equation set presented above, we consider the data of Kulick et al. (1993) and Paris et al. (2001). These data sets are challenging to

predict with simple models and a more sophisticated model is needed (Graham, 2000). Eaton (1995) claims that a new term within the dissipation rate equation is needed to account for the production of dissipation due to particles. The dissipation model derived in Chapter 3, Eq. (3.93), includes a production of dissipation due to particles.

Kulick et al. (1993) and Paris et al. (2001) used the same experimental setup. This was a high aspect ratio (11.4:1) vertical channel with a development section of 5.2 m. The particles fell down the channel in the same direction that the air was traveling and the particle response time was on the order of 130 ms. The volume fractions of the particles are on the order of 10^{-5}, which is clearly two-way coupling and according to Elghobashi (1994), thus particle-particle interaction could be ignored. With these data points, the particles should have reached a terminal velocity and the particle velocity should have been higher than the air velocity throughout the channel. However, all the data sets show that air velocity exceeds the particle velocity at the center of the channel, yet the particle velocity exceeds the air velocity near the wall. Yamamoto et al. (2001) simulated Kulick's data using large eddy simulation (LES) and a particle collision model. Their study shows that particle collisions increase transverse mixing and suggest that this mechanism is responsible for the flat particle velocity and concentration profile across the channel. The study of Nasr et al. (2007) also included a particle-particle and particle-wall collision model and compared the results to the data of Kulick et al. (1993). They showed that the particle collisions were responsible for flattening the particle velocity profile across the channel and also concluded that particle collisions were responsible for turbulence attenuation. They also showed that in the absence of particle collisions, the particle velocity exceeds the gas velocity and the carrier phase turbulence is augmented.

The data presented by Kulick et al. (1993) and Paris et al. (2001) are for steady, fully developed, particle laden, turbulent channel flow. For such a flow, a simple 1-D modeling approach can be taken. Additional assumptions are: uniform particle diameter, no mass transfer between the dispersed and continuous phase, particle rotational effects are neglected, and the RMS velocity fluctuations of the particles are negligible compared to the mean slip velocity. The formulations for steady, fully developed continuous phase flow are as follows.

Continuous Phase Momentum:

$$0 = -\alpha_c \frac{\partial \langle P \rangle}{\partial x} + \alpha_c \rho_c g_i + \alpha_c \frac{\partial}{\partial y}\left((\mu + \mu_T) \frac{\partial \langle u_i \rangle}{\partial y} \right) - \frac{3\pi \mu_c}{V} \sum_n \left[f D (u - v) \right]_n \tag{6.18}$$

which can be rewritten as

$$0 = -\alpha_c \frac{\partial \langle P \rangle}{\partial x} + \alpha_c \rho_c g + \alpha_c \frac{\partial}{\partial y}\left((\mu + \mu_T) \frac{\partial \langle u \rangle}{\partial y} \right) - \beta_V \left(\langle u \rangle - \langle v \rangle \right) \tag{6.19}$$

where β_V is described by Eq. (2.19).

Continuous Phase Turbulent Kinetic Energy:

$$0 = \alpha_c \nu_T \left(\frac{\partial \langle u \rangle}{\partial y} \right)^2 + \frac{\beta_V}{\rho_c} \left[\langle u \rangle - \langle v \rangle \right]^2 + \alpha_c \frac{\partial}{\partial y}\left[\left(\nu + \frac{\nu_T}{\sigma_k} \right) \frac{\partial k}{\partial y} \right] - \alpha_c \varepsilon \tag{6.20}$$

Continuous Phase Turbulent Dissipation:

$$0 = C'_{\varepsilon 1} \alpha_c \nu_T \left(\frac{\partial \langle u \rangle}{\partial y} \right)^2 \frac{\varepsilon}{k} - C'_{\varepsilon 2} \alpha_c \frac{\varepsilon^2}{k} + C_{\varepsilon 3} \frac{v^2}{V} \sum_n f_n \frac{|u - v|_n^2}{D_n} + \alpha_c \frac{\partial}{\partial y}\left[\left(\nu + \frac{\nu_T}{\sigma_\varepsilon} \right) \frac{\partial \varepsilon}{\partial y} \right] \tag{6.21}$$

By assuming that the particle diameter is uniform and neglecting the deviation in particle velocity, the above equation can be rewritten as

$$0 = C'_{\varepsilon 1} \alpha_c \nu_T \left(\frac{\partial \langle u \rangle}{\partial y} \right)^2 \frac{\varepsilon}{k} - C'_{\varepsilon 2} \alpha_c \frac{\varepsilon^2}{k} + \alpha_d C_{\varepsilon 3} \frac{6 v^2}{\pi D^4} f \left[\left(\langle u \rangle - \langle v \rangle \right)^2 + 2k \right] + \alpha_c \frac{\partial}{\partial y}\left[\left(\nu + \frac{\nu_T}{\sigma_\varepsilon} \right) \frac{\partial \varepsilon}{\partial y} \right] \tag{6.22}$$

where the turbulent kinematic viscosity (ν_T) is modeled by Eq. (2.15) and the coefficients shown in the above equation are given in Table 6.1. At the wall, the velocity of the fluid is zero; the shear at the wall is modeled by

$$\tau_w = \frac{\rho C_\mu^{1/4} k^{1/2}}{u^+} u \tag{6.23}$$

Near the wall, the production of turbulent kinetic energy is balanced by the dissipation and the diffusion is assumed negligible. The dissipation near the wall is determined by Eq. (6.4) and the turbulent kinetic energy is found from Eq. (6.7).

The finite volume approach was used to model Eqs. (6.19), (6.20), and (6.22). The boundary conditions applied at the wall were Eqs. (6.4), (6.7) and (6.23). The particle velocity profile was determined from the experimental data. The turbulent kinetic energy was found from the experimental data by assuming that the stream-wise fluctuations can be summed with twice the transverse fluctuations, shown as

$$2k = \overline{u_1'^2} + 2 \cdot \overline{u_2'^2} \tag{6.24}$$

For the un-laden case, the standard coefficients were used in the k-ε model; for the laden cases, the single phase coefficients were used in addition to effects of the dispersed phase (see Table 6.1 for the un-laden and laden coefficients). The un-laden piezometric pressure gradient was determined from the data of Kulick et al. (1993) and found to be -14.28 Pa/m. Kulick et al. (1993) could not measure the laden pressure gradient; Paris et al. (2001) did measure the laden pressure gradient but could not justify why it was so high. In the experiments of Kulick et al. (1993) and Paris et al. (2001), the continuous phase mass flow rate was adjusted for the different particle loadings in order to maintain a constant centerline velocity, shown in Table 6.2. In the model, for the laden cases, the

piezometric pressure gradient was iterated until the centerline velocity matched that of the experimental data.

6.2.1 Comparison of the Model to Experimental Data

The un-laden velocity profile and turbulent kinetic energy predicted by the model were compared to the data of Kulick et al. (1993) and Paris et al. (2001). For this case, the standard k-ε model was used with the standard coefficients (shown in Table 6.1). The velocity was normalized by the centerline velocity and plotted in terms of y^+. The normalized un-laden velocity profile predicted by the model agrees well with the measurements, shown in Figure 6.1. The un-laden turbulent kinetic energy determined by Kulick et al. (1993) using LDA and Paris et al. (2001) using Particle Image Velocimetry (PIV) appear to agree well in the range of $200 < y^+ < 400$ but deviated for $y^+ < 200$. The un-laden turbulent kinetic energy predicted by the model show better agreement with the data of Paris et al. (2001) than Kulick et al. (1993) near the wall (shown in Figure 6.2). Towards the center of the channel, the predictions of the model show good agreement with both data sets.

Kulick et al. (1993) obtained air velocity measurements using LDA for various particle sizes (50 – 90 μm) and loadings (0 – 0.8). The data collected by Kulick et al. (1993) demonstrate that 50 μm and 90 μm glass particles produce little attenuation, yet 70 μm copper particles at mass loadings of greater than 0.1 produce significant turbulence attenuation. For the case of 70 μm copper particles at mass loadings of 10% and 20%, the experimental data of Kulick is compared to the model predictions. For the particle laden case, the coefficients used in the k-ε equation are shown in Table 6.1. The

velocity is normalized by the centerline velocity and shown in Figure 6.3. For the 10% and 20% mass loading cases, the model tends to under-predict the velocity magnitude near the wall. It is also noticed that the velocity profiles predicted by the model are quite different than those found from the experimental data. The velocity profile predicted by the model for a mass loading of 10% shows a slight increase in the carrier velocity near the center of the channel while the increase in velocity for a mass loading of 20% is more pronounced for $y/h > 0.6$. The turbulent kinetic energy predicted by the model is compared to experimental data for 10% mass loading (Figure 6.4) and 20% mass loading (Figure 6.5). The model compares well with the experimental data near the wall, but deviates towards the center of the channel. For the 20% mass loading case, a flat profile is noticed near the center of the channel. Although not seen in this data set, a similar flat profile for the turbulent kinetic energy near the centerline of a pipe is found in the data of Tsuji et al. (1984) and Sheen et al. (1993) for small particles. However, for both 10% and 20% mass loadings, the model tends to under-predict the data near the center of the channel. To determine if the model shows a decrease in TKE with increased mass loading, a comparison of the two mass loadings is shown in Figure 6.6. Near the wall, the model shows turbulence attenuation for increased mass loading, in good agreement with the experimental data. Near the centerline of the channel, the predictions deviate from the measured data.

Paris et al. (2001) used the same experimental set up as Kulick et al. (1993), however Paris used PIV instead of LDA to measure the air velocity and was able to reproduce the un-laden flow characteristics found by Kulick et al. (1993). The data of Paris et al. (2001) stops short of the centerline of the channel; no reason is given. The

particle size and loading is listed in Table 6.2. A comparison of the velocity profile normalized by the centerline velocity for the laden case of 20% mass loading is shown in Figure 6.7. The magnitude of the velocity profile is slightly lower than the experimental values. However, unlike the prediction of Kulick's data, the velocity trend predicted by the model agrees well with the data of Paris. The predicted turbulent kinetic energy is compared with the measurements and shown in Figure 6.8. It can be seen that the model agrees well in the range of $0.4 < y/h < 0.6$ but deviates near the wall.

Part of the reason for these deviations may be explained by the assumption of neglecting the re-distribution terms. For most cases involving particle laden flows, $\left[\langle u\rangle - \langle v\rangle\right]^2 >> \langle \delta v_i \delta v_i\rangle - \langle \delta u_i \delta v_i\rangle$ and the last terms may be neglected for such cases. However, for cases when $\left[\langle u\rangle - \langle v\rangle\right]^2 \approx 0$ the redistribution terms may play a significant role in modeling turbulent kinetic energy near the wall. In the data of Kulick (1993) and Paris (2001), there is a point in the flow where the continuous phase and dispersed phase velocities are equal. However, the data set does not give correlations for $\langle \delta u_i \delta v_i\rangle$.

Another reason for the deviation of turbulent kinetic energy near the center of the channel is the fact that the coefficient ($C_{\varepsilon 3}$) was calibrated with minimal data at low relative Reynolds numbers. The data at low relative Reynolds numbers suggested that particle loading affects the coefficient. To evaluate the effectiveness of the additional production term in the dissipation model, the production coefficient ($C_{\varepsilon 3}$) is varied. Within this coefficient, the fit coefficient ($C_{\varepsilon p}$) is varied from zero to 0.060, but the exponent *m* remained at 1.416. The effect of $C_{\varepsilon p}$ on TKE is shown in Figure 6.9. When the coefficient is zero the additional production term due to particle surfaces is suppressed, yet the effects of the particles are still included in the turbulent kinetic energy

equation. For such a case the dissipation is modeled as the single phase dissipation with the standard coefficients. This formulation shows a nearly constant turbulent kinetic energy across the channel. Increasing the coefficient to 0.015 shows a drastic reduction in TKE. For a coefficient of 0.015, the TKE profile is nearly matched; however the predicted magnitude is higher than seen from the experimental data. As the coefficient is increased to 0.060 the TKE near the wall matches well, but near the center of the channel, the model under-predicts the measurements and shows a constant TKE. The normalized velocity profiles show that as the production coefficient is reduced, the trend and magnitude of the velocity profiles better match the data, shown in Figure 6.10. It can be seen that if the production coefficient were zero, the velocity profile would be over predicted; this substantiates that a production of dissipation is needed. Nonetheless a better calibration of the coefficient is needed at lower particle Reynolds numbers.

The other unknown is the production coefficient ($C'_{\varepsilon l}$) due to the mean velocity gradient. In the derivation of the dissipation equation, the production coefficient was assumed to vary with one or more of the fundamental non-dimensional parameters found in particle laden flows, namely: particle loading, Stokes number, particle Reynolds number, or the Reynolds number of the flow. The calibration of this coefficient is complex and depends on the shear velocity and von Karman constant, both of which are unknown in the data presented in the literature. To simplify, the production coefficient ($C'_{\varepsilon l}$) was assumed constant between the wall and the center of the channel. To better understand the effect of the coefficient, it was varied from its standard value of 1.44 (see Figure 6.11). In Figure 6.11, the fit coefficient for the production of dissipation by particles ($C_{\varepsilon p}$) is set to 0.025, and the magnitude of TKE at the center of the channel is

matched with the data. The production of dissipation ($C'_{\varepsilon l}$) due to mean velocity gradients was varied to understand the effects. The piezometric pressure gradient was iterated for each case to maintain the centerline velocity at 10.5 m/s. If $C'_{\varepsilon l}$ = 1.6 and $C_{\varepsilon p}$ = 0.025, the TKE is matched near the wall and at the center of the channel. However, the results show that there is still a constant TKE near the center of the channel and the TKE predicted by the model deviates slightly from the data between 0.4 < y/h < 0.9. The normalized velocity profile is shown in Figure 6.12.

The predictions of the turbulent dissipation model with an additional production term due to the presence of particles are shown to improve the prediction of TKE near the wall. This additional term also accounts for changes in particle mass loading. Overall, it is an improvement over the standard single phase turbulent dissipation model. For flows with low particle Reynolds numbers, the prescribed coefficients are invalid and additional studies are needed to validate these conditions. This type of flow is challenging to predict, yet a first attempt at using the volume averaged equations to predict simple channel flows appears promising.

TABLE 6.1: Model Coefficients

Coefficient	Time Averaged Equation Set	Volume Averaged Equation Set
$C'_{\varepsilon 1}$	1.44	1.44 + unknown
$C'_{\varepsilon 2}$	1.92	$1.92 + 0.362*(C/St)^{0.76}$
$C_{\varepsilon 3}$	-	$0.058*(1.92 + 0.362*(C/St)^{0.76})*Re_p^{1.416}$
κ	0.4	0.4
C_μ	0.09	0.09
σ_k	1.0	1.0
σ_ε	1.3	1.3

TABLE 6.2: Data Parameters

Parameter	Kulick et al. (1993)	Paris et al. (2001)
Particle Material	Copper	Glass
Particle Diameter (D), μm	70	150
Particle Density (ρ_d), kg/m^3	8800	2500
Particle Loading	10%, 20%	20%
Continuous Phase	air	air
Centerline Gas Velocity (U_{cl}), m/s	10.5	10.5
Piezometric Pressure Gradient (dP_z/dx), Pa/m	-14.28	-27.56

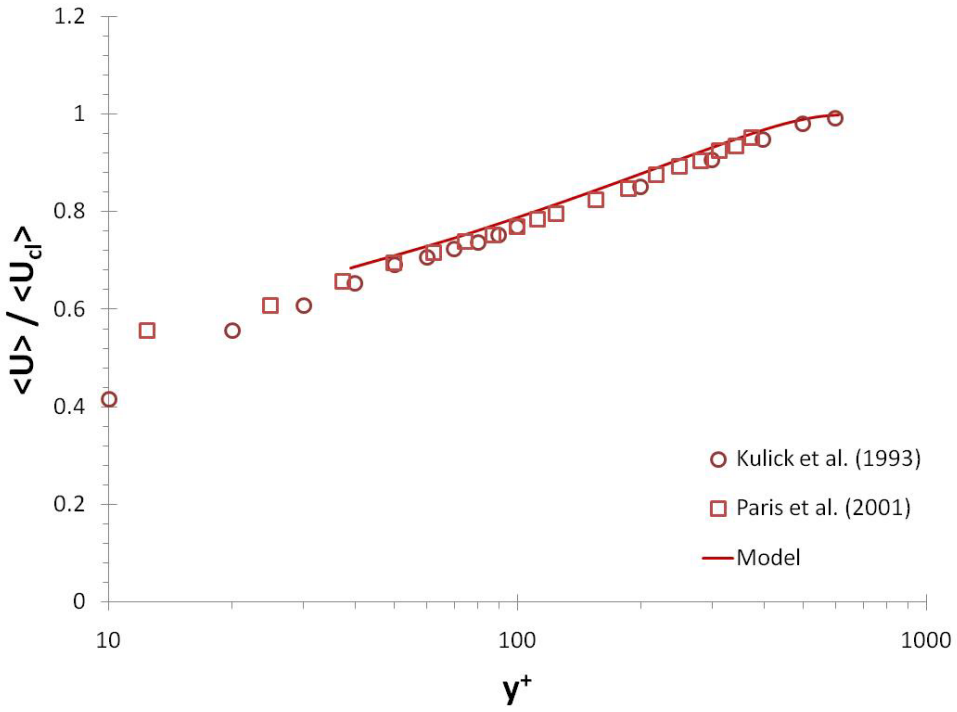

Figure 6.1: Comparison of the un-laden velocity profiles predicted by the model to the experimental data of Kulick et al. (1993) and Paris et al. (2001).

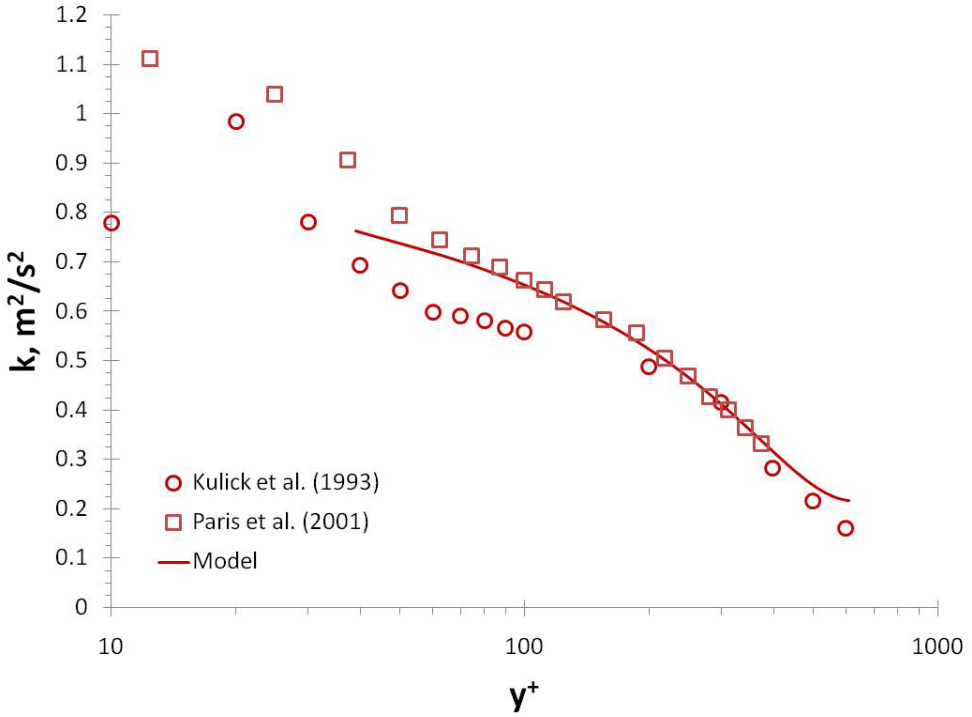

Figure 6.2: Comparison of the un-laden turbulent kinetic energy profiles predicted by the model to the experimental data of Kulick et al. (1993) and Paris et al. (2001).

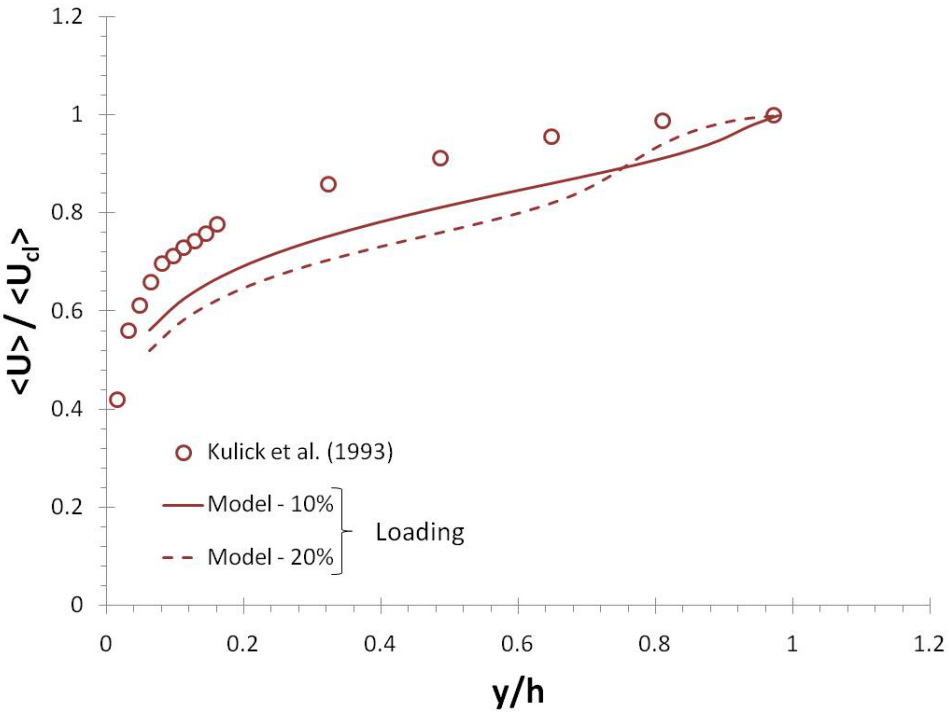

Figure 6.3: Comparison of the velocity profiles predicted by the model to the experimental data of Kulick et al. (1993) – Copper particles, 70 μm dia., mass loading indicated in legend.

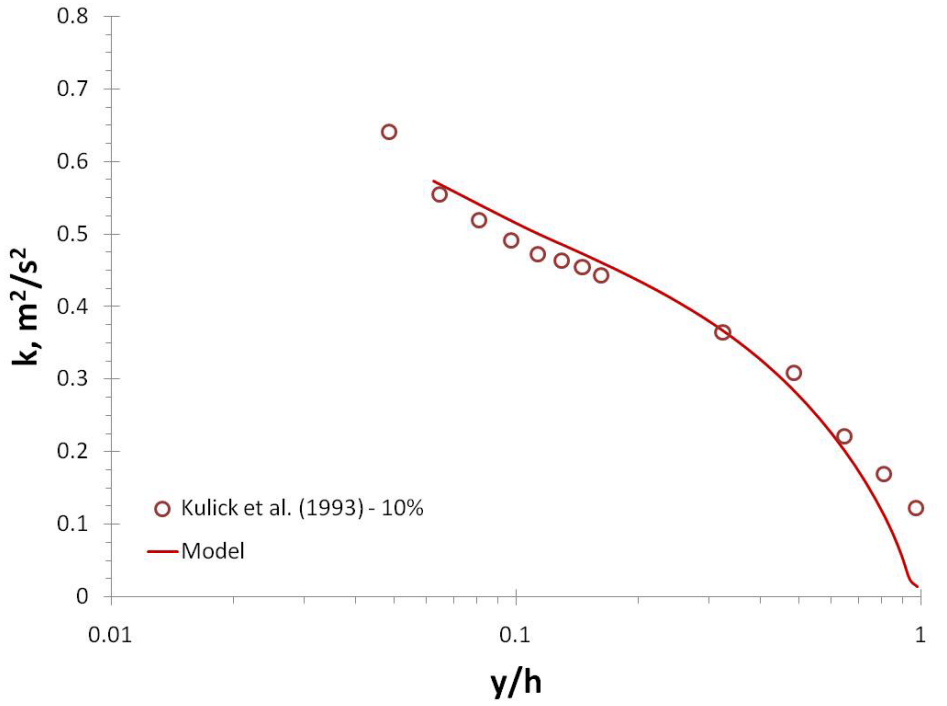

Figure 6.4: Comparison of the particle laden turbulent kinetic energy profiles predicted by the model to the experimental data of Kulick et al. (1993) – Copper particles, 70 μm dia., 10% mass loading.

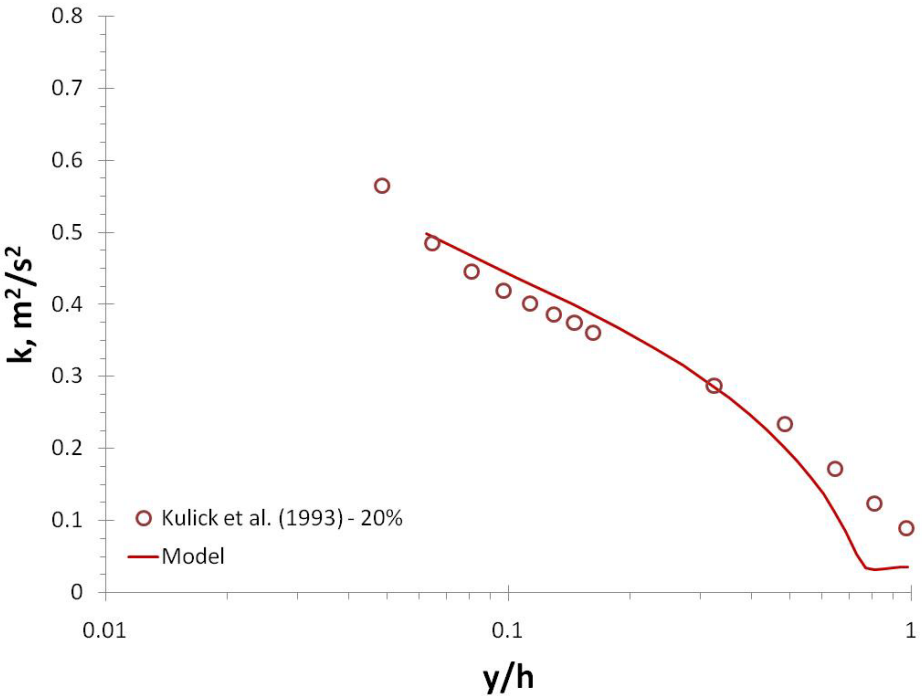

Figure 6.5: Comparison of the particle laden turbulent kinetic energy profiles predicted by the model to the experimental data of Kulick et al. (1993) – Copper particles, 70 μm dia., 20% mass loading.

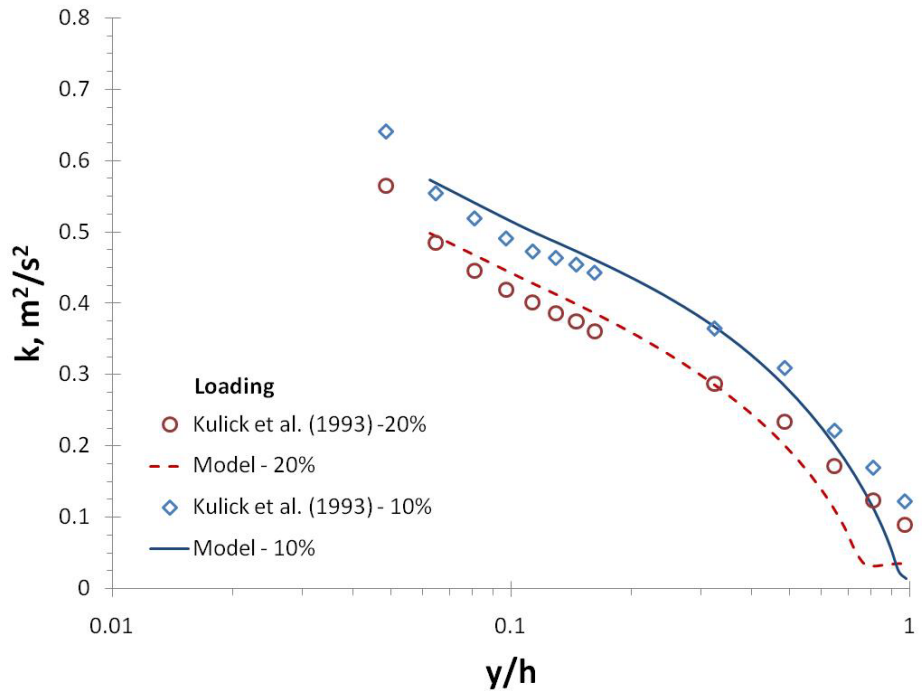

Figure 6.6: Comparison of the particle laden turbulent kinetic energy profiles predicted by the model to the experimental data of Kulick et al. (1993) – Copper particles, 70 μm dia., mass loading indicated in the legend.

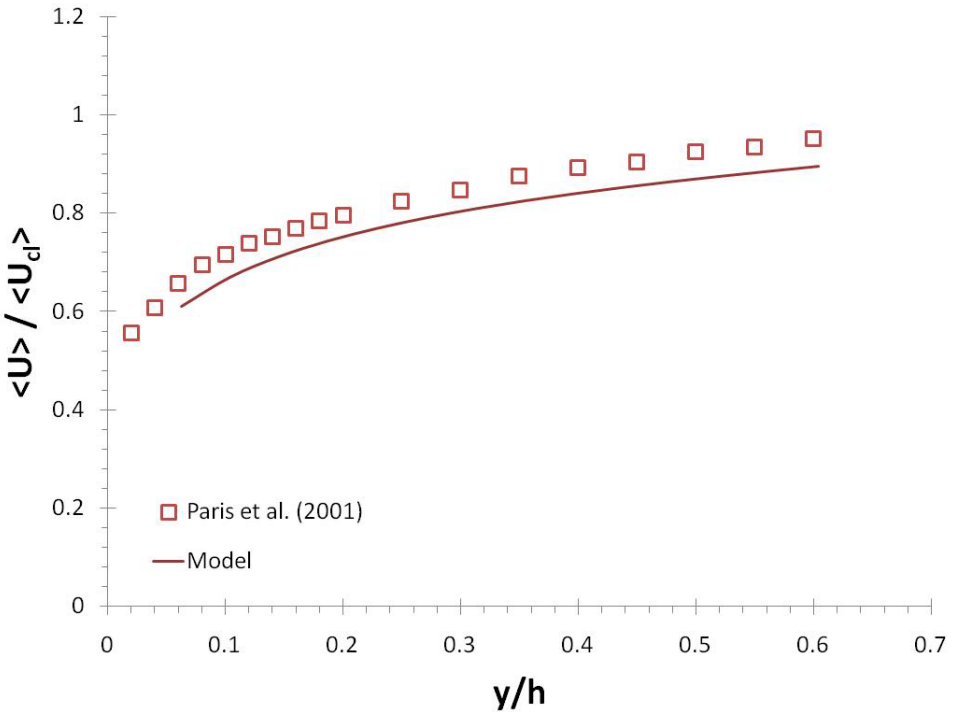

Figure 6.7: Comparison of the velocity profile predicted by the model to the experimental data of Paris et al. (2001) – Glass particles, 150 μm dia., 20% loading.

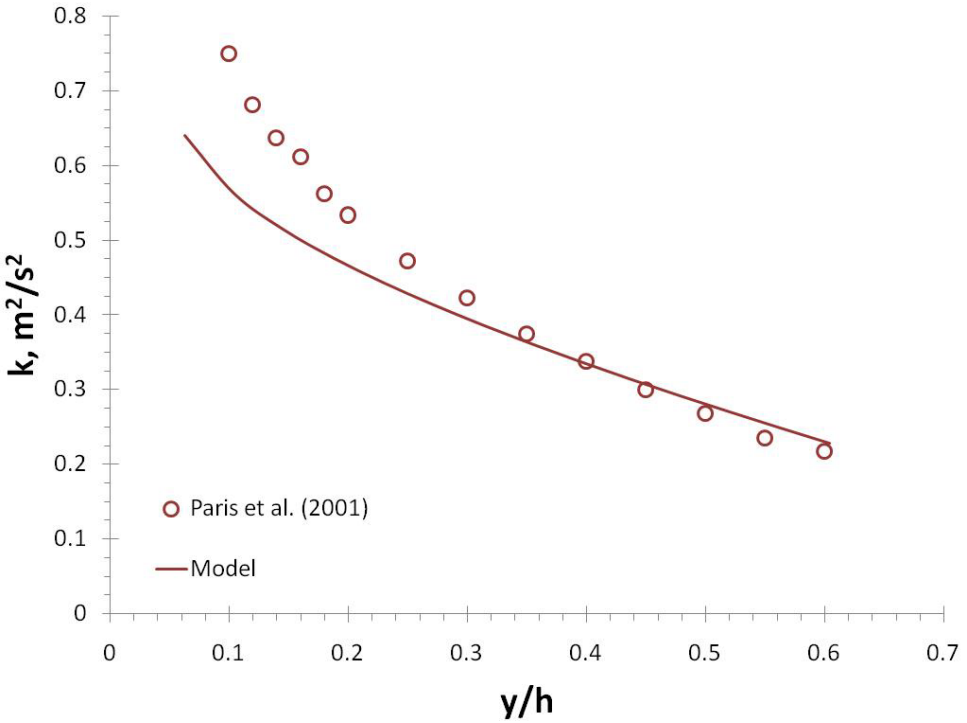

Figure 6.8: Comparison of the turbulent kinetic energy profile predicted by the model to the experimental data of Paris et al. (2001) – Glass particles, 150 μm dia., 20% loading.

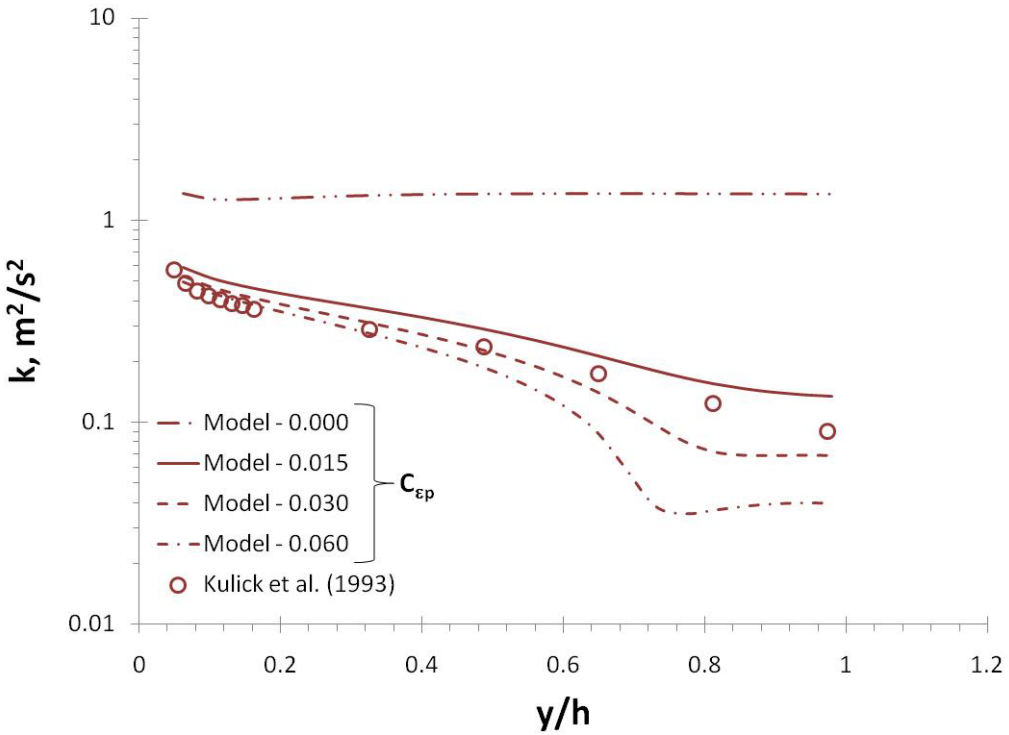

Figure 6.9: Evaluation of the production of dissipation coefficient due to the particles – Kulick et al. (1993), 20% loading, $C_{\varepsilon p}$ indicated in the legend.

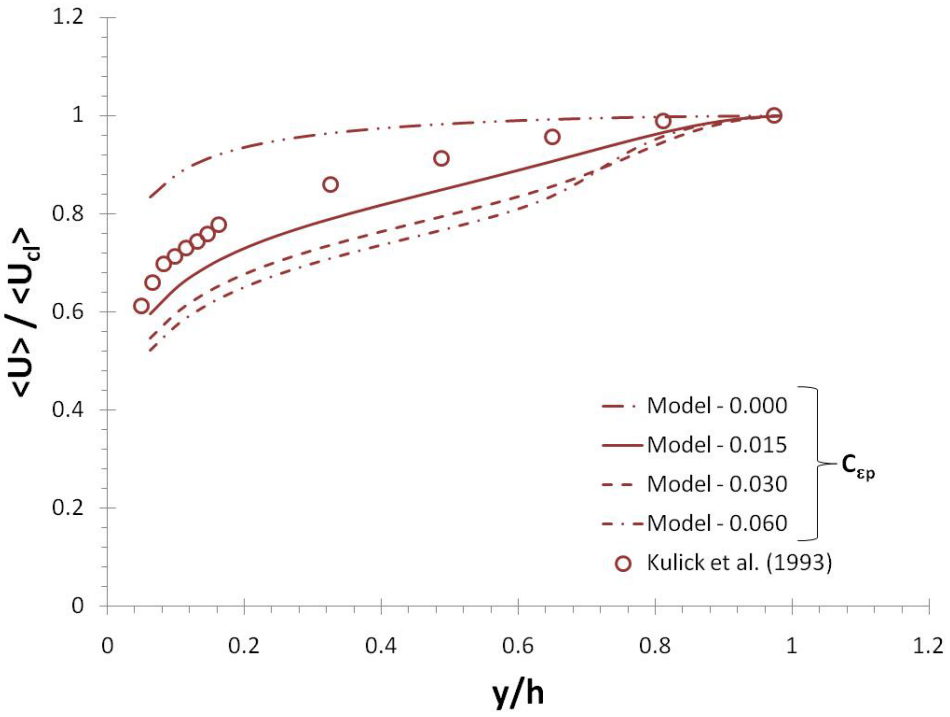

Figure 6.10: Effect of the production of dissipation on the velocity profile – Kulick et al. (1993), 20% loading, $C_{\varepsilon p}$ indicated in the legend.

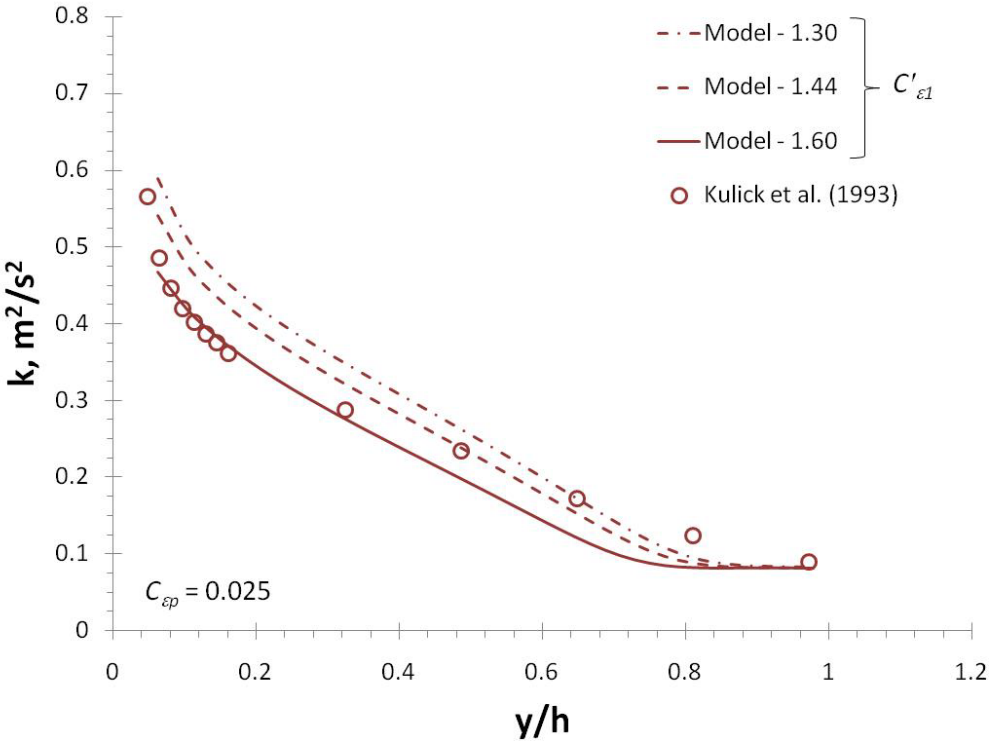

Figure 6.11: Evaluation of the production of dissipation coefficient due to the mean velocity gradient – Kulick et al. (1993), 20% loading, $C'_{\varepsilon 1}$ indicated in the legend.

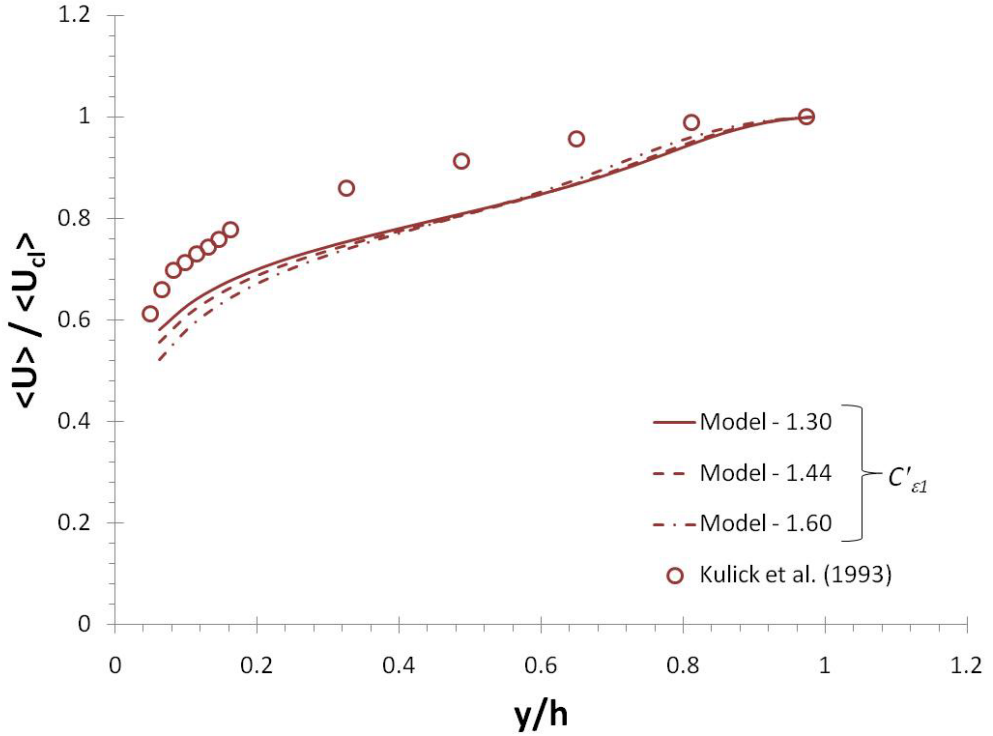

Figure 6.12: Effect of the production of dissipation coefficient due to the velocity profile – Kulick et al. (1993), 20% loading, $C'_{\varepsilon 1}$ indicated in the legend.

CHAPTER SEVEN

CONCLUSION AND FUTURE WORK

The current work is unique in providing a fundamental approach to obtaining a dissipation transport equation for particle laden turbulent flows. The equation is found from volume averaging process and new coefficients are studied and identified.

7.1 Conclusion

Volume averaging proves to be a powerful tool for analyzing multi-phase flows. In this work, a volume averaged turbulence dissipation transport equation that accounts for the turbulence dissipation caused by particle surfaces within a turbulent flow is derived from fundamentals. The derivation process reveals an additional production of dissipation term that is related to the instantaneous relative velocity gradients at the particle surface. The dissipation rate equation is valid for incompressible flows with no mass transfer between the dispersed and continuous phases. By setting the volume fraction of the continuous phase to unity, the volume average dissipation equation reduces to the single phase equivalent of the time averaged dissipation equation.

The dissipation transport equation was applied to experimental data involving generation of homogeneous turbulence by particles. The ratio of the new production of dissipation coefficient (due to the presence of particles) and the dissipation of dissipation coefficient was found to be related to the particle diameter and the Taylor length scale. At high relative Reynolds numbers, the ratio of the coefficients was found to correlate well with the relative Reynolds number of the particles, and at low relative Reynolds numbers, the ratios of coefficients appears to be a function of loading in addition to the particle Reynolds number.

The coefficient of the dissipation of dissipation term was determined numerically (using DNS) by modeling isotropic homogeneous turbulence decay in a field of stationary particles. The particles were represented by point forces and were placed at every grid point within a DNS domain. The study focused on two Reynolds numbers, 12.5 and 3.3. The results show that the coefficient for the dissipation of dissipation due to the presence of particles can be correlated to a ratio of the particle mass concentration and the Stokes number (C/St) and that this coefficient increased significantly for high mass concentration and low Stokes number.

The coefficient of the production of dissipation term was determined analytically, however the data lack the necessary parameters to calibrate this coefficient. Therefore, a numerical model was developed and applied to particles in a turbulent channel flow. The model was compared to the data of Kulick et al. (1993) and Paris et al. (2001) and is shown to reasonably predict the TKE for turbulent flow with particles in a high aspect ratio vertical channel. This study also shows that the production coefficient due to mean velocity gradients and the production coefficient due to the presence of particles are not

calibrated correctly for low particle Reynolds number flows. Additional data are needed to understand the effect of particle loading at low particle Reynolds numbers; these data should provide better calibration of these coefficients.

7.2 Future Work

The coefficients in the dissipation rate equation are studied for simple cases and the effects are noted. However, a significant amount of data is lacking for the parameters needed to better understand these coefficients over a wide range of conditions. Thus future work should focus on experimental data in areas of particle laden homogeneous turbulent decay, or validating these coefficients at higher Reynolds numbers using DNS. Additionally, the von Karman constant should be experimentally studied in particle laden turbulent flows in pipes and channels. And the shear and pressure gradient should be measured and validated to understand the effect of the particles. In addition, the results for particle laden jet flows should be studied with the insight provided by the models introduced in this work.

BIBLIOGRAPHY

Bernard, P. S. and J. M. Wallace, 2002. Turbulent Flow: Analysis, Measurement, and Prediction. John Wiley and Sons, Inc.

Burton, T. M. and J. K. Eaton, 2005. Fully Resolved Simulations of Particle-Turbulence Interaction. J. Fluid. Mech., **545**, 67 – 111.

Chen, J. H. and G. M. Faeth, 2000. Interwake Turbulence Properties of Homogeneous Dilute Particle-Laden Flows. AIAA J., **38**, 995 – 1001.

Chen, C. P. and P. E. Wood, 1985. A Turbulence Closure Model for Dilute Gas-Particle Flows. Canadian J. of Chem. Eng., **63**, 349 – 360.

Crowe, C.T. (editor), 2006. "Multiphase Flow Handbook". CRC, Taylor and Francis.

Crowe, C. T., 2000. On Models for Turbulence Modulation in Fluid-Particle Flows. *Intl.* J. Multiphase Flow, **26**, 719 – 727.

Crowe, C. T., 2001. Carrier-phase Turbulence in Dispersed Phase Flows. Intl. Conf. on Multiphase Flows. New Orleans. Presentation.

Crowe, C. T. and I. Gillandt, 1998. Turbulence Modulation of Fluid-Particle Flows – A Basic Approach. 3rd Intl. Conf. on Multiphase Flows. Lyon, France, June 8-12.

Crowe, C. T., M. Sommerfeld and Y. Tsuji, 1998. "Multiphase Flows with Droplets and Particles". CRC Press LLC.

Crowe, C. T. and P. Wang, 2000. Towards a Universal Model for Carrier-Phase Turbulence in Dispersed Phase Flows. ASME Fluids Eng. Div. Summer Meeting. Boston, MA, June 11-15.

Curtis, J. S., and B. van Wachem, 2004. Modeling Particle-Laden Flows: A Research Outlook. AIChE J., **50**, 2638 – 2645.

de Bruyn Kops, S. M., and J. J. Riley, 1998. Direct Numerical Simulation of Laboratory Experiments in Isotropic Turbulence. Physics of Fluids. **10**, 2125 – 2127.

Eaton, J. K., 2006. Turbulence Modulation by Particles. Crowe, C. T. (editor) "Multiphase Flow Handbook". CRC, Taylor and Francis.

Eaton, J. K., 1995. Turbulence Modification by Particles in Shear Flows. ASME FED **228**, 273 – 278.

Elghobashi, S., 1994. On Predicting Particle-Laden Turbulent Flows. App. Sci. Res., **52**, 309 – 329.

Elghobashi, S. E. and T. W. Abou-Arab, 1983. A Two-Equation Turbulence Model for Two-Phase Flows . Physics of Fluids, **26**, 931 – 938.

Ferrante, A. and S. Elghobashi, 2003. On the Physical Mechanisms of Two-Way Coupling in Particle-laden Isotropic Turbulence. Physics of Fluids, **15**, 315 – 328.

Fessler, J. R. and J. K. Eaton. 1995. Particle-Turbulence Interactions in a Backward-Facing Step Flow. Report MD-70, Dept. Mech. Eng., Stanford University.

Geiss, S., A. Sadiki, A. Maltsev and A. Dreizler, 2001. Investigations of Turbulence Modulation in Turbulent Particle Laden Flows. ZAMM Z. Angew. Math. Mech., **81**, S527 – S528.

Geiss, S., A. Dreizler, Z. Stojanovic, M. Chrigui, A. Sadiki and J. Janicka, 2004. Investigation of Turbulence Modification in a Non-Reactive Two-Phase Flow. Exp. Fluids, **36**, 344 – 354.

Gore, R. A. and C. T. Crowe, 1989. Effect of Particle Size on Modulating Turbulent Intensity. Int. J. Multiphase Flow, **15**, 279 – 285.

Graham, D. I., 2000. Turbulence Attenuation by Small Particles in Simple Shear Flows. J. Fluids Eng. 122, 134 – 137.

Hestroni, G., 1989. Particles – Turbulence Interaction. Int. J. Multiphase Flow, **15**, 735 – 746.

Hinze, J. O., 1975. "Turbulence". McGraw Hill, New York, NY.

Hosokawa, S., A. Tomiyama, M. Morimura, S. Fujiwara and T. Sakaguchi. Influences of Relative Velocity on Turbulent Intensity in Gas-Solid Two-Phase Flow in a Vertical Pipe. 3rd Int. Conf. Multiphase Flow. Lyon, France, June 8-12, 1998.

Kenning, V. M. and C. T. Crowe, 1997. On the Effect of Particles on Carrier Phase Turbulence in Gas-Particle Flows. Intl. J. Multiphase Flow, **23**, 403 – 408.

Kenning, V. M. and C. T. Crowe. Particle Induced Turbulence in Initially Quiescent Flows. ASME FEDSM 97-3191.

Kulick, J. D., J. R. Fessler and J. K. Eaton, 1993. On the Interactions between Particles and Turbulence in a Fully Developed Channel Flow in Air. Report No. MD-66, Dept. Mech. Eng., Stanford University.

Kulick, J. D., J. R. Fessler and J. K. Eaton, 1994. Particle Response and Turbulence Modification in Fully-developed Channel Flow. J. Fluid Mech., **277**, 109 – 134.

Lain, S., D. Broder and M. Sommerfeld, 1999. Experimental and Numerical Studies of the Hydrodynamics in a Bubble Column. Chem. Eng. Sci., **54**, 4913 – 4920.

Lance, M. and J. Bataille, 1982. Turbulence in the Liquid Phase of a Uniform Bubbly Air-Water Flow. J. Fluid. Mech., **22**, 95 – 118.

Lee, S. L. and F. Durst, 1982. On the Motion of Particles in Turbulent Duct Flows. Intl. J. Multiphase Flow, **8**, 125 – 146.

Lightstone, M. F. and S. M. Hodgson, 2004. Turbulence Modulation in Gas-Particle Flows: A comparison of Selected Models. Can. J. Chem. Eng. **82**, 209 – 219.

McMurtry, P. A., 1987. Direct Numerical Simulations of a Reacting Mixing Layer with Chemical Heat Release. Ph.D. Dissertation. University of Washington.

Mizukami, M., R. N. Parthasarathy and G. M. Faeth, 1992. Particle -Generated Turbulence in Homogeneous Dilute Dispersed Flows. Int. J. Multiphase Flow. **18**, 397 – 412.

Mohanarangam, K. and J. Y. Tu, 2007. Two-Fluid Model for Particle-Turbulence Interaction in a Backward-Facing Step. AIChE J. **53**, 2254 – 2264.

Mostafa, A. A. and H. C. Mongia, 1988. On the Interaction of Particles and Turbulent Fluid Flow. Int. J. Heat and Mass Trans. 31, 2063 – 2075.

Nasr, H. and G. Ahmadi, 2007. The Effect of Two-Way Coupling and Inter-particle Collisions on Turbulence Modulation in a Vertical Channel Flow. Int. J. Heat and Fluid Flow, **28**, 1507 – 1517.

Orzag, S. A. and G. S. Patterson Jr., 1972. Numerical Simulation of Turbulence. In Statistical Models and Turbulence (eds. J. Ehlers, K. Hepp, and H.A. Weidenmuller), Lecture Notes in Physics, **12**, 127 – 147.

Paris, A. D. and J. K. Eaton, 2001. Turbulence Attenuation in a Paricle-laden Channel Flow. Report No. TSD-137, Dept. Mech. Eng., Stanford University.

Parthasarathy, R. N. and G. M. Faeth, 1990. Turbulence Modulation in Homogeneous Dilute Particle-Laden Flows. J. Fluid Mech., **220**, 485 – 514.

Pope, S. B., 2000. “Turbulent Flows”. Cambridge University Press.

Rogallo, R. S., 1981. Numerical Experiments in Homogeneous Turbulence. NASA Tech. Memo. 81315.

Savolainen, K. and R. Karvinen, 1998. The Effect of Particles on Gas Turbulence in a Vertical Upward Pipe Flow. 3rd Int. Conf. Multiphase Flow. Lyon, France, June 8-12.

Schreck, S. and S. J. Kleis, 1993. Modification of Grid-Generated Turbulence by Solid Particles. J. Fluid Mech. **249**, 665 – 688.

Sheen, H., Y. Chang and Y. Chiang, 1993. Two Dimensional Measurements of Flow Structure in a Two-Phase Vertical Pipe Flow". Proc. Natl. Sci. Counc., **17**, 200 – 213.

Simonin, O. and K. D. Squires, 2003. On Two-Way Coupling in Gas-Solid Turbulent Flows. 4th ASME_JSME Joint Fluids Engineering Conf. Honolulu, HI, June 6-10.

Slattery, J. C., 1972. "Momentum, Energy, and Mass Transfer in a Continua". McGraw Hill, New York.

Squires, K. D. and J. K. Eaton, 1990. Particle Response and Turbulence Modification in Isotropic Turbulence. Physics of Fluids A, **2**, 1191 – 1203.

Squires, K. D. and J. K. Eaton, 1992. On the Modeling of Particle-Laden Turbulent Flows. Proceedings of the Sixth Workshop on Two-Phase Flow Predictions. Erlangen, Germany.

Tsuji, Y., Y. Morikawa and H. Shiomi, 1984. LDV Measurements of an Air-Solid Two-Phase Flow in a Vertical Pipe. J. Fluid Mech., **139**, 417 – 434.

Varaksin, A. Y., Y. Kurosaki, I. Satch, Y. V. Polezhaev and A. F. Polyahov, 1998. Experimental Study of the Direct Influence of Small Particles on Carrier Air Turbulence Intensity for Pipe Flow. 3rd Int. Conf. Multiphase Flow. Lyon, France, June 8-12.

Vermorel, O., B. Bedat, O. Simonin and T. Poinsot, 2003. Numerical Study and Modelling of Turbulence Modulation in a Particle Laden Slab Flow. J. of Turbulence, **4**, 1 – 39.

White, F. M., 1974. "Viscous Fluid Flow". McGraw Hill, New York, NY.

Yamamoto, Y., M Potthoff, T. Tanaka, T. Kajishima and Y. Tsuji, 2001. Large-eddy Simulation of Turbulent Gas-Particle Flow in a Vertical Channel: Effect of considering Inter-particle Collisions. J. Fluid Mech. **442**, 303 – 334.

Yan, F., M. F. Lightstone and P. E. Wood, 2007. Numerical Study on Turbulence Modulation in Gas-Particle Flows. *Heat and Mass Transfer*, **43**, 243 – 253.

Yarin, L. P. and G. Hetsroni, 1994. Turbulence Intensity in Dilute Two-phase Flows – 3: The Particles-Turbulence Interaction in Dilute Two-Phase Flow. Int. J. Multiphase Flow, **20**, 27 – 44.

Yokomine, T. and A. Shimizu, 1995. Prediction of Turbulence Modulation by using k-ε Model for Gas-Solid Flows. In: Serizawa A., Fukano T., Bataille J. (eds) Advances in Multiphase Flow. Elsevier, Amsterdam.

Yu, Y., L. Zhou and B. Wang, 2006. Modeling of Fluid Turbulence Modification using Two-time-scale Dissipation Models and Accounting for the Particle Wake Effect. Chinese J. Chem. Eng., **14**, 314 – 320.

Yuan, Z. and E. E. Michaelides, 1992. Turbulence Modulation in Particulate Flows – A Theoretical Approach. Int. J. Multiphase Flow, 18, 779 – 785.

Zhang, Y. and J. M. Reese, 2001. Particle-Gas Turbulence Interactions in a Kinetic Theory Approach to Granular Flows. Int. J. Multiphase Flow. **27**, 1945 – 1964.

Zhang, Y. and J. M. Reese, 2003. Gas Turbulence Modulation in a Two-Fluid Model for Gas-Solid Flows. AIChE J., **49**, 3048 – 3065.

Zhang, D. Z. and A. Prosperetti, 1994. Ensemble Phase-Averaged Equations for Bubbly Flows. Physics of Fluids, **6**, 2956 – 2970.

Zhou, L. X. and T. Chen, 2001. Simulation of Swirling Gas-particle Flows using USM and k-ε-kp Two-phase Turbulence Models. Powder Technology, **114**, 1 – 11.

APPENDIX A

DETAILS ON VOLUME AVERAGE IDENTITIES

A.1 Background:

The single phase momentum equations can be derived from a control (finite) volume approach. The finite differences of a property are then changed to derivatives of that property using the fundamental theorem of calculus. Ideally, as the limit goes to zero, a derivative can be defined at a point; but the derivative of a property of a fluid or any physical phenomena cannot be defined at a point. A true point does not exist in the real world. In a continuum, a point is defined as a volume in the range for which the averaged values of the atoms remain constant (see Figure A1). Thus the derivative in a continuum is understood to have a minimal volume of atoms associated with it such that it can be mathematically defined as a point.

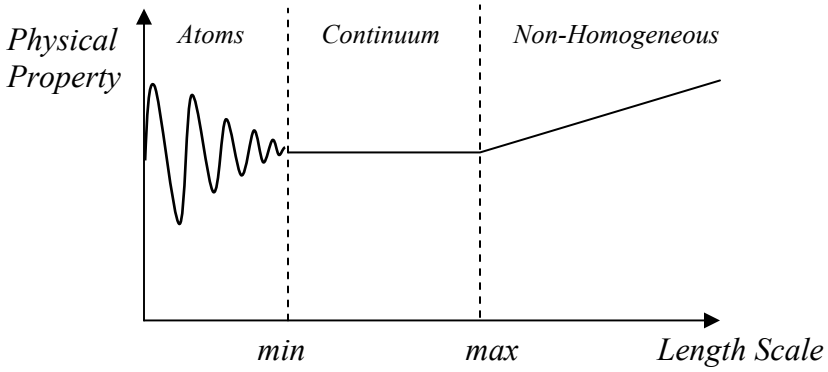

Figure A1: Range of a Continuum

In the continuous phase of a multi-phase fluid, it is presumed that a viscous shear layer develops near the surface of the dispersed phase particles due to the no-slip condition. Ideally, a continuum point model would be correct; practically, there are many particles with shear layers that have to be accounted for. To complicate matters, in a turbulent multi-phase flow, the height of the boundary layer around such small particles

can be much less than the particle diameter. Thus a continuum point model for the continuous phase is impractical with our current computational abilities. Using traditional finite volume approaches, an extremely fine moving mesh would be necessary to account for all the boundary layers around all particles within the flow field.

To improvise, an interim solution is proposed. Just as in the continuum model, volume averaging is a solution to account for the turbulent properties along with the properties in the boundary layers developed over the particles. It is assumed that there is a length scale (l) that is much less than the large scale structure (L) as shown in Figure A2. The minimum volume average length scale (l) is chosen such that an incremental change in the length scale does not affect the volume average of the continuous phase property. Consider the parameter B that is a function of space and time only:

$$B = B(x, y, z, t)$$

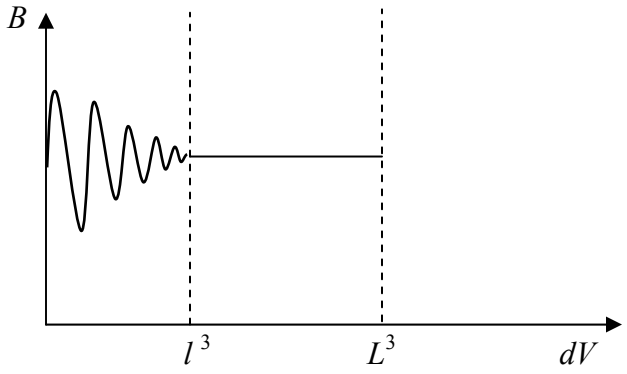

Figure A2: Range of Volume Average

The volume average of parameter B is defined as:

$$\overline{B} = \frac{1}{V_c}\int_{V_c} B dV$$

A.2 Volume Averaging the Spatial Derivative:

Traditional single phase equations modeling fluid flow involve a spatial gradient. In two-phase flow, the volume average is applied to the continuous phase in order to account for all the surface effects near the particles. To use a volume averaged parameter in the continuous phase, the volume average of a gradient must also be known. The volume average of a spatial gradient of parameter B is defined as:

$$\overline{\frac{\partial B}{\partial x_i}} = \frac{1}{V_c}\int_{V_c} \frac{\partial B}{\partial x_i} dV$$

Consider the 3-D multi-phase flow shown in Figure A3 (the third dimension is into the page). This flow represents particles in a gas flowing through a pipe. Particle-wall and particle-particle collisions are also shown to understand the effect of volume averaging the gradient of a parameter of the continuous phase.

The flow shown in Figure A3 is considered a snapshot of the actual flow at time t = t_o. Thus the dispersed and continuous phases are frozen in space at a single time (the volume average of a time gradient will be discussed later). The red box is a sample volume of size l^3. The vector x_k represents the center of the sample volume relative to some absolute coordinate reference frame. The vector γ_k extends from the center of the sampling volume to the center of every particle of the dispersed phase. The vector ξ_k extends from the center of the particle to the surface of the particle. The vector ψ_k is the sum of the vectors x_k , γ_k , and ξ_k. The incremental change in the position of the sampling volume is represented by Δx_k (shown by the dashed magenta box).

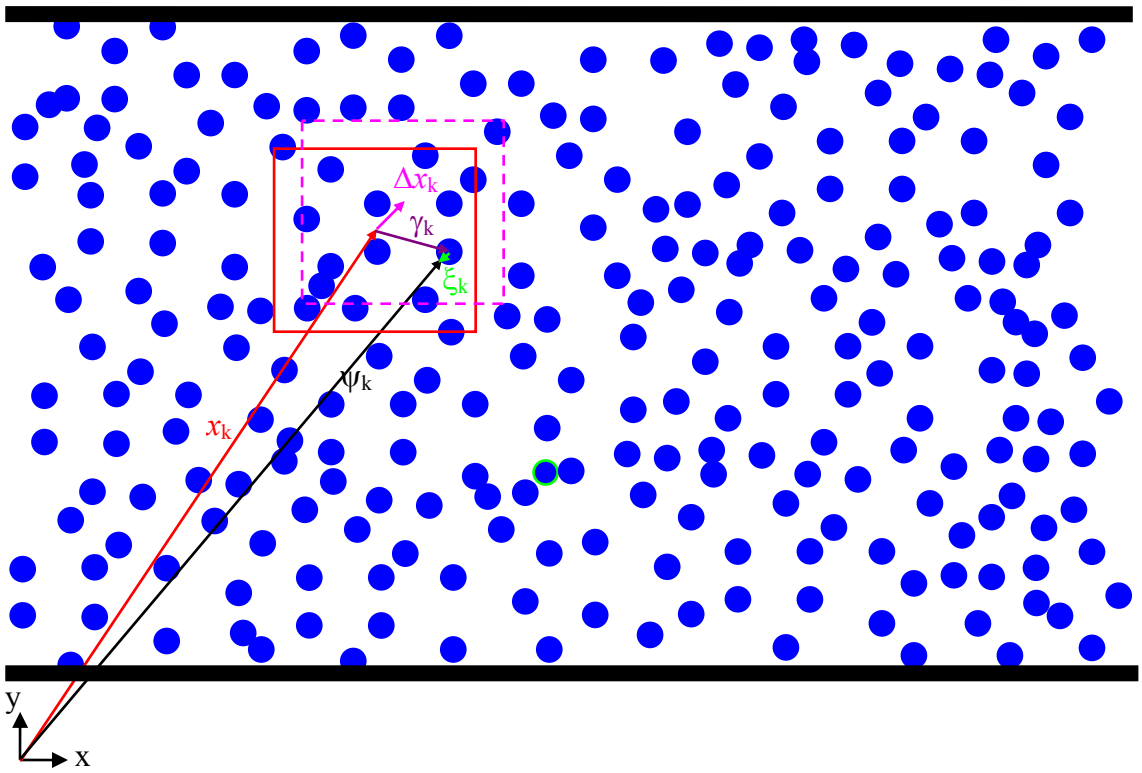

Figure A3: Multiphase Flow Frozen in Time and Space with Particle-Particle Collision and Particle-Wall Collision at time t = t_o with averaging volume l^2 and large scale L^2.

It can be shown that the derivative of an integrated parameter is equal to the integrated rate of change of that parameter at the boundary as shown in equation [1],

$$\frac{\partial}{\partial x_i}\int_{V_c} B d\lambda = \int_{S_d} B\frac{\partial \psi_k}{\partial x_i} n_k d\varpi + \int_{S_v} B\frac{\partial \varphi_k}{\partial x_i} n_k d\zeta \qquad [1]$$

where S_d represents all the surfaces of the dispersed phase within the sample volume and S_v represents the continuous phase boundary surfaces on edges of the sampling volume and n_k is the unit vector outward normal to the surface. Analyzing the first term on the right hand side of Eqn [1], it is found that for all particles (including collision and those crossing the sampling volume surface) within the sampling volume the gradient of ψ_k with respect to x_i is the tangent vector at the surface of the particle.

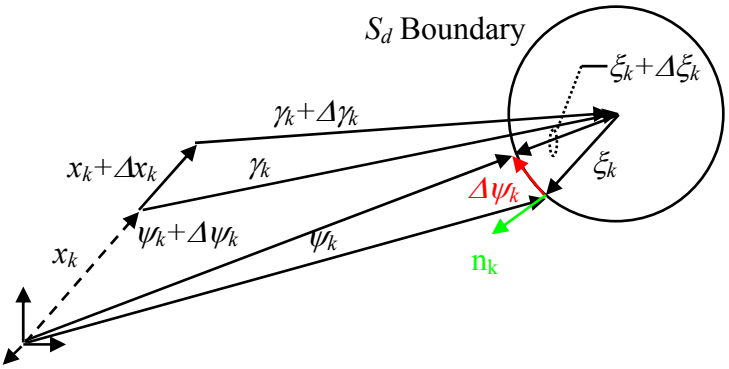

Figure A4: Representation of the change in ψ_k vector in relation to the tangent along the surface

The surface vector can be represented by the following equation:

$$\psi_k = \gamma_k + x_k + \xi_k \qquad [2]$$

Displacing the vector x_k by a distance Δx_k, then the total is shown to be:

$$\psi_k + \Delta\psi_k = \gamma_k + \Delta\gamma_k + x_k + \Delta x_k + \xi_k + \Delta\xi_k \qquad [3]$$

Subtracting Eq. [2] from Eq. [3] shows the displacement of the surface vector:

$$\Delta\psi_k = \Delta\gamma_k + \Delta x_k + \Delta\xi_k \qquad [4]$$

Dividing Eq. [4] by Δx_i and taking the limit as $\Delta x_i \to 0$ yields:

$$\frac{\partial\psi_k}{\partial x_i} = \frac{\partial\gamma_k}{\partial x_i} + \frac{\partial x_k}{\partial x_i} + \frac{\partial\xi_k}{\partial x_i} \qquad [5]$$

Since the vector γ_k terminates at the center of the particle, and the center position of the particle is stationary, taking a small step in the x_k direction shows that $\Delta\gamma_k = -\Delta x_k$ (shown in Figure A4). Thus Eq. [5] is shown to be:

$$\frac{\partial\psi_k}{\partial x_i} = -\frac{\partial x_k}{\partial x_i} + \frac{\partial x_k}{\partial x_i} + \frac{\partial\xi_k}{\partial x_i} \qquad [6]$$

$$\frac{\partial\psi_k}{\partial x_i} = \frac{\partial\xi_k}{\partial x_i} \qquad [7]$$

Eq. [7] shows that the vector $\Delta\psi_k$ is equal to the vector $\Delta\xi_k$ from the center of the particle to the surface of the particle. Thus $\Delta\psi_k$ lies tangent to the surface of the particle since the particle surface is not changing. Substituting Eq. [7] into the first term on the right hand side of Eq. [1] shows the tangent vector dotted with the normal vector:

$$\int_{S_d} B\frac{\partial\psi_k}{\partial x_i}n_k d\varpi = \int_{S_d} B\frac{\partial\xi_k}{\partial x_i}n_k d\varpi = 0 \qquad [8]$$

Substituting Eq. [8] into Eq. [1]:

$$\frac{\partial}{\partial x_i}\int_{V_c} B d\lambda = \int_{S_v} B\frac{\partial\varphi_k}{\partial x_i}n_k d\zeta \qquad [9]$$

The resultant vector φ_k is the sum of the vector representing the center of the sampling volume (x_k) in addition to the vector emanating from the center of the sampling volume to the surface of the sampling volume (ω_k) – see Figure A5. Mathematically, this is shown to be:

$$\varphi_k = x_k + \omega_k \qquad [10]$$

Using the same technique outlined above, Eq. [10] can altered to form:

$$\frac{\partial\varphi_k}{\partial x_i} = \frac{\partial x_k}{\partial x_i} + \frac{\partial\omega_k}{\partial x_i} \qquad [11]$$

Here it is assumed that the sample volume boundaries do not change with a change in the position of the sample volume (see Figure A5). In other words, if the position of the sample volume changes, the volume does not rotate or deform (as shown in Figure A5), thus $\frac{\partial\omega_k}{\partial x_i} = 0$ (zero tensor). However, the partial of x_k with respect to x_i is zero for all terms other than when k = i. Thus Eq. [11] is reduced to:

$$\frac{\partial\varphi_k}{\partial x_i} = \frac{\partial x_k}{\partial x_i} = \delta_{ik} \qquad [12]$$

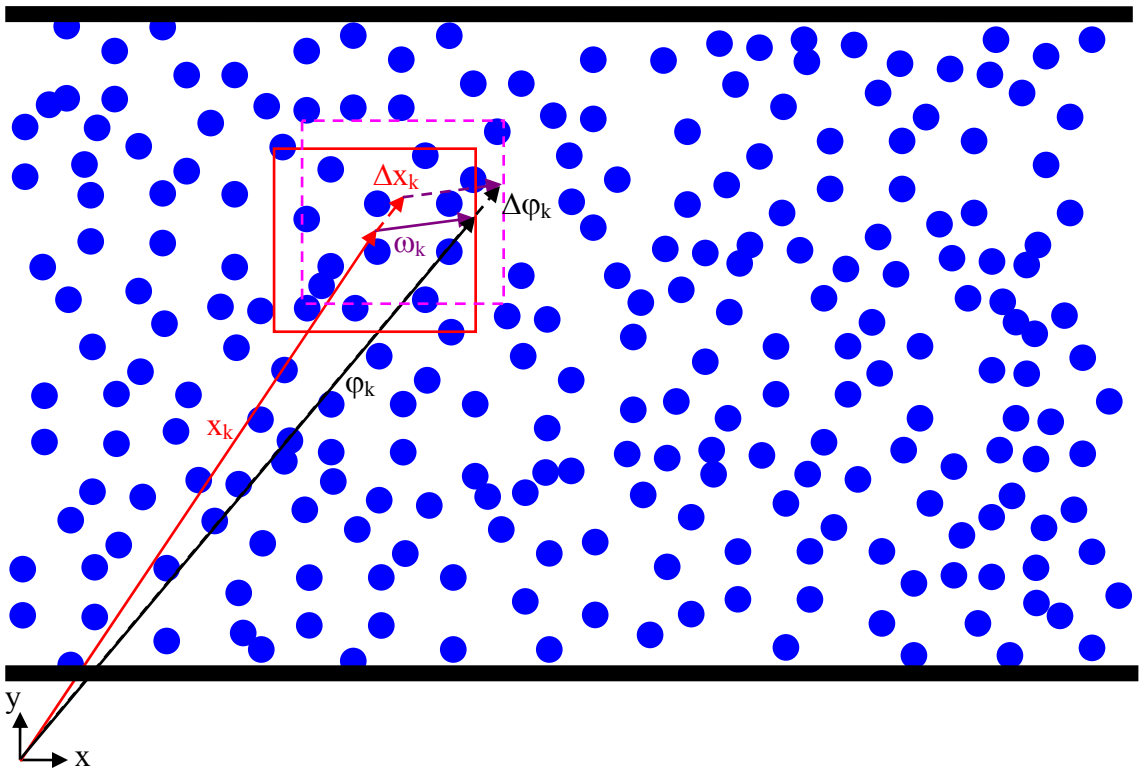

Figure A5: Representation of the change in ψ_i vector in relation to the change in position of the sampling volume

Substituting Eq. [12] into Eq. [9], and recalling that the size of the sample volume is constant and independent of position, then

$$\frac{\partial}{\partial x_i}\frac{1}{V_c}\int_{V_c} B d\lambda = \frac{1}{V_c}\int_{S_v} B\delta_{ik} n_k d\zeta \qquad [13]$$

Recall that in tensor notation, $\delta_{ik} n_k = n_i$. Also recall that Eq. [1] holds if λ = V and ζ = S. Thus Eq. [13] is then reduced to:

$$\frac{\partial}{\partial x_i}\frac{1}{V_c}\int_{V_c} B dV = \frac{1}{V_c}\int_{S_v} B n_i dS \qquad [14]$$

In order to account for the parameter flux at the particle surface, Green's theorem for the continuous phase is used:

$$\frac{1}{V_c}\int_{V_c}\frac{\partial B}{\partial x_i} dV = \frac{1}{V_c}\int_{S_v} B n_i dS + \frac{1}{V_c}\int_{S_d} B n_i dS \qquad [15]$$

Solving Eq. [15] for the surface flux term and substituting it into Eq. [14]:

$$\frac{\partial}{\partial x_i}\frac{1}{V_c}\int_{V_c} B dV = \frac{1}{V_c}\int_{V_c}\frac{\partial B}{\partial x_i}dV - \frac{1}{V_c}\int_{S_d} B n_i dS \qquad [16]$$

Eq. [16] is the volume averaged equation; it can be shown that the volume average of the gradient of parameter $B(x,y,z,t)$ is then:

$$\overline{\frac{\partial B}{\partial x_i}} = \frac{\partial \overline{B}}{\partial x_i} + \frac{1}{V_c}\int_{S_d} B n_i dS \qquad [17]$$

Taking n_i to be outward normal from the dispersed phase, then

$$\overline{\frac{\partial B}{\partial x_i}} = \frac{\partial \overline{B}}{\partial x_i} - \frac{1}{V_c}\int_{S_d} B n_i dS \qquad [18]$$

A.3 Volume Averaging the Temporal Derivative

Consider a particle such that its central position is spatially frozen and the surface varies with time only. If the mass transfer across the surface of the particle is zero, then the particle diameter is constant and the volume average of the parameter B is then:

$$\overline{\frac{\partial B}{\partial t}} = \frac{\partial \overline{B}}{\partial t} \qquad [19]$$

However, if there is mass transfer across the boundary, or if the diameter changes with time (as shown in Figure A6), then the position of the particle surface is represented by:

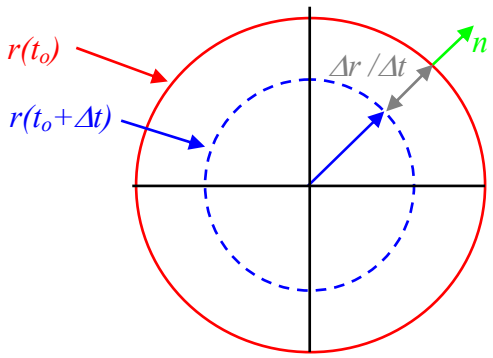

Figure A6: Representation of the change in radius of a particle for a change in time.

$$\frac{\partial}{\partial t}\int_{V_c} B dV = \int_{V_c} \frac{\partial B}{\partial t} dV + \int_{S_d} B \frac{\partial}{\partial t}(\chi_i + r_i n_i) n_i dS + \int_{S_v} B \frac{\partial \psi_i}{\partial t} n_i dS \quad [20]$$

where χ_i is the position of the center of the particle. The boundary surfaces of the continuous phase sample volume do not change with time (i.e. $\psi_i = f(x_i)$ only), thus:

$$\int_{S_v} B \frac{\partial \psi_i}{\partial t} n_i dS = 0 \quad [21]$$

If evaporation or condensation is occurring, then mass transfer is occurring at the particle surface and the radius of the surface of the particles can change will change with time. Applying Eq. [21] to Eq. [20] yields:

$$\frac{\partial}{\partial t}\int_{V_c} B dV = \int_{V_c} \frac{\partial B}{\partial t} dV + \int_{S_d} B \frac{\partial}{\partial t}(\chi_i + r_i n_i) n_i dS \quad [22]$$

Since the sampling volume is constant with time, the above equation is shown to be:

$$\frac{\partial}{\partial t}\frac{1}{V_c}\int_{V_c} B dV - \frac{1}{V_c}\int_{S_d} B \frac{\partial}{\partial t}(\chi_i + r_i n_i) n_i dS = \frac{1}{V_c}\int_{V_c} \frac{\partial B}{\partial t} dV$$

The above equation shows that n_i is in the direction from the continuous phase to the dispersed phase. It makes sense to make n_i outward normal from the dispersed phase, thus the volume average of a time derivative of a property is then shown to be:

$$\overline{\frac{\partial B}{\partial t}} = \frac{\partial \overline{B}}{\partial t} + \frac{1}{V_c}\int_{S_d} B(v_i n_i + \dot{r}_i) dS \quad [23]$$

where v_i is the velocity at the center of the particle.

APPENDIX B

FORTRAN CODE

```
C~~~~~~~~~~~~~~~~~~~~~~~~~~~~~~~~~~~~~~~~~~~~~~~~~~~~~~~~~~~~~~~~~~~~~~~~~~~~
C~~~~~~~~~~  PARTICLE_LADEN TURBULENT FLOW SOLVER ~~~~~~~~~~~~~~
C~~~~~~~~~~~~~~~~~~~~~~~~~~~~~~~~~~~~~~~~~~~~~~~~~~~~~~~~~~~~~~~~~~~~~~~~~~~~
C~~~~~~~~~~~~~~1D, Uniform Grid, Steady, Fully Developed Flow ~~~~~~~~~~~~~~~~
C~~~~~~~~~~~~~~~~~~~~~~~~~~~~~~~~~~~~~~~~~~~~~~~~~~~~~~~~~~~~~~~~~~~~~~~~~~~~

C~~~~~Variable Definitions ~~~~~~~~~~~~~~~~~~~~~~~~~~~~~~~~~~~~~~~~~~~~~~~~
C     yl = domain length in j direction
C     rho = density
C     amu = molecular viscosity
C     n = iteration number
C     jpmax = total grid points in j direction
C     jp = j direction counter
C     u = u cell velocities
C     epsu, = u-vel convergence criteria.
C     anu,asu,apu = coefficients for u-momentum equations
C     ank,ask,apk = coefficients for turb kinetic energy equation
C     ane,ase,ape = coefficients for turb dissipation equation
C     u_pre = holds the previous values of velocity for convergence check
C     y_cor = provide correct y values for file output.
C     a = used to hold coefficients for TDMA
C     b = used to hold source term in TDMA
C     utau = friction velocity
C     tauw = shear at the wall
C     pdx = piezometric pressure gradient
C     uplus = nondimensional velocity in wall coordinates
C     yplus = nondimensional length in wall coordinates
C     eps = turbulent dissipation
C     kpr,epr,amutpr = previous kin, epsilon, turb visc
C     kin = turbulent kinetic energy
C     amut = turbulent viscosity (dynamic)
C     prod = component of turbulent production--(du/dy)**2
C     tauwtl,tauwtu = turb shear at the wall (l=lower, u=upper)
C     ce1, ce2 = dissipation coefficients (1.44, 1.92)
C     sigk, sige = turbulent schmidt numbers of k and epsilon eq. (1.0, 1.3)
C~~~~~~~~~~~~~~~~~~~~~~~~~~~~~~~~~~~~~~~~~~~~~~~~~~~~~~~~~~~~~~~~~~~~~~~~~~~~~
C~~~~~~~~~~~~~~~~~~~~~~~~~~~~~~~~~~~~~~~~~~~~~~~~~~~~~~~~~~~~~~~~~~~~~~~~~~~~~

      implicit none

C     INITIALIZE GLOBAL VARIABLES
      INTEGER jpmax
      INTEGER n,jp,jn,mx,jpp,jnp,itr,itm,ito,nke
      PARAMETER (jpmax=50,mx=50)
      DOUBLE PRECISION yl,y_cor(jpmax),pdy(jpmax),yp
      DOUBLE PRECISION rho(jpmax),pdx,aspra,amas,tauw
      DOUBLE PRECISION u(jpmax),u_pre(jpmax),asu(jpmax),anu(jpmax)
      DOUBLE PRECISION apu(jpmax),amutpr(jpmax),prodpr(jpmax)
      DOUBLE PRECISION amu(jpmax),amut(jpmax),prod(jpmax)
      DOUBLE PRECISION utau(jpmax),uplus(jpmax),yplus(jpmax)
      DOUBLE PRECISION kin(jpmax),eps(jpmax),kpr(jpmax),epr(jpmax)
      DOUBLE PRECISION cmu,ce1,ce2,sigk,sige,kap,ero,gr
      DOUBLE PRECISION ru,rk,re,rp,rlamu,rlamk,rlame,rlamp,tauwtl,tauwtu
      DOUBLE PRECISION adrp,rhop(jpmax),fdr(jpmax),rer(jpmax),pno(jpmax)
      DOUBLE PRECISION alphd(jpmax),cst(jpmax),v(jpmax),betav(jpmax)
      DOUBLE PRECISION conc(jpmax),taup(jpmax),adf(jpmax)
      DOUBLE PRECISION adi(jpmax),ain(jpmax)

C     GEOMETRY PARAMETERS
      PARAMETER (yl=0.04) !chan height = m
      PARAMETER (aspra = 11.425) !chan aspect ratio (width to height)

C     PARTICLE PARAMETERS
      PARAMETER (adrp = 70.0E-6)!m, particle diameter
      PARAMETER (amas = 0.2)! mdot_d/mdot_c

C     TURBULENCE PARAMETERS
      PARAMETER (cmu=0.09,sigk=1.0,sige=1.3,kap=0.41)
      PARAMETER (ero=9.8)! wall roughness parameter (E), see Schliting, smooth=9.8
      PARAMETER (nke=0)! 0=single phase, 1=particles present
```

```
      if(nke.eq.0) then
       ce1 = 1.44
       ce2 = 1.92
      else
       ce1 = 1.44
       ce2 = 1.92
      endif

C     GRAVITY
      gr = 9.81 !m/s^2
C
C     Define density, viscosity, and particle parameters
      do 27 jp=1,jpmax
      rho(jp) = 1.2 ! kg/m^3 - fluid density
      rhop(jp) = 8800. ! kg/m^3 - particle density
      amu(jp) = 1.8E-5 ! kg/m*s
      fdr(jp) = 1.0 ! drag factor
      rer(jp) = 1.0 ! relative reynolds number
      pno(jp) = 10000 ! number of particles
      alphd(jp) = 0.000001 ! dispersed phase volume fraction
   27 continue

      do jp=2,jpmax
      u_pre(jp)=0.0
      enddo

C     SPECIFY THE PRESSURE GRADIENT
C     this term is manually iterated
      pdx = -14.28 !Pa/m  (peiziometric) pressure gradient (dp/dx)

C     CONVERGENCE CRITERIA (u-velocity)
      rlamu=0.001
      rlamk=0.001
      rlamp=0.001
      rlame=0.001

C     SETUP THE STRUCTURED OR UNSTRUCTURED GRID
      call grid(jpmax,yl,pdy,y_cor)

C     DETERMINE SHEAR STRESS AT THE WALL, INITIALIZE U+ AND Y+ VALUES
      tauwtl = -pdx*yl/2.*aspra/(1.+aspra)
      tauwtu = -pdx*yl/2.*aspra/(1.+aspra)
      utau(2) = sqrt(tauwtl/rho(2))
      utau(jpmax-1) = sqrt(tauwtu/rho(jpmax-1))
      yplus(2) = rho(2)/amu(2)*(y_cor(2))*utau(2)
      if(yplus(2).lt.1.0) then
      print*, 'yplus(2) =',yplus(2)
      pause
      else
      do jp = 2,jpmax/2
       jn = jpmax+1-jp
      yplus(jp) = rho(jp)/amu(jp)*(y_cor(jp))*utau(2)
      uplus(jp) = 1/kap*dlog(ero*yplus(jp))
      yplus(jn) = yplus(jp)
      uplus(jn) = uplus(jp)
      enddo
      yplus(1) = 0.
      yplus(jpmax) = 0.
      uplus(1) = 0.
      uplus(jpmax) = 0.
      endif

C     SETTING WALL BOUNDARY CONDITIONS
      u(1) = 0.
      u(jpmax) = 0.
      u(2) = uplus(2)*utau(2)
      u(jpmax-1) = uplus(jpmax-1)*utau(2)
      do jp = 3,jpmax-2
      u(jp) = uplus(jp)*utau(2)
      enddo
```

```
      kin(1) = 0.
      kin(jpmax) = 0.
      kin(2) = utau(2)**2/sqrt(cmu)
      kin(jpmax-1) = utau(jpmax-1)**2/sqrt(cmu)
      eps(2) = utau(2)**3*uplus(2)/(pdy(2)/2.)
      eps(jpmax-1) = utau(jpmax-1)**3*uplus(jpmax-1)/(pdy(jpmax-1)/2.)
      eps(1) = eps(2)
      eps(jpmax) = eps(jpmax-1)
      amut(1) = 0.
      amut(2) = cmu*kin(2)**2/eps(2)
      amut(jpmax-1) = cmu*kin(jpmax-1)**2/eps(jpmax-1)
      amut(jpmax) = 0.

     open(9,file='y-u-plus.dat')
     write(9,*)'j,ycor,yplus,uplus,u'
     do 411 jp=1,jpmax
     write(9,410)jp,',',y_cor(jp),',',yplus(jp),',',uplus(jp),',',u(jp)
  410 format(i8,a2,f15.10,a2,f15.10,a2,f15.10,a2,f15.10)
  411 continue
     close(unit=9)

C    INITIALIZING TURBULENCE PARAMETERS K, EPSILON AND TURB VISC.
     do jp = 2,jpmax-1
     v(jp) = 1. !this cannot be initialized as zero
     kin(jp) = kin(2)
     eps(jp) = eps(2)
     amut(jp) = amut(2)
     amutpr(jp) = amut(jp)
     kpr(jp) = kin(jp)
     epr(jp) = eps(jp)
     enddo

C    SOLVE FOR THE VELOCITY GRADIENTS IN THE PRODUCTION TERM
     call bousq(jpmax,u,prod,kin,amut,rho,pdy,eps,utau,kap)
     if(nke.eq.0) goto 189
     call partv(jpmax,mx,u,v,y_cor,pdy,rho,gr,rer,adrp,fdr,amu,
    1               pno,alphd,cst,rhop,betav,amas,conc,yl,taup)
  189 continue

C    INITIALIZING ITERATION COUNTER
     ito = 0
C=====MAIN ITERATION LOOP=============================================
C
  200 ito = ito + 1

C    SETTING PREVIOUS VELOCITY, TKE AND TURB VISC VALUES VALUES
     do jp=2,jpmax-1
     u_pre(jp)=u(jp)
     kpr(jp) = kin(jp)
     epr(jp) = eps(jp)
     prodpr(jp) = prod(jp)
     amutpr(jp) = amut(jp)
     enddo
C
     do 230 itr = 1,100

C    SOLVE TURBULENT DISSIPATION EQUATION
     call diss(mx,jpmax,pdy,epr,kpr,eps,tauwtl,tauwtu,nke,
    1  u,rho,amut,prod,kin,amu,y_cor,ce1,ce2,sige,cmu,kap,amutpr,
    1  fdr,alphd,adrp,v,rer,cst,utau,uplus,betav,ito)

C    UPDATE THE TURBULENT VISCOSITY, UPLUS AND YPLUS
     do jp = 2,jpmax-1
     amut(jp) = rho(jp)*cmu*kin(jp)**2/eps(jp)
     enddo
  230 continue

C    SOLVE TURBULENT KINETIC ENERGY EQUATION
     call kinen(mx,jpmax,pdy,sigk,cmu,kin,utau,kap,tauwtl,tauwtu,
    1 rho,amut,prod,eps,amu,u,y_cor,uplus,kpr,epr,amutpr,betav,nke,
```

```
     1 v,alphd,ito)

C    UPDATE THE TURBULENT VISCOSITY, UPLUS AND YPLUS
     do jp = 2,jpmax-1
     amut(jp) = rho(jp)*cmu*kin(jp)**2/eps(jp)
     enddo

     do 240 itr = 1,1000
C    SOLVE FOR CELL PARTICLE-VELOCITY
     if(nke.eq.0) goto 235
     call partv(jpmax,mx,u,v,y_cor,pdy,rho,gr,rer,adrp,fdr,amu,
    1           pno,alphd,cst,rhop,betav,amas,conc,yl,taup)
  235 continue

C    SOLVE FOR CELL U-VELOCITY
     call uvel(mx,rho,amu,pdy,kin,pdx,y_cor,
    1   u_pre,u,jpmax,amut,cmu,uplus,amutpr,tauwtl,tauwtu,nke,
    1   v,alphd,rhop,fdr,taup,eps,ito)
  240 continue

C    SOLVE FOR THE VELOCITY GRADIENTS IN THE PRODUCTION TERM
     call bousq(jpmax,u,prod,kin,amut,rho,pdy,eps,utau,kap)

C    UPDATE U+ AND Y+
     do itr = 1,100
      tauw = rho(2)*cmu**0.25*kin(2)**0.5/uplus(2)*u(2)
      tauwtl = tauw
      tauwtu = tauw
      utau(2) = sqrt(tauw/rho(2))
      yplus(2) = rho(2)/amu(2)*(y_cor(2))*utau(2)
      if(yplus(2).le.11.63) then
      uplus(2) = yplus(2)
      endif
C
      if(yplus(2).gt.11.63) then
      uplus(2) = 1/kap*dlog(ero*yplus(2))
      endif
      yplus(jpmax-1) = rho(jpmax-1)/amu(jpmax-1)*(y_cor(2))*utau(2)
      if(yplus(jpmax-1).le.11.63) then
      uplus(jpmax-1)=yplus(jpmax-1)!*(1.-0.25*(yplus(jpmax-1)/14.5)**3)
      endif
C
      if(yplus(jpmax-1).gt.11.63) then
      uplus(jpmax-1) = 1/kap*dlog(ero*yplus(jpmax-1))
      endif
      enddo
C
      do jp = 3,jpmax-2
       jn = jpmax+1-jp
      uplus(jp) = u(jp) / utau(2)
      if(jp.le.jpmax/2) then
      yplus(jp) = y_cor(jp)*utau(2)*rho(jp)/amu(jp)
      yplus(jn) = yplus(jp)
      endif
      enddo

C    CHECK THE CONVERGENCE OF THE SOLUTION
     ru = 0.
     rk = 0.
     rp = 0.
     re = 0.
     do jpp=2,jpmax-1
     ru=ru+(u(jpp)-u_pre(jpp))**2
     rk=rk+(kin(jpp)-kpr(jpp))**2
     rp=rp+(prod(jpp)-prodpr(jpp))**2
     re=re+(eps(jpp)-epr(jpp))**2
     enddo
     ru = sqrt(ru/(jpmax-2))
     rk = sqrt(rk/(jpmax-2))
     rp = sqrt(rp/(jpmax-2))
```

```
      re = sqrt(re/(jpmax-2))
      if(ru.gt.rlamu.or.rk.gt.rlamk.or.rp.gt.rlamp.
     1or.re.gt.rlame) then
      if (mod(ito,20).eq.0)then
      write(*,*)'iteration number',ito
      print*,'residuals are not converged'
      write(*,*)'u-res  k-res  prod-res  eps-res'
      write(*,*) ru,rk,rp,re
      print*,'velocity =',u(2),u(3),u(4),u(jpmax/2)
      print*,'Tau_wall_turb =',tauw
      print*,'u+ =',uplus(2),'  y+ =',yplus(2)
      print*,'KE =',kin(2),kin(3),kin(4),kin(10)
      print*,'DISS =',eps(2),eps(3),eps(4),eps(10)
      print*,'PROD=',prod(2),prod(3),prod(4),prod(10)
      print*,'AMUT=',amut(2),amut(3),amut(4),amut(10)
      endif
      goto 200
      endif
C     PRINT FINAL VALUES
      write(*,*)'final values'
      write(*,*)'u-res  k-res  prod-res  eps-res'
      write(*,*) ru,rk,rp,re
      print*, u(2)
      print*,'Tau_wall =',tauw
      print*,'u+ =',uplus(2),'  y+ =',yplus(2)
      write(*,*)'total iterations: ',ito,'\n'

C     WRITE DATA TO FILES
      open(73,file='vel2.dat')
      write(73,*) 'TITLE = "1-D CHANNEL FLOW"'
      write(73,*) 'VARIABLES = "Y-DIR", "U", "UPLUS", "YPLUS","KE",
     1 "DISS"'
      write(73,*) 'ZONE T = "VEL", J = ',jpmax,
     & ', F = POINT'
      do  jp=1,jpmax
      write(73,450)y_cor(jp),u(jp),uplus(jp),yplus(jp),kin(jp),eps(jp),
     1amut(jp),v(jp),alphd(jp),cst(jp),rer(jp),prod(jp)
  450 FORMAT(2X,F12.6,2X,F12.6,2X,F12.6,2X,F20.14,2X,F30.14,2X,F30.14,
     12X,F30.14,2X,F12.6,2X,F20.14,2X,F20.14,2X,F20.14,2X,F20.6)
      enddo
      close(unit = 73)

      write(*,*) 'Program is done'

      STOP
      END

C~~~~~~~~~~~~~~~~~~~~~~~~~~~~~~~~~~~~~~~~~~~~~~~~~~~~~~~~~~~~~~~~~~~~~~~~~~~~~~~
C~~~~~~~~~~~~~~~~~~~~~~~~~~ END MAIN PROGRAM ~~~~~~~~~~~~~~~~~~~~~~~~~~~~~~~~~~~~
C~~~~~~~~~~~~~~~~~~~~~~~~~~~~~~~~~~~~~~~~~~~~~~~~~~~~~~~~~~~~~~~~~~~~~~~~~~~~~~~


C~~~~~~~~~~~~~~~~~~~~~~~~~~~~~~~~~~~~~~~~~~~~~~~~~~~~~~~~~~~~~~~~~~~~~~~~~~~~~~~
C~~~~~~~~~~~~~~~~~~~~~~~~~~~~~~~~~~~~~~~~~~~~~~~~~~~~~~~~~~~~~~~~~~~~~~~~~~~~~~~
C~~~~~~~~~~~~~~~~~~~~~~~~~~~~~~~~~~~~~~~~~~~~~~~~~~~~~~~~~~~~~~~~~~~~~~~~~~~~~~~


      subroutine grid(jpmax,yl,pdy,y_cor)

      INTEGER jpmax,jp
      DOUBLE PRECISION pdy(jpmax),yl,yint
      DOUBLE PRECISION y_cor(jpmax)

C     UNIFORM GRID----------------------------------------------------
      do 13 jp=1,jpmax
      pdy(jp) = yl/(float(jpmax-2))
   13 continue

      do j=1,jpmax
      if (j.eq.1) then
      y_cor(j)=0.0
```

```
      elseif (j.eq.2) then
      y_cor(j)=pdy(1)/2.
      elseif (j.gt.2.and.j.lt.jpmax)  then
      y_cor(j)=y_cor(j-1)+pdy(j)
      elseif (j.eq.jpmax) then
      y_cor(j)=y_cor(j-1)+pdy(j)/2.0
      endif
      enddo

C-----------------------------------------------------------------------

      open(9,file='grid.dat')
      write(9,*)'j,ycor,pdy'
      do 422 jp=1,jpmax
      write(9,409)jp,',',y_cor(jp),',',pdy(jp)
  409 format(i8,a2,f15.10,a2,f15.10)
  422 continue
      close(unit=9)

      RETURN
      END

C~~~~~~~~~~~~~~~~~~~~~~~~~~~~~~~~~~~~~~~~~~~~~~~~~~~~~~~~~~~~~~~~~~~~~~~~~~~
C~~~~~~~~~~~~~~~~~~~ U-VELOCITY SOLVER SUBROUTINE ~~~~~~~~~~~~~~~~~~~~~~~~~~
C~~~~~~~~~~~~~~~~~~~~~~~~~~~~~~~~~~~~~~~~~~~~~~~~~~~~~~~~~~~~~~~~~~~~~~~~~~~

      subroutine uvel(mx,rho,amu,pdy,kin,pdx,y_cor,
     1  u_pre,u,jpmax,amut,cmu,uplus,amutpr,tauwtl,tauwtu,nke,
     1  v,alphd,rhop,fdr,taup,eps,ito)
      INTEGER jp,jpmax,k,nke,ito
      DOUBLE PRECISION asu(jpmax),anu(jpmax),apu(jpmax)
      DOUBLE PRECISION u(jpmax),uplus(jpmax),kin(jpmax),u_pre(jpmax)
      DOUBLE PRECISION pdy(jpmax),y_cor(jpmax),uvpri(jpmax),cmu,pdx
      DOUBLE PRECISION a(mx,3),b(mx),wu,pi,alp,sc(jpmax),sp(jpmax)
      DOUBLE PRECISION amup(jpmax),fdr(jpmax),v(jpmax)
      DOUBLE PRECISION rho(jpmax),amu(jpmax),amut(jpmax),amutpr(jpmax)
      DOUBLE PRECISION fs3,fn2,fnj2,fsj1,tauwtl,tauwtu
      DOUBLE PRECISION taup(jpmax),alphd(jpmax),rhop(jpmax),eps(jpmax)

      alp = 1.0
      do jp=1,jpmax
      if (ito.gt.500000) then
      amup(jp) = amut(jp)
      else
      amup(jp) = amut(jp)+amu(jp)
      endif
      enddo
C     Velocity under relaxation factor
      wu = 0.8

      pi = 4.0*atan(1.0)
C     Setting the coefficients

      do 12 jp=3,jpmax-2
      anu(jp)=2.0*(amup(jp)*amup(jp+1)/(amup(jp)+amup(jp+1)))
     1 /(pdy(jp))
      asu(jp)=2.0*(amup(jp)*amup(jp-1)/(amup(jp)+amup(jp-1)))
     1 /(pdy(jp))
      if(nke.eq.0) then
      sp(jp)=0.
      else
      sp(jp)= alphd(jp)/(1-alphd(jp))*rhop(jp)*fdr(jp)/taup(jp)
      endif
      apu(jp)=(anu(jp)+asu(jp)+sp(jp)*pdy(jp))/wu
      if(apu(jp).lt.0.) print*,'apu =',apu(jp)
   12 continue

      anu(2)=2.0*(amup(2)*amup(3)/(amup(2)+amup(3)))
     1 /(pdy(2))
      asu(2)=0.
```

```
      if(nke.eq.0) then
      sp(2)= rho(2)*cmu**0.25*kin(2)**0.5/uplus(2)
      else
      sp(2)= rho(2)*cmu**0.25*kin(2)**0.5/uplus(2)
     1      +alphd(2)/(1-alphd(2))*rhop(2)*fdr(2)/taup(2)*pdy(2)
      endif
      apu(2)=(anu(2)+asu(2)+sp(2))/wu

      anu(jpmax-1)=0.
      asu(jpmax-1)=2.0*(amup(jpmax-1)*amup(jpmax-2)/
     1 (amup(jpmax-1)+amup(jpmax-2)))/(pdy(jpmax-1))
      if(nke.eq.0) then
      sp(jpmax-1)= rho(jpmax-1)*cmu**0.25*kin(jpmax-1)**0.5
     1 /uplus(jpmax-1)
      else
      sp(jpmax-1)= rho(jpmax-1)*cmu**0.25*kin(jpmax-1)**0.5
     1 /uplus(jpmax-1)
     1 +alphd(jpmax-1)/(1-alphd(jpmax-1))*rhop(jpmax-1)
     1 *fdr(jpmax-1)/taup(jpmax-1)*pdy(jpmax-1)
      endif
      apu(jpmax-1)=(anu(jpmax-1)+asu(jpmax-1)+sp(jpmax-1))
     1 /wu

C~~~~~TDMA~~~~~~~~~~~~~~~~~~~~~~~~~~~~~~~~~~~~~~~~~~~~~~~~~~~~~~~~~~~~~~~~~~~~~~~
      do 17 jp=2,jpmax-1
      k=jp-1
      a(k,3)=-anu(jp)
      a(k,2)=apu(jp)
      a(k,1)=-asu(jp)
      if(nke.eq.0) then
      b(k)=-pdx*pdy(jp)+(1.-wu)*apu(jp)*u_pre(jp)
      else
      b(k)=-pdx*pdy(jp)
     1 +alphd(jp)/(1.-alphd(jp))*rhop(jp)*fdr(jp)/taup(jp)*v(jp)*pdy(jp)
     1 +(1.-wu)*apu(jp)*u_pre(jp) !particle source is linearized source
      endif
   17 continue

C     Call TDMA
      call thomas(jpmax-2,mx,a,b)
      do 18 jp=2,jpmax-1
   18 u(jp)=b(jp-1)

      RETURN
      END
C
C~~~~~~~~~~~~~~~~~~~~~~~~~~~~~~~~~~~~~~~~~~~~~~~~~~~~~~~~~~~~~~~~~~~~~~~~~~~~~~~
C~~~~~~~~~~~~~~~~~~ PARTICLE VELOCITY SUBROUTINE ~~~~~~~~~~~~~~~~~~~~~~~~~~~~~~
C~~~~~~~~~~~~~~~~~~~~~~~~~~~~~~~~~~~~~~~~~~~~~~~~~~~~~~~~~~~~~~~~~~~~~~~~~~~~~~~
      subroutine partv(jpmax,mx,u,v,y_cor,pdy,rho,gr,rer,adrp,fdr,amu,
     1              pno,alphd,cst,rhop,betav,amas,conc,yl,taup)

      INTEGER jpmax,mx,jp,itrn
      DOUBLE PRECISION y_cor(jpmax),pdy(jpmax),fdr(jpmax),pno(jpmax)
      DOUBLE PRECISION cst(jpmax),taup(jpmax),betav(jpmax),vpr(jpmax)
      DOUBLE PRECISION u(jpmax),rho(jpmax),amu(jpmax),alphd(jpmax),yl
      DOUBLE PRECISION v(jpmax),rhop(jpmax),rer(jpmax),adrp,gr,sumv,ucl
      DOUBLE PRECISION resv,avelp(jpmax),tauf(jpmax),amas,conc(jpmax)
      REAL pi
       pi = 4.0*atan(1.0)

  101 continue
      sumv = 0.

      do 10 jp = 2,jpmax-1
      vpr(jp) = v(jp)
      avelp(jp) = rho(jp)*u(jp)/(rhop(jp)*v(jp))
C     Particle volume fraction
      alphd(jp) = amas*avelp(jp)/(1+amas*avelp(jp))
C     Relative Reynolds number
```

```
      rer(jp) = rho(jp)/amu(jp)*abs(u(jp)-v(jp))*adrp
C     Drag fractor
      fdr(jp) = 1.0 + 0.15*rer(jp)**0.687
C     Particle response time
      taup(jp) = rhop(jp)*adrp**2/(18.*amu(jp))
C     Fluid reponse time
      tauf(jp) = yl/u(jp)
C     Particle concentration
      conc(jp) = alphd(jp)*rhop(jp)/((1-alphd(jp))*rho(jp))
C     Particle Number per unit Volume
      pno(jp) = alphd(jp)/(pi/6*adrp**3)
C     hydraulic drag factor
      betav(jp) = alphd(jp)*rhop(jp)*fdr(jp)/taup(jp)
C
C     TERMINAL VELOCITY EQN
C      v(jp) = gr*adrp**2*(rhop(jp)-rho(jp))/(18.0*amu(jp)*fdr(jp))
C     1 + u(jp)
C
C     FIXED VELOCITY EQN - Determined from Kulick's data
      if(jp.le.jpmax/2) then
       jn = jpmax+1-jp
       if(amas.eq.0.1) then
       v(jp) = -5625.4*y_cor(jp)**2 + 266.5*y_cor(jp) + 5.6956
       else
       v(jp) = -2460.2*y_cor(jp)**2 + 144.13*y_cor(jp) + 6.153
       endif
       v(jn) = v(jp)
      endif
C     Concentration over Stokes Number (C/St)
      cst(jp) = conc(jp)*tauf(jp)/taup(jp)
      sumv = sumv+(v(jp)-vpr(jp))**2
   10 continue
      resv = sqrt(sumv)
      if(resv.gt.1.E-9) goto 101
      RETURN
      END

C ====== TURBULENCE SUROUTINES ==========================================
C~~~~~~~~~~~~~~~~~~~~~~~~~~~~~~~~~~~~~~~~~~~~~~~~~~~~~~~~~~~~~~~~~~~~~~~~
C~~~~~~~~~~~~~~~~ BOUSINESQ APPROX. AND PRODUCTION TERM ~~~~~~~~~~~~~~~~
C~~~~~~~~~~~~~~~~~~~~~~~~~~~~~~~~~~~~~~~~~~~~~~~~~~~~~~~~~~~~~~~~~~~~~~~~
      subroutine bousq(jpmax,u,prod,kin,amut,rho,pdy,eps,utau,kap)
      INTEGER jpmax,jp
      DOUBLE PRECISION u(jpmax),pdy(jpmax),amut(jpmax),rho(jpmax)
      DOUBLE PRECISION prod(jpmax),kin(jpmax),eps(jpmax)
      DOUBLE PRECISION adudy(jpmax),utau(jpmax),kap

C     Determine the velocity gradients (central diff scheme)
      do jp=3,jpmax-2

      adudy(jp) = (u(jp+1)-u(jp-1))/(2.0*pdy(jp))
      prod(jp) = (adudy(jp)*adudy(jp))

      if(prod(jp).lt.0.) print*,'prod <0',jp,prod(jp)
      enddo
C
      prod(2) = (utau(2)/(kap*pdy(2)/2.))**2
      prod(jpmax-1) = (utau(jpmax-1)/(kap*pdy(2)/2.))**2

      RETURN
      END
C
C~~~~~~~~~~~~~~~~~~~~~~~~~~~~~~~~~~~~~~~~~~~~~~~~~~~~~~~~~~~~~~~~~~~~~~~~
C~~~~~~~~~~~~ TURBULENT KINETIC ENERGY EQN SOLVER SUBROUTINE ~~~~~~~~~~~
C~~~~~~~~~~~~~~~~~~~~~~~~~~~~~~~~~~~~~~~~~~~~~~~~~~~~~~~~~~~~~~~~~~~~~~~~
      subroutine kinen(mx,jpmax,pdy,sigk,cmu,kin,utau,kap,tauwtl,tauwtu,
     1 rho,amut,prod,eps,amu,u,y_cor,uplus,kpr,epr,amutpr,betav,nke,
     1 v,alphd,ito)

      INTEGER mx,jpmax,jp,nke,ito
```

```
      DOUBLE PRECISION pdy(jpmax),amut(jpmax),amup(jpmax),rho(jpmax)
      DOUBLE PRECISION ask(jpmax),ank(jpmax),apk(jpmax),sp(jpmax)
      DOUBLE PRECISION sc(jpmax),sigk,cmu,kap,pi,adrp,wk,alp,fs3,fnj2
      DOUBLE PRECISION atk(mx,3),btk(mx),kin(jpmax),utau(jpmax)
      DOUBLE PRECISION amutpr(jpmax),tauwtl,tauwtu
      DOUBLE PRECISION prod(jpmax),eps(jpmax),amu(jpmax),fdr(jpmax)
      DOUBLE PRECISION pno(jpmax),alphd(jpmax),betav(jpmax)
      DOUBLE PRECISION uplus(jpmax),y_cor(jpmax),u(jpmax),v(jpmax)
      DOUBLE PRECISION kpr(jpmax),epr(jpmax),amun(jpmax),amus(jpmax)

      wk = 0.6
      pi = 4.0*atan(1.0)

      do jp=2,jpmax-1
      if(ito.gt.500000) then
      amun(jp) = amut(jp+1)/sigk
      amus(jp) = amut(jp-1)/sigk
      amup(jp) = amut(jp)/sigk
      else
      amun(jp) = amut(jp+1)/sigk+amu(jp+1)
      amus(jp) = amut(jp-1)/sigk+amu(jp-1)
      amup(jp) = amut(jp)/sigk+amu(jp)
      endif
      enddo

C     Setting the center region coefficients for TKE
      do 2 jp=3,jpmax-2
      ank(jp)=2.0*(amup(jp)*amun(jp)/(amup(jp)+amun(jp)))
     1 /(pdy(jp))
      ask(jp)=2.0*(amup(jp)*amus(jp)/(amup(jp)+amus(jp)))
     1 /(pdy(jp))
      if(nke.eq.0) then
      sp(jp) = rho(2)**2*cmu*kpr(jp)/amut(jp)
      else
      sp(jp) = rho(2)**2*cmu*kpr(jp)/amut(jp)
      endif

      if(sp(jp).lt.0.) print*,'sp-k',jp,sp(jp)
      apk(jp)=(ank(jp)+ask(jp)+sp(jp)*pdy(jp))/wk
      if(apk(jp).lt.0.) print*,'apk =',apk(jp)
    2 continue
      ask(2) = 0.
      ank(2) = 2.0*(amup(2)*amun(2)/(amup(2)+amun(2)))
     1 /(pdy(2))
      if(nke.eq.0) then
      sp(2) = rho(2)*cmu**0.75*kpr(2)**0.5*uplus(2)/(pdy(2)/2.)
      else
      sp(2) = rho(2)*cmu**0.75*kpr(2)**0.5*uplus(2)/(pdy(2)/2.)
      endif
      apk(2) = (ask(2)+ank(2)+sp(2)*pdy(2))/wk

      ask(jpmax-1) =2.0*(amup(jpmax-1)*amus(jpmax-1)
     1 /(amup(jpmax-1)+amus(jpmax-1)))/(pdy(jpmax-1))
      ank(jpmax-1) = 0.
      if(nke.eq.0) then
      sp(jpmax-1) = rho(jpmax-1)*cmu**0.75*kpr(jpmax-1)**0.5
     1 *uplus(jpmax-1)/(pdy(jpmax-1)/2.)
      else
      sp(jpmax-1) = rho(jpmax-1)*cmu**0.75*kpr(jpmax-1)**0.5
     1 *uplus(jpmax-1)/(pdy(jpmax-1)/2.)
      endif
      apk(jpmax-1)=(ask(jpmax-1)+ank(jpmax-1)+sp(jpmax-1)
     1 *pdy(jpmax-1))/wk

C~~~~TDMA~~~~~~~~~~~~~~~~~~~~~~~~~~~~~~~~~~~~~~~~~~~~~~~~~~~~~~~~~~~~~~~~~~~~~~~

      do 31 jp=2,jpmax-1
      k=jp-1
      atk(k,1)=-ask(jp)
      atk(k,2)=apk(jp)
```

```
      atk(k,3)=-ank(jp)
      if(nke.eq.0) then
      sc(jp) = amut(jp)*prod(jp)
      else
      sc(jp) = amut(jp)*prod(jp)
     1 + betav(jp)
     1 *(u(jp)-v(jp))**2
     1 /((1-alphd(jp)))
      endif
      if(sc(jp).lt.0.) print*,'sc-k',jp,sc(jp)
      btk(k)= sc(jp)*pdy(jp)
     1 +apk(jp)*kpr(jp)*(1.-wk)

   31 continue
      if(nke.eq.0) then
      btk(1)=tauwtl*u(2)/(pdy(2)/2.)*pdy(2)
     1 +apk(2)*kpr(2)*(1.-wk)

      else
      btk(1)=tauwtl*u(2)/(pdy(2)/2.)*pdy(2)
     1 *1./sqrt(1.-(1./(1.+utau(2)**3/(kap
     1 *pdy(2)/2.*betav(2)/((1.-alphd(2))*rho(2))*(u(2)-v(2))**2))))
     1 + apk(2)*kpr(2)*(1.-wk)
      endif

      btk(jpmax-2)=btk(1)

C     CALL TDMA
      call thomas(jpmax-2,mx,atk,btk)
      do 32 jp=2,jpmax-1
      kin(jp)=btk(jp-1)
   32 continue


      RETURN
      END


C~~~~~~~~~~~~~~~~~~~~~~~~~~~~~~~~~~~~~~~~~~~~~~~~~~~~~~~~~~~~~~~~~~~~~~~~~~~~~~~
C~~~~~~~~~~~~~ TURBULENT DISSIPATION EQN SOLVER SUBROUTINE ~~~~~~~~~~~~
C~~~~~~~~~~~~~~~~~~~~~~~~~~~~~~~~~~~~~~~~~~~~~~~~~~~~~~~~~~~~~~~~~~~~~~~~~~~~~~~
      subroutine diss(mx,jpmax,pdy,epr,kpr,eps,tauwtl,tauwtu,nke,
     1  u,rho,amut,prod,kin,amu,y_cor,ce1,ce2,sige,cmu,kap,amutpr,
     1 fdr,alphd,adrp,v,rer,cst,utau,uplus,betav,ito)

      INTEGER mx,jpmax,jp,nke,ito
      DOUBLE PRECISION y_cor(jpmax),pdy(jpmax),amut(jpmax),amup(jpmax)
      DOUBLE PRECISION ase(jpmax),ane(jpmax),ape(jpmax),rho(jpmax)
      DOUBLE PRECISION amutpr(jpmax),u(jpmax),sc(jpmax),sp(jpmax)
      DOUBLE PRECISION a(mx,3),b(mx),kin(jpmax),fdr(jpmax),v(jpmax)
      DOUBLE PRECISION prod(jpmax),eps(jpmax),amu(jpmax),alphd(jpmax)
      DOUBLE PRECISION kpr(jpmax),epr(jpmax),rer(jpmax),ce3(jpmax)
      DOUBLE PRECISION ce1,ce2,cmu,sige,kap,pi,adrp,alp,ce2pr(jpmax)
      DOUBLE PRECISION tauwtl,tauwtu,amun(jpmax),amus(jpmax),cst(jpmax)
      DOUBLE PRECISION utau(jpmax),uplus(jpmax),betav(jpmax),cep
      REAL we
      cep = 0.058
      we = 0.6
      pi = 4.0*atan(1.0)

C     Setting the turbulent viscosity
      do jp=2,jpmax-1
      if(ito.gt.500000) then
      amun(jp) = amut(jp+1)/sige
      amus(jp) = amut(jp-1)/sige
      amup(jp) = amut(jp)/sige
      else
      amun(jp) = amut(jp+1)/sige+amu(jp+1)
      amus(jp) = amut(jp-1)/sige+amu(jp-1)
      amup(jp) = amut(jp)/sige+amu(jp)
```

```
      endif
      enddo

C     Setting the coefficients for dissipation in the central domain
      do 2 jp=3,jpmax-2
      ane(jp)=2.0*(amup(jp)*amun(jp)/(amup(jp)+amun(jp)))
     1 /(pdy(jp))
      ase(jp)=2.0*(amup(jp)*amus(jp)/(amup(jp)+amus(jp)))
     1 /(pdy(jp))
      if(nke.eq.0) then
      sp(jp) = dmax1((2.*rho(jp)**2*ce2*cmu*kin(jp)/amut(jp)),0.D0)
      else
      sp(jp) = dmax1((2.*rho(jp)**2*ce2*cmu*kin(jp)/amut(jp)),0.D0)
      endif

      if(sp(jp).lt.0.) print*, 'sp-e',jp,sp(jp)
      ape(jp)=(ane(jp)+ase(jp)+sp(jp)*pdy(jp))/we
      if(ape(jp).lt.0.) print*,'ape =',ape(jp)
      ce2pr(jp)=0.362*cst(jp)**0.76+ce2
      ce3(jp)=cep*rer(jp)**1.416*ce2pr(jp)
    2 continue

      ane(2) = 2.0*(amup(2)*amun(2)/(amup(2)+amun(2)))
     1 /(pdy(2))
      ase(2) = 0.
      if(nke.eq.0) then
      sp(2) = 10**30
      else
      sp(2) = 10**30
      endif
      ape(2) = (ane(2)+ase(2)+sp(2))/we
      ce2pr(2)=0.362*cst(2)**0.76+ce2
      ce3(2)=cep*rer(2)**1.416*ce2pr(2)

      ane(jpmax-1) = 0.
      ase(jpmax-1) = 2.0*(amup(jpmax-1)*amus(jpmax-1)
     1 /(amup(jpmax-1)+amus(jpmax-1)))/(pdy(jpmax-1))
      if(nke.eq.0) then
      sp(jpmax-1) = 10**30
      else
      sp(jpmax-1) = 10**30
      endif
      ape(jpmax-1)=(ane(jpmax-1)+ase(jpmax-1)+sp(jpmax-1)
     1 )/we
      ce2pr(jpmax-1)=0.362*cst(jpmax-1)**0.76+ce2
      ce3(jpmax-1)=cep*rer(jpmax-1)**1.416*ce2pr(jpmax-1)

C~~~~~TDMA~~~~~~~~~~~~~~~~~~~~~~~~~~~~~~~~~~~~~~~~~~~~~~~~~~~~~~~~~~~~~~~~~~~~~~~~~~~~
      do 31 jp=2,jpmax-1
      k=jp-1
      a(k,1)=-ase(jp)
      a(k,2)=ape(jp)
      a(k,3)=-ane(jp)
      if(nke.eq.0) then
      sc(jp)=ce1*rho(jp)*prod(jp)*kin(jp)*cmu
     1 +ce2*rho(jp)**3*cmu**2*kin(jp)**3/amut(jp)**2
      else
      sc(jp)=ce1*rho(jp)*prod(jp)*kin(jp)*cmu
     1 + ce2pr(jp)*rho(jp)**3*cmu**2*kin(jp)**3/amut(jp)**2
     1 + 6.*rho(jp)*ce3(jp)*alphd(jp)*(amu(jp)/rho(jp))**2
     1 *(u(jp)**2 + v(jp)**2 - 2*u(jp)*v(jp)+ 2*kin(jp))
     1 *fdr(jp)/(pi*adrp**4*(1-alphd(jp)))
      endif

      if(sc(jp).lt.0.) print*,'sc-e', jp,sc(jp)
      b(k)=sc(jp)*pdy(jp)
     1 +ape(jp)*epr(jp)*(1.-we)
   31 continue
      if(nke.eq.0) then
       b(1)=cmu**0.75*kin(2)**1.5/(kap*pdy(2)/2.)*10**30
```

```
     1 +ape(2)*epr(2)*(1.-we)
      else
      b(1)=cmu**0.75*kin(2)**1.5/(kap*pdy(2)/2.)*10**30
     1 + betav(2)*(u(2)-v(2))**2/(rho(2)*(1-alphd(2)))*10**30
     1 + ape(2)*epr(2)*(1.-we)
      endif
      b(jpmax-2)=b(1)

C     CALL TDMA
      call thomas(jpmax-2,mx,a,b)
      do 32 jp=2,jpmax-1
       eps(jp)=b(jp-1)
   32 continue

      RETURN
      END

C===== END TURB SUBROUTINE ==========================================

C~~~~~~~~~~~~~~~~~~~~~~~~~~~~~~~~~~~~~~~~~~~~~~~~~~~~~~~~~~~~~~~~~~~~~~~~
C~~~~~~~~~~~~~~~~~~~ TDMA (Thomas) ALGORITHM ~~~~~~~~~~~~~~~~~~~~~~~~~~~
C~~~~~~~~~~~~~~~~~~~~~~~~~~~~~~~~~~~~~~~~~~~~~~~~~~~~~~~~~~~~~~~~~~~~~~~~
      subroutine thomas(n,max,a,b)

      INTEGER max,n,i
      DOUBLE PRECISION a(max,3),b(max)
C     With reference to Patankar's book (pp. 52-53)
C     a(i,2) = ai, a(i,3)=bi, a(i,1)=ci, b(i)=di (on RHS of eq below)
C     a(1,3) = P1
      a(1,3)=-a(1,3)/a(1,2)
C     b(1) = Q1
      b(1)=b(1)/a(1,2)
      do 51 i=2,n
C     a(i,3) = Pi
      a(i,3)=-a(i,3)/(a(i,2)+a(i,1)*a(i-1,3))
C     b(i) = Qi
      b(i)=(b(i)-a(i,1)*b(i-1))/(a(i,2)+a(i,1)*a(i-1,3))
   51 continue
      do 52 i=n-1,1,-1
      b(i)=a(i,3)*b(i+1)+b(i)
   52 continue

      return
      end
```